



Norwegian University of  
Science and Technology

# Stress Analysis, Lay-up and Production Process For The Tail Section Of A Composite Glider Used For Energy Generation.

**Erik Vassøy Olsen**

Materials Science and Engineering

Submission date: August 2017

Supervisor: Nils Petter Vedvik, MTP

Norwegian University of Science and Technology  
Department of Mechanical and Industrial Engineering



## PREFACE

This project was carried out at the department of engineering design and materials, at the Norwegian University of Science and Technology (NTNU), spring 2017. The thesis is written in cooperation with Kongsberg Defense systems (KDS) and Kitemill.

The idea of this assignment was brought up during a visit as KDS's production facility in March 2016. Kitemill is related to KDS through Kongsberg Innovasjon. KDS support them with their knowledge about composite materials. From this cooperation, this thesis was formed.

I have always had a passion for engineering. Kitemill's concept immediately took my attention as a genuinely interesting way of producing energy. I also found this to be a great opportunity to learn from experiences engineers at both Kitemill and KDS.

I want to thank KDS for making this thesis possible. Especially Tor Sigurd Breivik, for all his support and help with arranging the thesis. I also want to thank Sture Smidt and Jo Grini at Kitemill for technical support and help with manufacturing test samples. A thank is also addressed to my fellow classmates Marcus Kolberg and Christer Kobbevik Oldeide for their help with software. At last I want to thank my supervisor at NTNU Associate Professor Nils Petter Vedvik.

A special thanks to Textreme and Evonik for sponsoring my thesis with test materials.

## ABSTRACT

Kitemill is developing a new concept to harness wind energy. Their concept is shaped like a glider, and takes advantage of the high wind speeds at high altitudes. Operations in such environments require strong and lightweight materials. This thesis will focus on the production method, material type and lay-up for a structural composite beam inside the horizontal stabilizer.

Kitemill currently use wet lay-up bladder moulding technique to make the part. In this process where an inflatable bicycle tube is used to generate pressure on the composite in a closed mould. The maximum load of the piece they made by this process was set as the benchmark loading.

The material used in this production method is a combination between Textreme (76 gsm) and Renlam M1 Epoxy. This material combination was tested according to the ASTM standard of composite testing, with some simplifications. The laminate constants were calculated from these results. These constants were used to create an Abaqus model which simulated the bladder moulded beam in a three-point bending test.

A second production technique was created. The aim was to build a sample that could take the benchmark loading, but weighing less. This was done by creating a parametric optimization of lay-up for composites with the software program Isight. This lay-up was used together with a compression moulding technique where a core-material is squeezed into the mould. Pre-Preg composite material was used for this concept.

The results indicated that the focus should be changes from the “maximum load” to “production quality”. The compression moulding production technique seems to be a better alternative than the bladder moulding technique due to air bubbles in the laminate. However, this is a more expensive production technique.

The structure of the optimization program is good, but it needs some adjustments before it can be useful for real design applications. The program was computational heavy because the program had too many variables. There was also a problem with the way the simulation was set up. The result at this was that Abaqus ignored the difference between a continuous ply and a non-continuous ply.

The conclusion is that the bladder molding technique can be used for the prototype glider, but the material should be changed to Pre-preg to minimize production flaws.

## SAMMENDRAG

Kitemill utviklet et nytt konsept for å utnytte vindenergien. Konseptet er en drage formet som en glider. Den utnytter de høye vindhastighetene høyt over bakken. Operasjoner i slike krevende miljøer krever sterke og lette materialer. Denne oppgaven vil fokusere på produksjonsmetoden, materialtype og lay-up for en strukturell komposittbjelke på innsiden av høyderor.

Kitemill bruker i dag en blærestøpingsteknikk til å produsere denne delen. I denne prosessen brukes en oppblåsbar sykkelslange på innsiden av lukket form til å lage press mot komposittmaterialet. Den maksimale lasten på bjelken i 3-punkt bøyetest, laget med denne teknikken ble satt som en referanselast.

Materialet som brukes i denne produksjonsmetoden er en kombinasjon mellom Textreme (76 gsm) og Renlam M1. Epoxy. Denne materialkombinasjonen ble testet i henhold til ASTM standarden for kompositt testing, med noen forenklinger. Disse resultatene ble brukt til å regne ut laminatkonstantene til materialet. Laminatkonstantene ble videre brukt i en Abaqus modell som beregner den maksimale lasten i en 3-punkts bøyetest.

Det ble også brukt en annen produksjonsteknikk. Målet var å lage et annet eksemplar med en annen metode som kunne ta samme referanselasten, men veie mindre. For disse prøvene ble det utviklet et optimaliseringsprogram for kompositter med i programvaren Isight. Komposittbjelken ble laget med en kompresjonsstøping teknikk, hvor et kjernemateriale ble presset ned i formen. Preimpregnerte komposittmaterialer ble brukt for dette konseptet.

Det ble konkludert med at fokuset burde endres fra å spare vekt til å heller finne eller utvikle en produksjonsmetode som gir høy produksjonskvalitet. Kompresjonsstøpet så ut til å fungere bedre enn blærestøpet, fordi den hadde færre luftbobler mellom lagene i laminatet. Ulempen med denne metoden er at det vil koste mer å produsere hvert eksemplar.

Strukturen i optimaliseringsprogrammet er bra, men det trenger mer arbeid før det kan fungere optimalt. Programmet krevde mye datakraft på grunn av mange design variabler. Det var også et problem med hvordan simuleringen var satt opp. Resultatet av dette var at Abaqus ignorerte forskjellen på sammenhengende og oppdelte lag med karbonfiber.

Konklusjonen er at blærestøpte teknikken er best for prototype glideflyet, men materialet burde byttes ut med pre-impregnert karbonfiber for å minimere produksjonsfeil.



# TABLE OF CONTENTS

<b>NOMENCLATURE</b>	<b>1</b>
<b>1. INTRODUCTION</b>	<b>2</b>
1.1. STRUCTURE OF THIS THESIS	2
1.2. A SOLUTION FOR RENEWABLE ENERGY	4
1.3. KITEMILLS AIRBOURNE WIND ENERGY CONCEPT	4
1.4. SCOPE OF THIS THESIS	6
<b>2. THEORY</b>	<b>8</b>
2.1. NAMES AND DEFINITIONS OF THE GLIDER	8
2.2. LOADCASE DEFINITION	9
2.2.1. AIRCRAFT MANEUVERING	9
2.2.2. ELIPTIC LIFT DISTRIBUTION	10
2.3. BALANCING OF THE GLIDER	11
2.4. FINITE ELEMENT SIMULATION	11
2.4.1. SHELL ELEMENTS	11
2.4.2. SOLID ELEMENTS	12
2.4.3. STATIC GENERAL SIMULATION	13
2.5. COMPOSITE MATERIALS	13
2.5.1. INTRODUCTION TO LAMINATES	13
2.5.2. INTRODUCTION TO ANISOTROPIC MATERIALS	15
2.5.3. FAILURE CRITERIA FOR COMPOSITES	15
2.6. INTRODUCTION TO COMPOSITE TESTING	17
2.6.1. TENSILE TESTING FG COMPOSITES	17
2.6.2. IN PLANE SHEAR TESTING OF COMPOSITES	18
2.6.3. COMPRESSIVE TESTING OF COMPOSITES	18
2.7. PARAMETERIZATION SOFTWARE	19
2.7.1. OPTIMIZATION ALGORITHM	20
<b>3. TESTING TEXTREME WITH RENLAM M1</b>	<b>21</b>
3.1. MOULD PREPARATION	21
3.2. LAY-UP	21
3.3. CURING	22
3.4. TEST SAMPLES	22
3.5. CLAMPING TABS	22
3.6. TESTING	24
3.6.1. TEST SETUP FOR TENSION TESTING	25
3.6.2. TEST SETUP FOR SHEAR TESTING	25

3.6.3.	TEST SETUP FOR COMPRESSION TESTING	26
<b>3.7.</b>	<b>TEST RESULTS</b>	<b>27</b>
3.7.1.	TENSION RESULTS	27
3.7.2.	SHEAR RESULTS	28
3.7.3.	COMPRESSION RESULTS	29
3.7.4.	SUMMARY TESTING RESULTS	31
<b>4.</b>	<b>BLADDER MOULDING (CONCEPT 1)</b>	<b>32</b>
<b>4.1.</b>	<b>MOULD PREPARATION</b>	<b>33</b>
<b>4.2.</b>	<b>CUTTING THE TEXTREME WEAVE</b>	<b>33</b>
<b>4.3.</b>	<b>WET LAY-UP OF CARBON FIBER</b>	<b>34</b>
<b>4.4.</b>	<b>STRUCTURE OF THE LAY-UP</b>	<b>34</b>
<b>4.5.</b>	<b>CURING</b>	<b>36</b>
<b>4.6.</b>	<b>DEMOULDING</b>	<b>37</b>
<b>4.7.</b>	<b>RESULTS</b>	<b>37</b>
<b>4.8.</b>	<b>3-POINT BENDING TEST</b>	<b>38</b>
<b>5.</b>	<b>OPTIMIZATION OF COMPOSITES</b>	<b>39</b>
<b>5.1.</b>	<b>BUILDING A FEA MODEL IN ABAQUS</b>	<b>39</b>
5.1.1.	SYMMETRY CONDITIONS	39
5.1.2.	MATERIAL PROPERTIES AND DEFINITIONS	40
5.1.3.	INTERACTION	40
5.1.4.	BOUNDARY CONDITIONS	41
5.1.5.	STEP AND LOADING	42
5.1.6.	SIMULATION ON A COMPRESSION MOULDED SAMPLE	42
5.1.7.	MESH	42
<b>5.2.</b>	<b>LAY-UP ZONES</b>	<b>44</b>
<b>5.3.</b>	<b>ABAQUS MACRO</b>	<b>45</b>
<b>5.4.</b>	<b>OPTIMALIZATION USING DATA EXCHANGER</b>	<b>45</b>
<b>5.5.</b>	<b>OPTIMIZATION USING OS EXCEL, OS COMMAND AND PYTHON</b>	<b>46</b>
<b>5.6.</b>	<b>PYTHON PROGRAM</b>	<b>48</b>
<b>5.7.</b>	<b>OPTIMIZED LAY-UP</b>	<b>49</b>
<b>6.</b>	<b>COMPRESSION MOULDING (CONCEPT 2)</b>	<b>50</b>
6.1.1.	REDESIGN OF THE MOULD	50
6.1.2.	PREPARATION OF THE MOULD	51
<b>6.2.</b>	<b>SIMPLYFING THE LAY-UP</b>	<b>53</b>
<b>6.3.</b>	<b>FIBERSIM</b>	<b>53</b>
<b>6.4.</b>	<b>LAY-UP</b>	<b>55</b>
<b>6.5.</b>	<b>CURING</b>	<b>56</b>
<b>6.6.</b>	<b>RESULT</b>	<b>57</b>

<b>7. TESTING</b>	<b>59</b>
<b>7.1. TESTRIG DESIGN</b>	<b>59</b>
<b>7.2. TEST SETUP</b>	<b>60</b>
<b>7.3. TEST RESULTS</b>	<b>60</b>
7.3.1. BLADDER MOULDED SAMPLES	60
7.3.2. COMPRESSION MOULDED SAMPLES	61
<b>8. DISCUSSION</b>	<b>62</b>
<b>8.1. TESTING TEXTREME</b>	<b>62</b>
8.1.1. TENSION TESTING	62
8.1.2. SHEAR TESTING	63
8.1.3. COMPRESSION TESTING	63
<b>8.2. BLADDER MOULDING</b>	<b>64</b>
8.2.1. PRODUCT QUALITY	64
8.2.2. FINDING THE FAILURE LOAD	65
<b>8.3. THE OPTIMIZATION PROGRAM</b>	<b>65</b>
8.3.1. OPTIMALIZATION ALGORITHM	66
8.3.2. THE RESULT	67
8.3.3. THE FEA SETUP	67
<b>8.4. COMPRESSION MOULDING</b>	<b>68</b>
8.4.1. QUALITY OF THE PRODUCT	68
<b>8.5. TESTING</b>	<b>69</b>
<b>8.6. GENERAL DISCUSSION</b>	<b>70</b>
8.6.1. CROSS SECTION MICROSCOPY COMPARISON	70
<b>9. CONCLUSION</b>	<b>72</b>
<b>10. FUTURE WORK</b>	<b>73</b>
<b>SOURCES</b>	<b>74</b>
<b>APPENDIX</b>	<b>75</b>



## NOMENCLATURE

$\Delta\gamma_{12}$  = Difference between the two engineering shear strain points ( $\approx 0,004\mu m$ )

$\Delta\varepsilon$  = Difference in strain ( $\approx 2000\mu\varepsilon$ )

$\Delta\sigma$  = Difference in the applied tensile stress corresponding to the strain

$\sigma_{uts}$  = Ultimate tensile strength

$\Delta\tau_{12}$  = Difference in applied engineering shear stress between two shear strain points

$\tau_{12}^m$  = Maximum in plane shear stress 0

$\nu_{12}$  = Poisson's ratio

$A$  = Average cross-sectional area

$CG$  = Centre of gravity

$CL_{max}$  = Maximum coefficient of lift

$CO_p$  = Center of pressure

$E_1$  = Young's modulus in 1 direction

$E_2$  = Young's modulus in 2 direction

$E^f$  = Expected flexural modulus

$E^{Chord}$  = Chord modulus of elasticity

$F^{cu}$  = Laminate compressive strength

$G_{12}$  = Shear modulus 1-2 plane

$G_{13}$  = Shear modulus 1-3 plane

$G_{23}$  = Shear modulus 2-3 plane

$G_{12}^{Chord}$  = Shear chord modulus of elasticity

$G_{xz}$  = Through the thickness (interlaminar) shear modulus

$h$  = Specimen thickness [mm]

$l_g$  = Length of gauge section [mm]

$NP$  = Neutral point

$P_f$  = Maximum load at failure [N]

$P^{max}$  = Maximum force before failure

$P^m$  = Maximum force below 5% engineering shear strain

$S_{12}$  = Shear strength in 1-2 plane

$X_T$  = Tensile strength in 1 direction

$X_C$  = Compressive strength in 1 direction

$Y_T$  = Tensile strength in 2 direction

$Y_C$  = Compressive strength in 2 direction

# 1. INTRODUCTION

## 1.1. STRUCTURE OF THIS THESIS

---

The experimental work of this thesis is written in the chronological order according to the workflow. This is done to give the reader an insight in the thought process. The workflow of this Thesis is represented by Figure 1.

### **Chapter 1: Introduction**

An introduction to the general insight and motivation for this thesis

### **Chapter 2: Theory**

Relevant theory for the analytical and practical work in this thesis.

### **Chapter 3: Testing Texteme with Renlam M1**

In this chapter the laminate constants for Texteme combined with Renlam M1 is found by testing. This chapter is heavily based on the preliminary study.

### **Chapter 4: Bladder moulding (concept 1)**

This chapter describes the current process Kitemill uses for production of their parts using a bladder moulding technique. The failure load of their concept was used as a benchmark for the parametric optimization.

### **Chapter 5: Parametric optimization of composites**

The process of making a parametric optimized lay-up for composites in Isight.

### **Chapter 6: Compression moulding (concept 2)**

The optimized lay-up was used to build new samples with a compression moulding technique.

### **Chapter 7: Testing**

This chapter gives an overview of how the testing was performed and the results.

### **Chapter 8: Discussion**

Discussion related to the results obtained during experimental and analytical work.

### **Chapter 9: Conclusion**

A conclusion of the results

### **Chapter 10: Further work**

Thoughts around further work

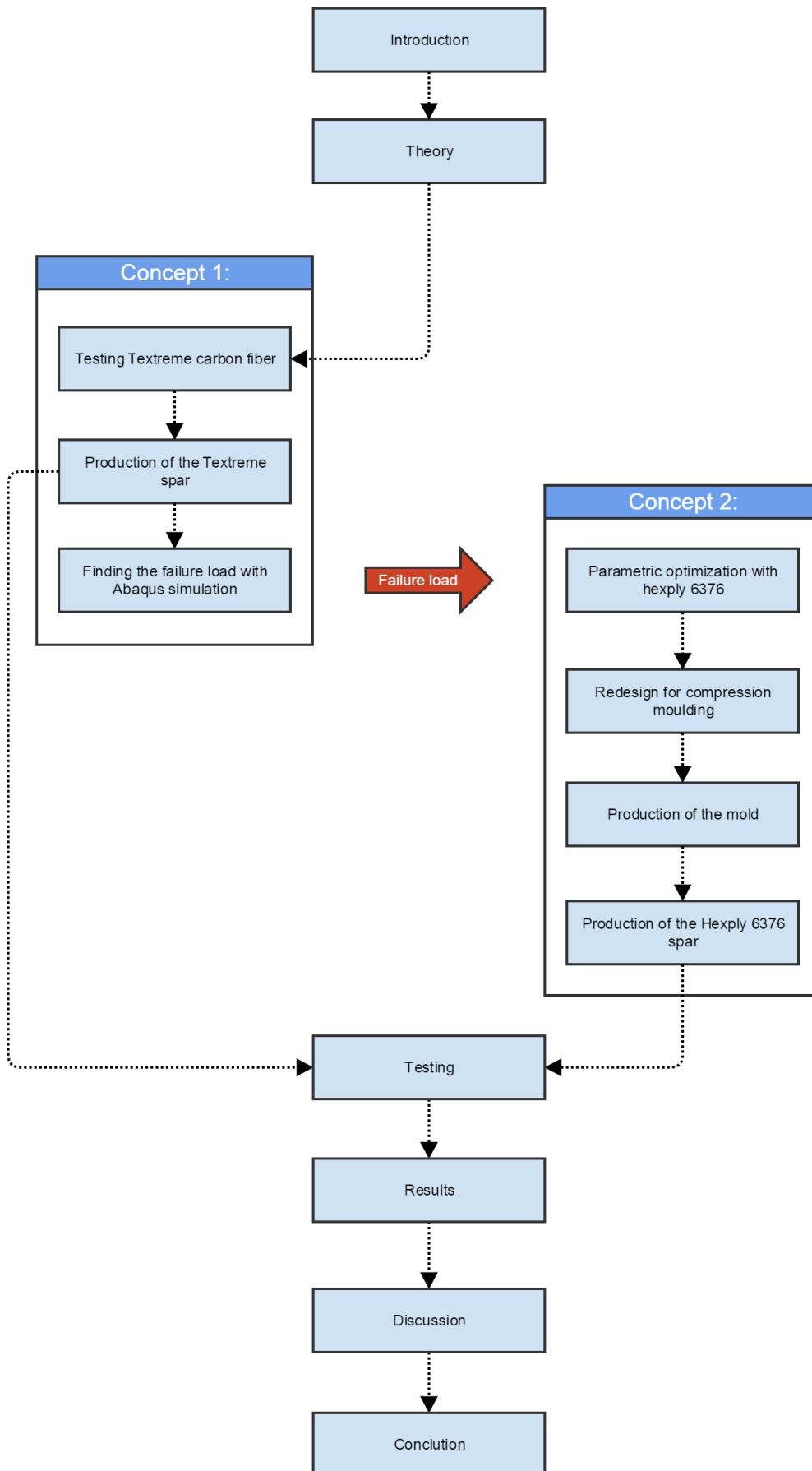


Figure 1: Workflow of this thesis

## 1.2. A SOLUTION FOR RENEWABLE ENERGY

As the standard of living grows worldwide, the requirement for energy resources also rises. Mankind is continually trying to find new ways to harness energy. The challenge is to find sustainable methods to harness the energy in an environmentally friendly way.

The 4<sup>th</sup> of November 2016 the Paris agreement took effect. In this agreement, 113 countries agreed to take precautions to halt the greenhouse gas emissions. The goal is to avoid a temperature rise of 1.5°C (2). This means that the demand for green energy will increase drastically in the near future.

## 1.3. KITEMILLS AIRBOURNE WIND ENERGY CONCEPT

Kitemill is a Norwegian company that was founded in 2008. Their expertise is technology that potentially can revolutionize the wind energy business. Traditionally, wind has been harnessed with wind turbines. These are often big and heavy structures, which means that the material and installation costs are high. Kitemill claim that their concept uses only 10% of the materials compared to traditional wind turbines with the same capacity. Today's wind turbines power output is strongly dependent on the wind speed. Kitemill's concept goes to higher altitude where the windspeed is higher and more stable, which means more energy can be generated.

A kite is a good model to illustrate the concept. As the wind is captured by the kite a pressure difference occurs across the kite membrane, much like an airplane wing, this pressure difference creates lift and drag, together these forces cause tension in the tether (pulling force). Figure 2 illustrates a free body diagram of a kite flying in the wind.

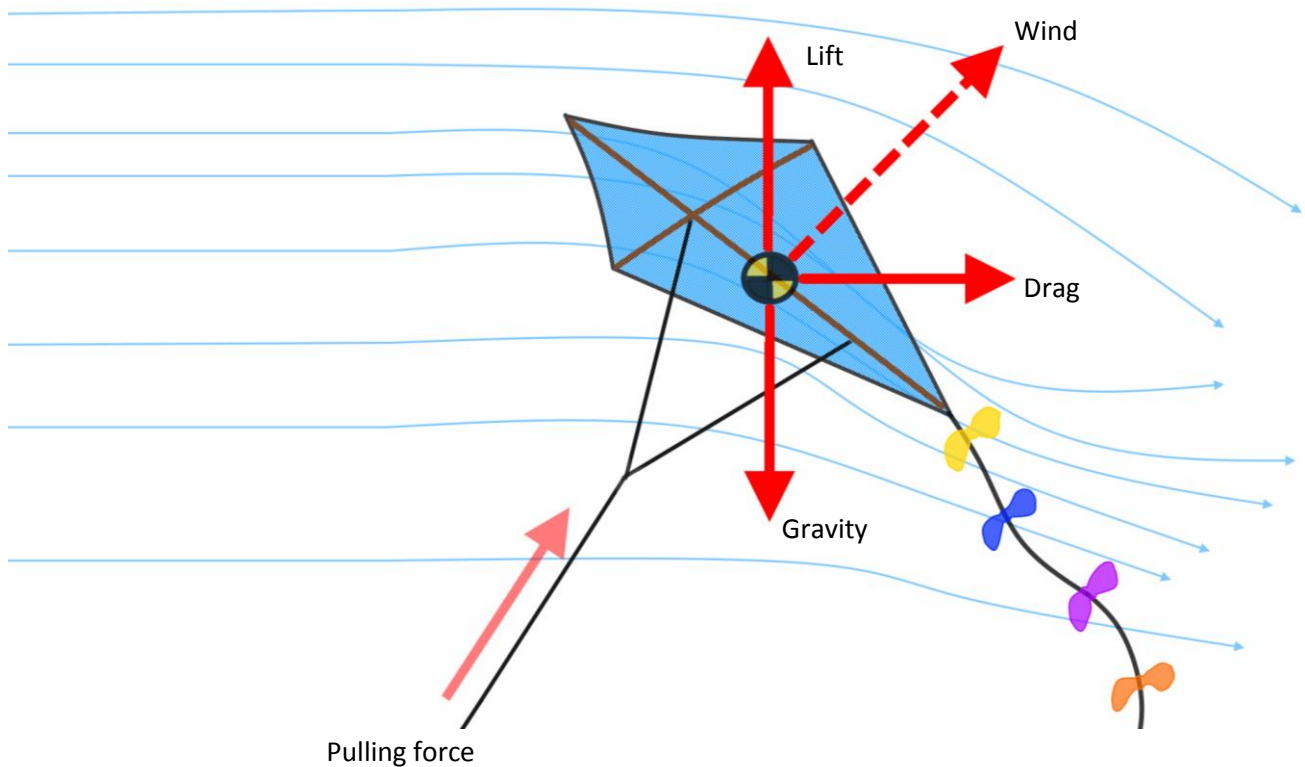


Figure 2: Free-body diagram of a kite

Kitemill's concept looks like an airplane (glider), but works the same way as a kite. Instead of holding it in your hand, the tether is wound up on a drum which is placed on the ground. The drum is coupled to a generator, which generates electricity when the kite is carried downstream by the wind. The nominal pulling force from a glider with a wingspan of 7.5m is estimated to be 7500N. With a wind speed of 12 m/s this results in a 30 kW of power generation(3). Figure 3 shows the founder of Kitemill; Thomas Hårklau and the production manager; Jo Grini with the first 30 kW prototype.



Figure 3: The first 30 kW prototype

To gather as much energy as possible from the wind, the glider flies in a helical path. This is illustrated in Figure 4. When the tether is fully extended, the glider turns to a horizontal gliding position. This is to minimize drag as the kite returns to the starting position. This is illustrated in Figure 5. These maneuvers are autonomously controlled by an onboard electrical control unit.

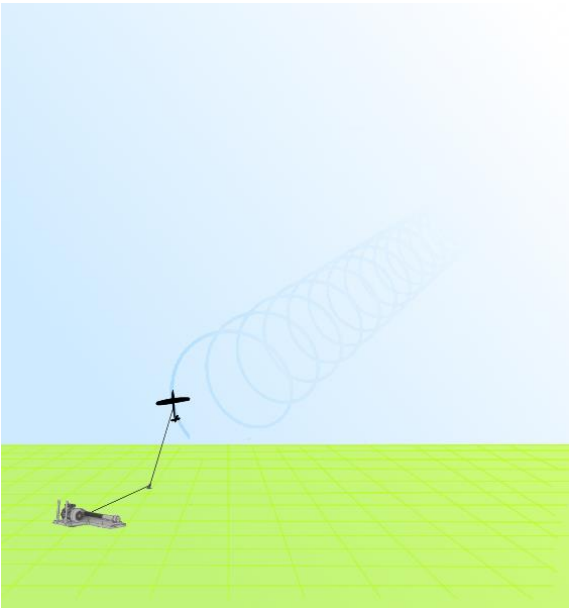


Figure 4: Glider enters helical path

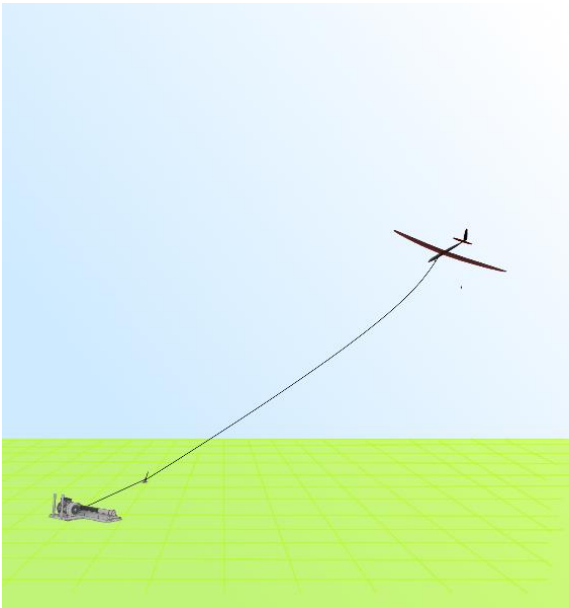


Figure 5: Return to start position

## 1.4. SCOPE OF THIS THESIS

---

The scope of this thesis is to improve the design and production process that Kitemill uses to make a load bearing spar placed in the horizontal stabilizer of their prototype glider. The tail section of the glider is illustrated in Figure 6. Half of the horizontal stabilizer spar is shown by the transparent view of the wing element.

There were no accurate estimations of the forces acting on the spar due to the kite being a prototype, thus in the early stage of development. It was therefore decided to go to Kitemill's production facility at Lista to produce two samples with Kitemill's manufacturing methods and equipment. These samples would set the benchmark loading, which was going to be used in the simulation. The material used in their process, is the same material that was tested in the preliminary study report. Finite Element Analysis (FEA) simulations will be compared to physical tests to find the accuracy of the results.

The benchmark loading will be set as the target when designing an optimization program for composites in Insight. This is a software that is made for parametric optimization through FEA. The idea is to use a different production technique and an optimized lay-up to create a new spar that can withstand the same loading but weigh less.

Two different production methods will be tested and discussed in this thesis. A bladder moulding technique and a compression moulding technique.

The author of this thesis is a material scientist. This thesis will therefore focus on the material parameters and production techniques, not the different load cases the part may be exposed to during operation. The physical dimensions and design is given by Kitemill.

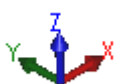
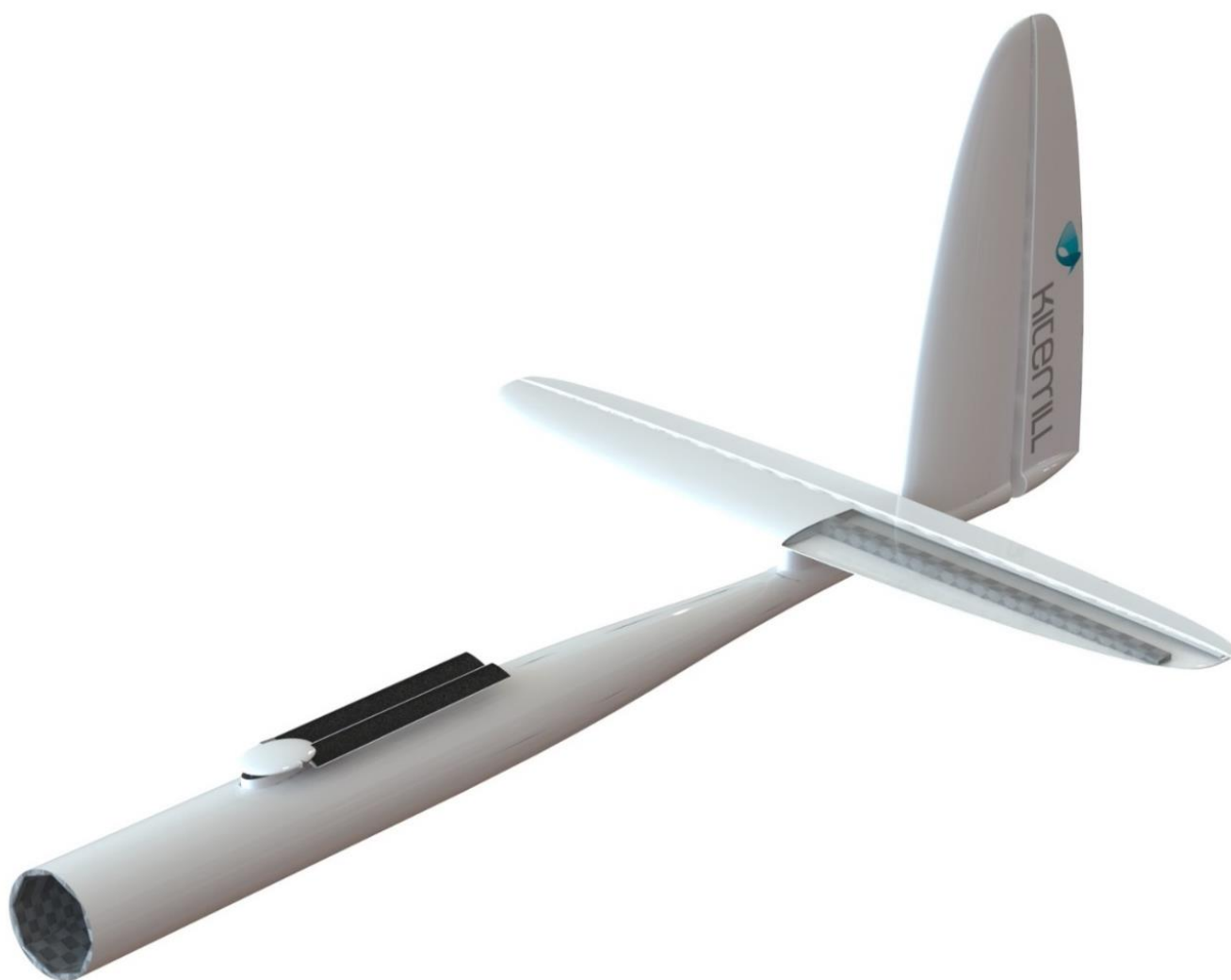


Figure 6: The tail section of the glider.

## 2. THEORY

### 2.1. NAMES AND DEFINITIONS OF THE GLIDER

When designing a glider, it is necessary to have a general understanding of the name convention used in aerospace. Figure 7 illustrates the glider with name conventions that will be used in this thesis. The Horizontal stabilizer spar is shown in Figure 8. The spar is the load bearing structure in the horizontal stabilizer.

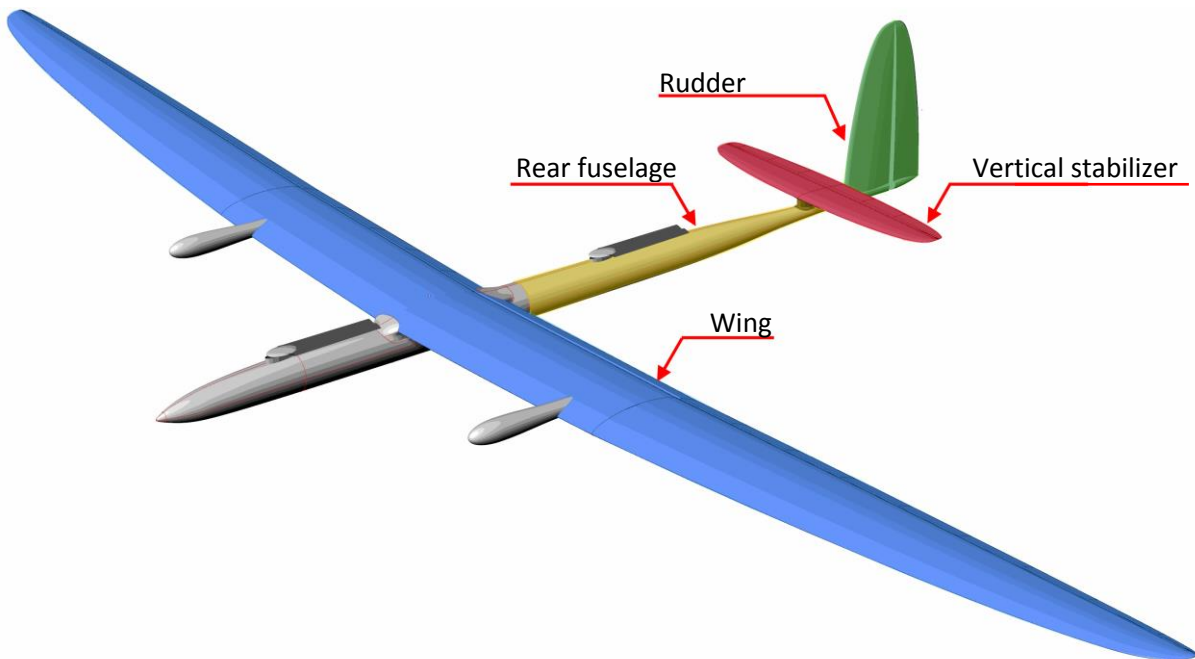


Figure 7: Name of the different zones on the glider



Figure 8: The Horizontal stabilizer spar

The spar is symmetric about the fuselage of the glider. The defined symmetry plane is shown in Figure 9.



Figure 9: Symmetry plane of the spar

## 2.2. LOADCASE DEFINITION

---

### 2.2.1. AIRCRAFT MANEUVERING

---

The glider is free to move in 6 degrees of freedom, when it is airborne. Figure 10 illustrates a glider with an orthogonal axis system. The origin of the coordinate system is chosen as the wing leading edge at the root:

- Rotation about the longitudinal axis is called roll
- Rotation about the vertical axis is called yaw
- Rotation about the lateral axis is called pitch

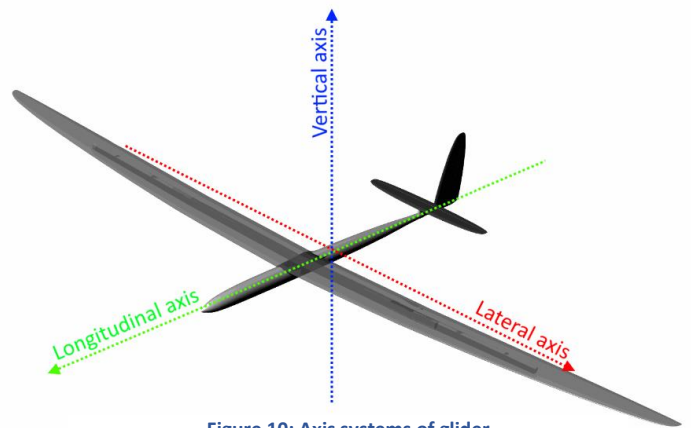


Figure 10: Axis systems of glider

The horizontal stabilizer is used to control the motion of the aircraft in pitch.

### 2.2.2. ELIPTIC LIFT DISTRIBUTION

The worst load case will be when the airplane performs a pitch maneuver, hence the dimensioning factor. The load distribution for a wing has an approximate elliptical lift distribution. The lift distribution for the horizontal stabilizer can be seen in Figure 11.

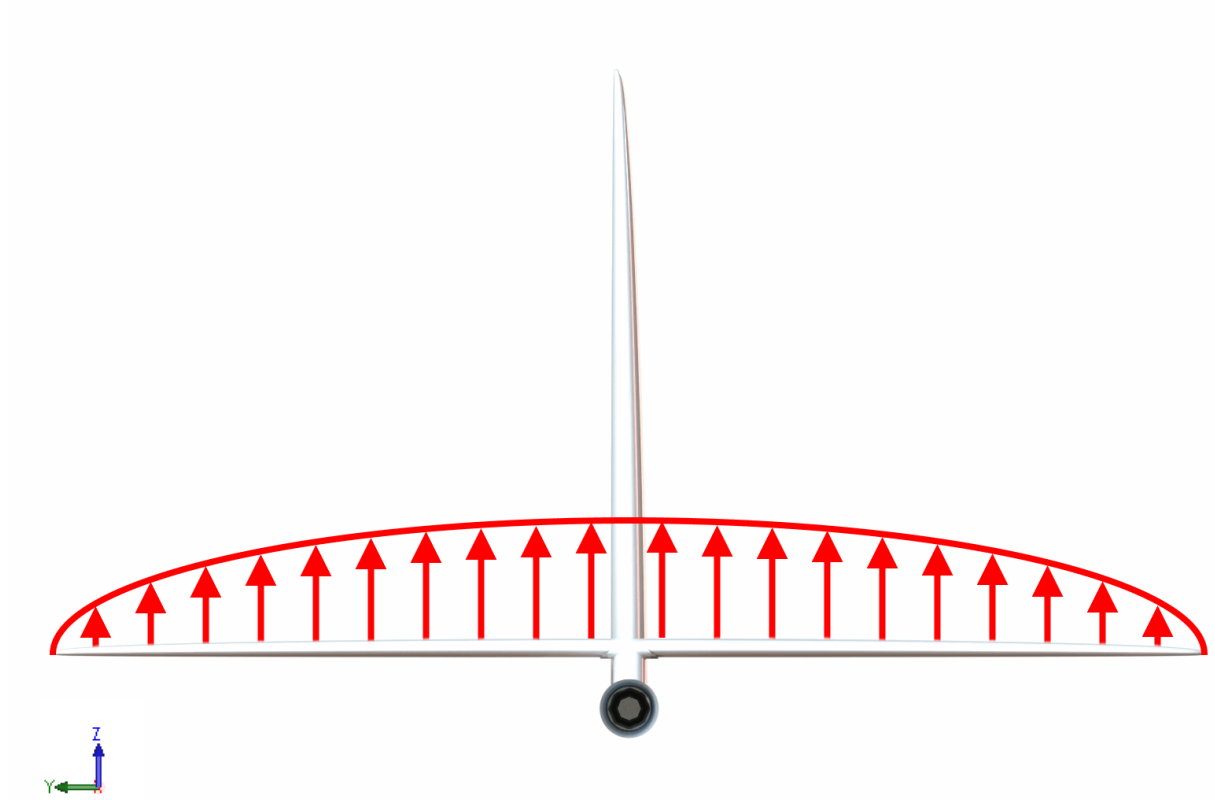


Figure 11: Lift distribution over the horizontal stabilizer

The center of pressure is for the horizontal stabilizer estimated to be ahead of the spar. This will create a torsional momentum. This is illustrated in Figure 12 (4).

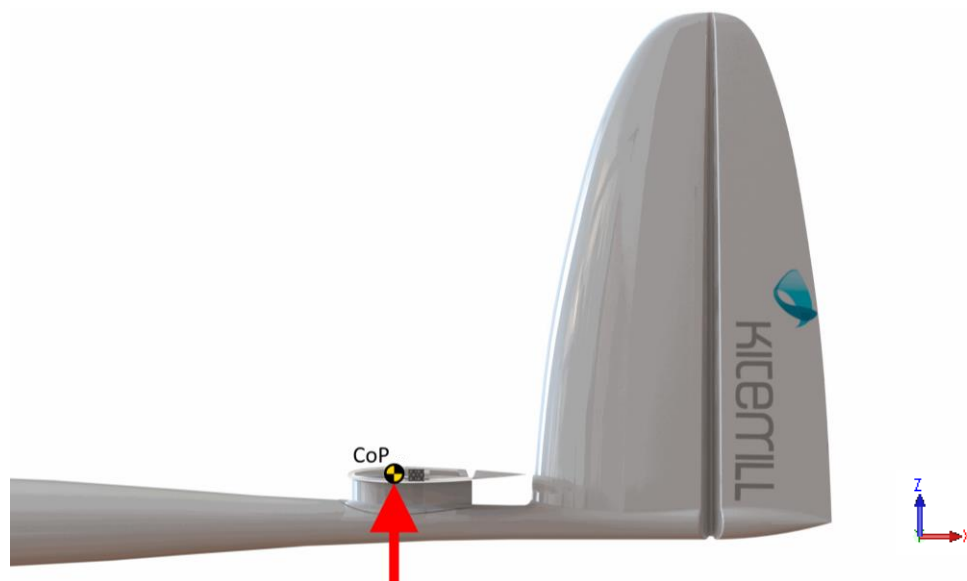


Figure 12: Centre of pressure ahead of the spar

## 2.3. BALANCING OF THE GLIDER

The summation of all the aerodynamic centres is called the neutral point (NP). A general design criterion in aerospace engineering is that this point needs to be behind the centre of gravity (CG) in the flight direction. If this criterion isn't met the glider will become unstable in pitch. Figure 13 illustrates where the CG should be placed relative to the NP. The centre of gravity can be adjusted by putting weight at the front. The downside is that a heavier glider would require more energy to stay airborne, which means that less energy will be generated(5).

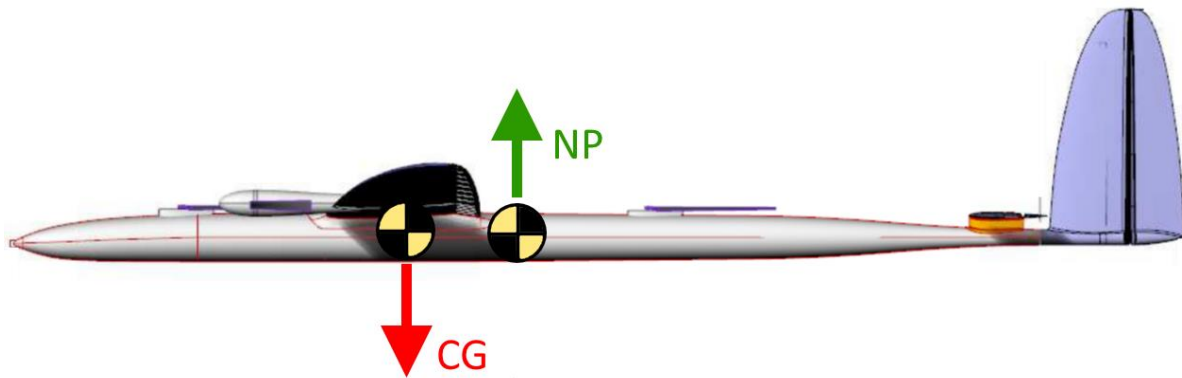


Figure 13: Center of gravity ahead of the neutral point in flying direction.

## 2.4. FINITE ELEMENT SIMULATION

### 2.4.1. SHELL ELEMENTS

Choosing the right element type is crucial to perform accurate simulations and limit the use of computational power. Abaqus CAE supports the elements S3R, S3RS, S4, S4R, S4RS, S4RSW, SC6R, SC8R and S8R for analysis of laminated composite shells (6). The element codes are explained in Figure 14. Figure 14: Explanation of the element codes for shell elements (7)

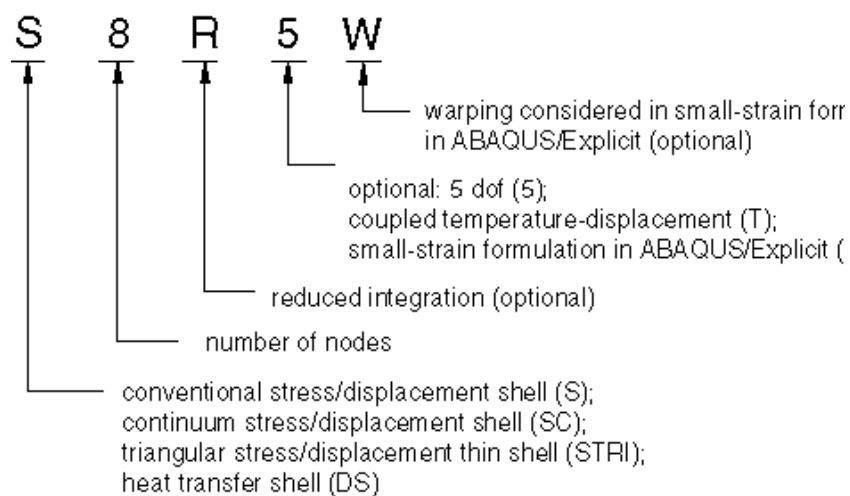


Figure 14: Explanation of the element codes for shell elements (7)

If the thickness is relatively small compared to the other dimensions on the structure, i.e. a shell structure, conventional shell elements is a good choice. These are defined as 2,5-dimension elements with no “out of plane” thickness. The thickness is assigned to the element by the material properties. If the thickness of the laminate is more than 1/15 of the length of the elements surface shell, conventional shell must be used. If the thickness is less than 1/15 the other dimensions a shell formulation can be used. These elements do not account for transverse shear deformation and is therefore not applicable for thick composite materials (7).

Abaqus provides elements with reduced integration. These elements use reduced (lower-order) integration to form the element stiffness. Reduced integration usually provides more accurate simulations. In cases where the transverse shear flexibility is important and second degree interpolation is desired, thick conventional shells are a good choice (8).

2.4.2. SOLID ELEMENTS

Solid elements are the standard volume elements in Abaqus. These elements can be used for both linear and non-linear analysis with contact involving plasticity and large deformations. Figure 15 explains the element codes of solid elements.

Triangular and tetrahedral elements are geometrically versatile and are good for complicated shapes. However, a good hexahedral mesh usually provides equivalent accuracy at less cost. If the geometrical shape is adequate, the hexahedral mesh should be chosen over the triangular and tetrahedral.

In Abaqus/Standard you can choose between full or reduced integration. Reduced integration uses a lower order integration to form the element stiffness. This reduces the running time of the simulation and saves computational power. Second-order, fully integrated elements are good to use close to the stress concentrations to capture the severe stress gradients. First order elements with reduced integration are good for large distortions(1).

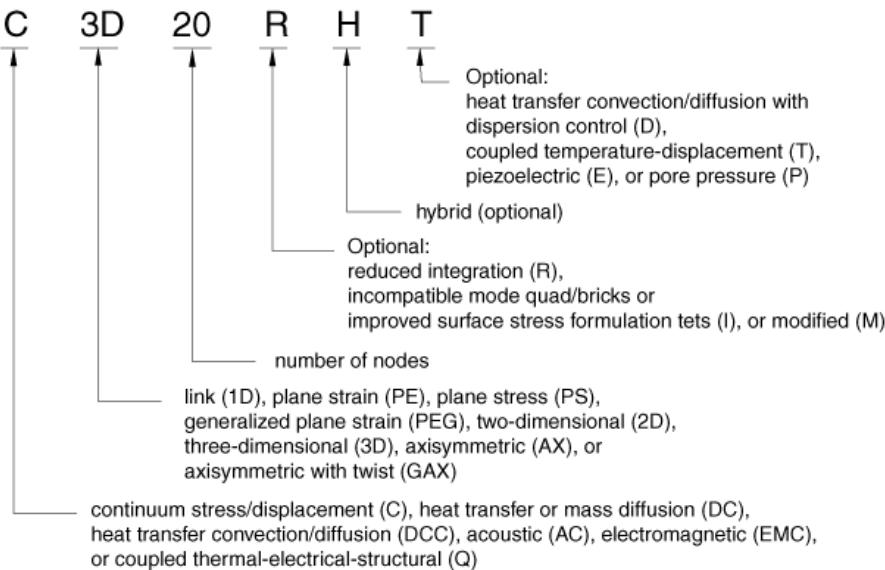


Figure 15: Explanation of the element codes for solid elements (1)

### 2.4.3. STATIC GENERAL SIMULATION

Static analyses can be used for both linear and nonlinear problems due to material and geometrical response. The time in this analysis is only used to control the load amplitudes. This means that time depended response is not accounted for in this type of analysis. Any stress/displacement elements can be used in this type of simulation (9).

## 2.5. COMPOSITE MATERIALS

### 2.5.1. INTRODUCTION TO LAMINATES

A composite material is a combination of two or more materials with different properties. Modern composite materials are often made by strong fibers embedded in a polymer matrix. This results in very strong and lightweight materials.

The properties of the fibers in the composite material have very high influence on the strength and stiffness of the material. This is because there is a significant strength and stiffness difference between the fibers and the matrix. This means composite materials can be defined as in plane anisotropic materials.

Carbon fibers is a type of fiber that offers superb strength/stiffness to weight ratio. To make it more convenient to handle, bunches of these fibers are woven together in fabrics. The fibers can be woven into different patterns and shapes. Carbon fibers are most commonly quantified by the following parameters.

- Type of weave
- Number of fibers in each tow (K-number)
- Weight (grams per square meter of weave (gsm))
- Characteristics of the type of carbon fiber used

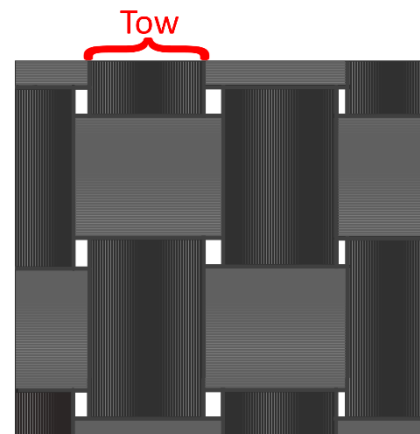


Figure 16: Plain weave

Figure 16 illustrates the plain weave of carbon fiber.

When a single fabric is combined with a resin it is referred to as a lamina or a layer. In general, there is a variety of different ways to combine the fabric and the matrix. The two main categories are pre-impregnated fabrics and wet-impregnated fabrics. The pros and cons with the impregnation method are listed in Figure 17.

Pre impregnated fabrics	Wet impregnated fabrics
Pre impregnated fabrics are bought as a lamina.	Fabric that needs to be impregnated
<ul style="list-style-type: none"> <li>+ Very good production control</li> <li>+ Specific material constants are often given</li> <li>+ Ease of production</li> <li>- Expensive</li> <li>- Needs to be stored at low temperature</li> <li>- Has a limited shelf time</li> </ul>	<ul style="list-style-type: none"> <li>+ Cheap</li> <li>+ Possible to combine a variety of different materials</li> <li>+ No expiration date</li> <li>- Very low production quality</li> <li>- Requires a more advanced production method</li> </ul>

Figure 17: Pros and cons for impregnation method of a composite fabric

A stack of laminas on top of each other and cured together under high pressure is called a laminate. The laminas can be oriented with different angles, this makes it possible to tailor a laminate for a specific loading. Figure 18 illustrates how the laminates can be stacked together to form a laminate.

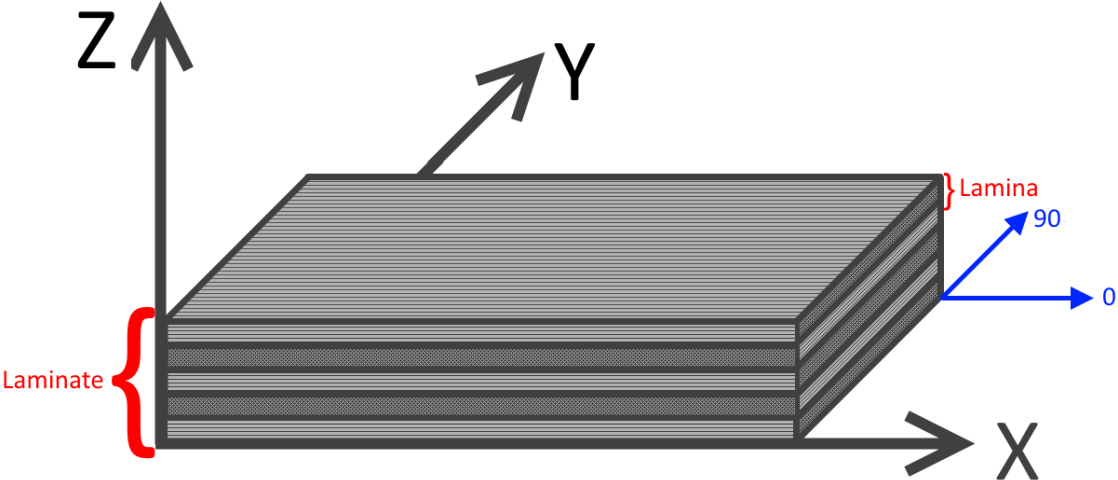


Figure 18: Global coordinate system for the laminate

Because the fabric is woven together there can be a slight difference in Young’s modulus in the different fiber directions. A roll of carbon fiber as illustrated in Figure 19. The width of the roll is called the weft, these fibers have been woven around the fibers in the longitudinal direction (warp). The warp fibers are straight, and this often results in a higher young’s modulus. The idea is that the spread tow fabrics are so thin that the difference in stiffness between warp and weft can be ignored.

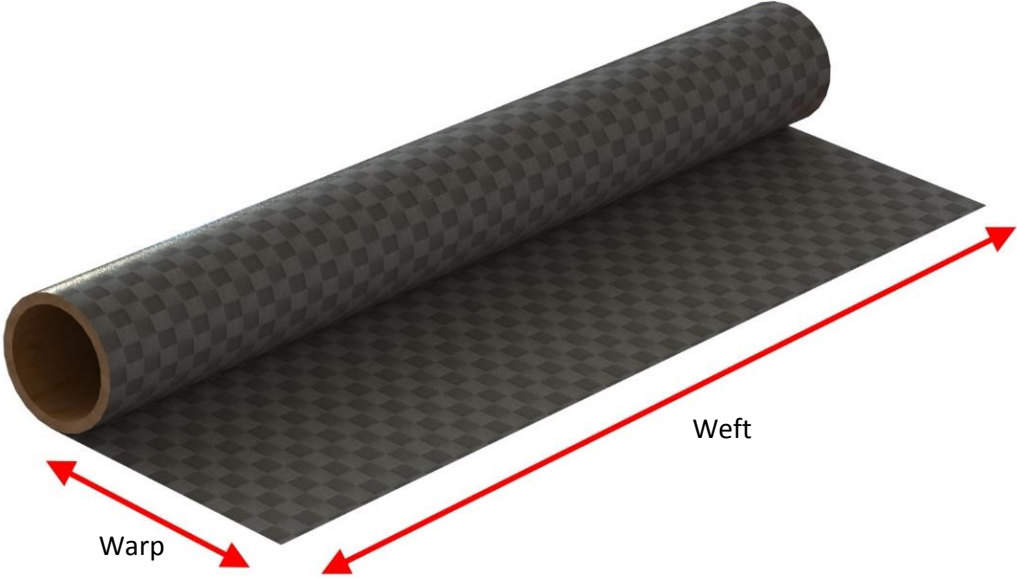


Figure 19: A roll of Textreme (spread tow carbon fiber)

## 2.5.2. INTRODUCTION TO ANISOTROPIC MATERIALS

Woven fabrics are defined as in plane anisotropic materials which means that the materials characteristics vary with the in-plane angle. Thin laminates are assumed to be in plane stress which reduces the amount of laminate constants that is needed to perform FEA simulations with a failure criterion.

If plane stress is used as an assumption, the following material constant are needed to perform a FEA simulation. The respective directions of a fabric are illustrated in Figure 20.

$E_1$  = Young's modulus in 1 direction

$E_2$  = Young's modulus in 2 direction

$\nu_{12}$  = Poisson's ratio in 1-2 plane

$G_{12}$  = Shear modulus 1-3

$G_{13}$  = Shear modulus 1-3 plane

$G_{23}$  = Shear modulus 2-3 plane

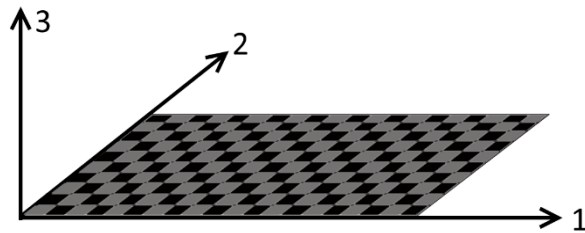


Figure 20: Local coordinate system for a lamina

It is important to emphasize that this is a local coordinate system for a lamina (hence 1,2 and 3 direction). This makes it possible to refer the fiber direction when the laminate is oriented by an arbitrary angle in the global coordinate system.

## 2.5.3. FAILURE CRITERIA FOR COMPOSITES

Because composites are anisotropic materials they need failure criteria that are suited for this. Failure of fiber-reinforced composites may be caused by fiber buckling, fiber breakage, matrix cracking, delamination or a combination of these. Typical failure modes of composites are shown in Figure 21(10). The failure modes from right to left are; micro buckling, fiber failure, matrix cracking and delamination.

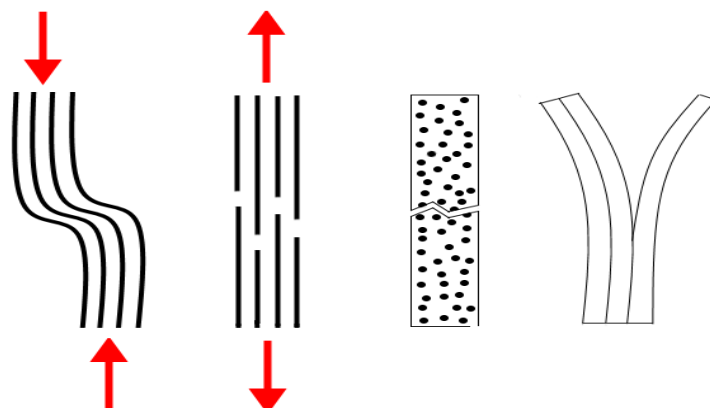


Figure 21: Typical failure modes of composites

## Tsai Wu

Tsai Wu is a failure criterion not associated with a failure mode. Tsai Wu as a plane stress failure criterion is defined as: Failure of a laminate occurs when  $f > 1$ .

$$f = F_1\sigma_1 + F_2\sigma_2 + F_{11}\sigma_1^2 + F_{22}\sigma_2^2 + F_{66}\tau_{12}^2 + 2F_{12}\sigma_1\sigma_2 \quad ( 1 )$$

where:

$$\begin{aligned} F_1 &= \frac{1}{X_T} - \frac{1}{X_C} & F_2 &= \frac{1}{Y_T} - \frac{1}{Y_C} \\ F_{11} &= \frac{1}{X_T X_C} & F_{22} &= \frac{1}{Y_T Y_C} \\ F_{66} &= \frac{1}{S_{12}^2} \end{aligned} \quad ( 2 )$$

The interaction coefficient  $F_{12}$  must be determined from additional biaxial testing. It can be estimated as:

$$\begin{aligned} F_{12} &= f_{ij}\sqrt{F_{11}F_{22}} \\ f_{ij} &= -0,5 \text{ or } 0 \end{aligned} \quad ( 3 )$$

This criterion does not consider the different damage mechanisms that promote laminate failure. Another issue worth noticing when using this criterion is the fact that it predicts that failure under biaxial tensile stress depends on the compressive strength (10).

## Maximum stress (MSTRS)

The maximum failure criterion is frequently used for orthotropic and transversely isotropic materials under plane-stress conditions. Failure does not occur if none of the stresses exceeds the strengths of the material. This is a simple and direct way to predict failure of composites, no interaction of the stresses acting of the lamina are considered. The advantage with this failure criteria is that it is associated with a failure mode (10).

For a unidirectional composite, failure will happen when:

$$\begin{aligned} \text{Fiber:} & \quad \sigma_1 \geq X_T \quad \text{or} \quad |\sigma_1| \geq X_C \\ \text{Matrix:} & \quad \sigma_2 \geq Y_C \quad \text{or} \quad |\sigma_2| \geq Y_C \\ \text{Shear:} & \quad |\sigma_{12}| \geq S_{12} \end{aligned}$$

## 2.6. INTRODUCTION TO COMPOSITE TESTING

---

To do lamina simulations in Abaqus, a total of six engineering constants are required. These engineering constants are often difficult/impossible to find when an arbitrary fiber is mixed with an arbitrary resin. These can be estimated using the rule of mixtures, but the results won't be as accurate as if the materials were tested together. Experimental tests can be used to find the material constants and the failure stress.

Composite materials that are woven (textile composites) must be tested according to an approved standard, such as the ASTM D6854. These materials often have a repeating geometrical pattern based on the manufacturing parameters. This geometrical pattern is referred to as a "unit cell" (11). Figure 22 illustrates the definition of a unit cell.

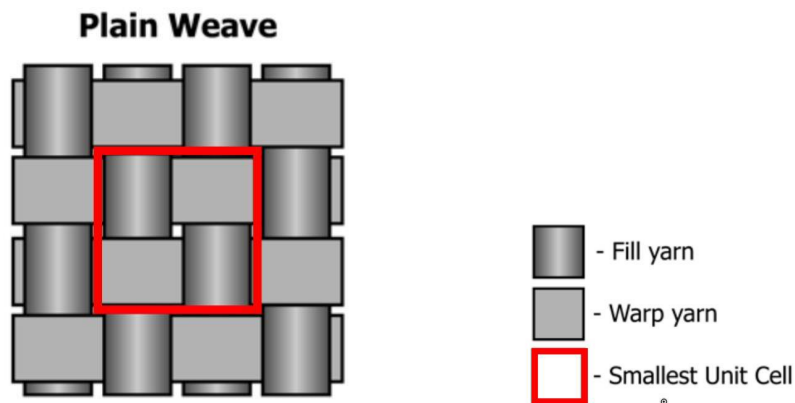


Figure 22: Definition of unit cell (12)

### 2.6.1. TENSILE TESTING FG COMPOSITES

---

Tensile testing of a rectangular composite material specimen will obtain the following material properties in the test direction(13).

- Ultimate tensile strength
- Tensile chord modulus of elasticity

This method is suitable for random, discontinuous, and continuous fibers, but is limited to materials that are symmetric with respect to the test direction.

#### Tensile strength calculation

The tensile strength is the maximum tensile stress the material can withstand before failure.

$$\sigma_{uts} = \frac{p^{max}}{A} \quad ( 4 )$$

#### Tensile Chord modulus of Elasticity

By selecting the appropriate strain range from  $1000\mu\epsilon$  to  $3000\mu\epsilon$ , and combining them with the corresponding stresses, it is possible to calculate the chord modulus of elasticity from the material. If

these exact points aren't available from the output data, the nearest two points will be chosen with its corresponding values. This method is only valid if stress vs strain is linear in the given area.

$$E^{Chord} = \frac{\Delta\sigma}{\Delta\varepsilon} \quad (5)$$

### 2.6.2. IN PLANE SHEAR TESTING OF COMPOSITES

This test method determines the in-plane shear response for a composite material. A rectangular specimen with fibers in [+45/-45] degrees orientation to the loading direction is tested in tension. The concept is illustrated in Figure 23.

It is important to emphasize that ASTM4762 describes this test as a poor test to determine the ultimate shear strength, due to large non-linear response while testing. However, this is a widely used test method because of its simplicity (14).

From the in-plane shear testing the following material parameters can be obtained.

- Maximum shear
- Shear modulus

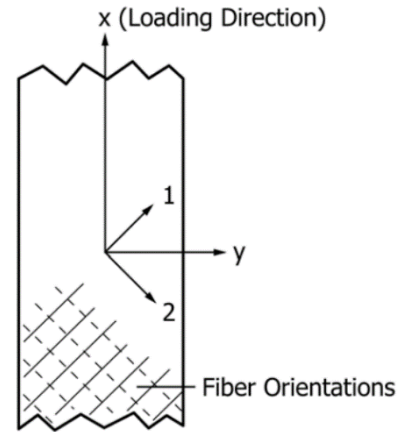


Figure 23: Fiber orientation for in plane shear testing.

#### Maximum shear

$$T_{12}^m = \frac{P^m}{2A} \quad (6)$$

#### Shear Modulus ( $G_{12}$ )

$$G_{12}^{Chord} = \frac{\Delta\tau_{12}}{\Delta\gamma_{12}} \quad (7)$$

### 2.6.3. COMPRESSIVE TESTING OF COMPOSITES

A straight sided specimen with a fiber orientation parallel to the loading direction is compressed until failure. The ratio between thickness of the specimen and the height must be sufficient to prevent buckling. The following formula calculates the minimum specimen thickness (15).

$$h \geq \frac{l_g}{0,9069 \sqrt{\left(1 - \frac{1,2F^{cu}}{G_{xz}}\right) \left(\frac{E^f}{F^{cu}}\right)}} \quad (8)$$

By doing compression testing, the following material properties can be obtained, for the given test direction:

- Ultimate compressive strength

### Ultimate compressive strength

$$F^{cu} = \frac{P_f}{wh} \quad (9)$$

## 2.7. PARAMETERIZATION SOFTWARE

---

Isight is an open system software that helps the user to combine different software applications to automate the execution of multiple simulations. By placing the software applications in a chronological order according to the simulation process, Isight can open the different software programs, run the simulation, and pass information along the chain to the next program. Isight has built-in optimization algorithms, the chain can be looped and Isight can iterate on a set of given parameters to see how this affects the output. This allows the user to save time, and improve the product by optimizing design by iterating the chosen variables.

Isight has built in functionality to work with a lot of different software. Some of the most common software programs are listed below:

- Python
- Excel
- Matlab
- Abaqus
- Catia
- Solidworks
- Word
- Mathcad

Isight also have some built in functions which is used to manipulate the data input or output from other computer programs. Both the data exchanger and the OS command has been used in this thesis. The functionality of these applications is described below.

### Data exchanger



The Data exchanger is a component within Isight that can be added to a loop. The optimization algorithm in Isight can use the data exchanger to update the input values to the simulation.

### OS command



A component that makes it possible to run the command prompt through Isight. By utilizing this component, you can run program that Isight normally doesn't support.

### 2.7.1. OPTIMIZATION ALGORITHM

---

Isight uses mathematical optimization algorithms to make iterations based on the design variables. There is a lot of different algorithms that is suitable for different types of optimization purposes. The different algorithms use different approaches to find local minima or local maxima.

Good design practice when designing an optimization program is to keep the number of variables to a minimum. This will make it easier for the optimization program to find the local maxima / local minima.

#### **Evol Optimization Algorithm**

Evol is an evolution based algorithm based on the works of Rechenberg and Schwefel. The algorithm mutates designs by adding a normally distributed random value to each design variable. The mutation strength is self-adaptive and changes during the optimization process(16).

## 3. TESTING TEXTREME WITH RENLAM M1

### 3.1. MOULD PREPARATION

The samples were moulded on a flat steel plate. To maintain a good surface finish and make the samples easy to demould, it is important to have a proper surface finish on the mould. This mould was prepared in the following way.

- 1) Deep surface scratches were removed by sanding using sandpaper with decreasing roughness from 40 to 2000. Figure 24 illustrates sanding of the mould with rough sandpaper.



Figure 24: Sanding to remove surface scratches

- 2) After sanding, the mould was properly cleaned with isopropanol three times with an interval of 15 minutes between each session.
- 3) 6 layers of Chemlease 712 EZ (sealer) were applied with 30 minutes between each coating.
- 4) 4 layers of Chemlease 2185 (release agent) was applied with a wipe-on/wipe-off technique.

### 3.2. LAY-UP

**Compression specimens:** Because the compression test required 18 layers of carbon fiber fabric, this laminate had to be produced separately. All layers had the same orientation and the difference between warp and weft were considered. The resin was applied to each fabric with a paint roller. For a compression test, good bonding between the layers is crucial. The laminate was therefore pressurized (debulked) for 1 minute every third layer.

**Tension and shear specimen:** These specimens only consist of three layers of carbon fiber, and there is therefore no need for debulking under production. All layers had the same orientation and the difference between warp and weft were considered.

### 3.3. CURING

The samples cured in room temperature with a pressure of 0,98 bar for 24 hours. After the 24 hours, the vacuum pump was shut off and the samples where post cured for 15 hours at 40°C.



Figure 25: Curing of laminates in room temperature

### 3.4. TEST SAMPLES

All the specimen samples were cut out of the laminate plate using a diamond saw. The respective cut out dimensions are shown in Figure 26.

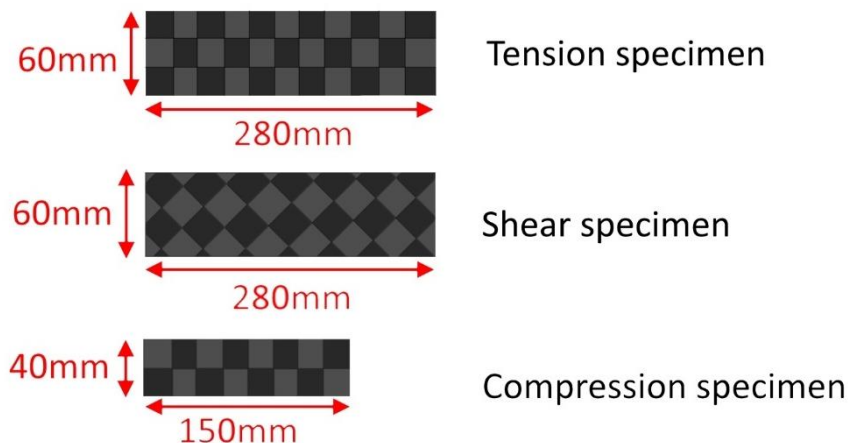


Figure 26: Specimen cut out size

### 3.5. CLAMPING TABS

In the ASTM standard it is recommended to use clamping tabs between the specimen and the clamping tool on the test machine. This will reduce the stress concentrations and give more accurate results. The material used for clamping tabs should have approximately the same stiffness as the

specimen, hence fiber glass tabs have been used in these experiments. They will have approximately the same stiffness in the clamping direction.

The tabs need to be properly attached to the specimen to make sure there is no slip between the specimen and the tab. Araldite 4858, a high strength epoxy two-component adhesive was used for this application. The tabs were slightly sanded and cleaned with isopropanol before the two parts were glued together and cured at 40°C for three hours.

Figure 27 and Figure 28 gives the dimensions of the clamping tabs used in this experiment. The tabs were cut out using a diamond saw, and for the specimen used for tension and shear testing, a 45° chamfer was made at the end to distribute the loads better from the clamp to the sample.

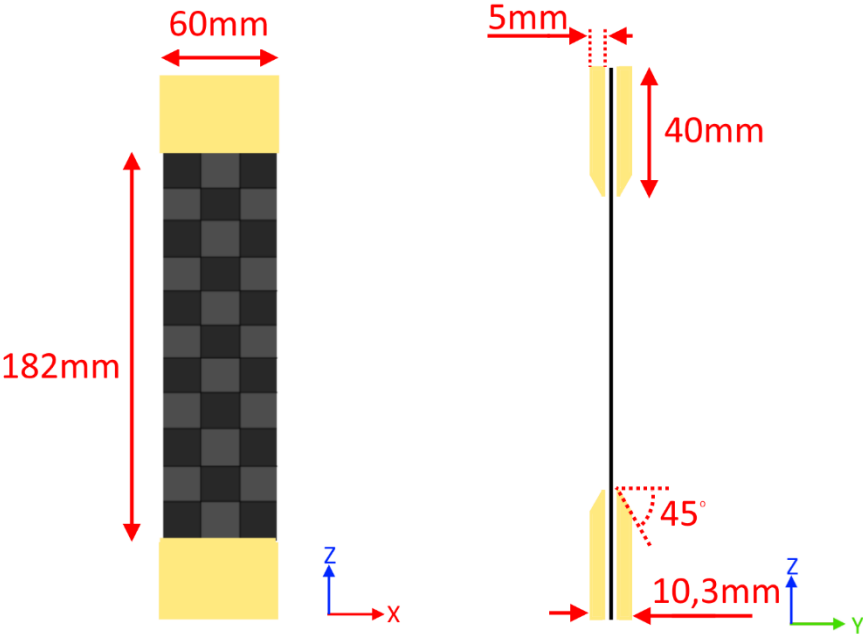


Figure 27: Tab dimensions for tension and shear specimen

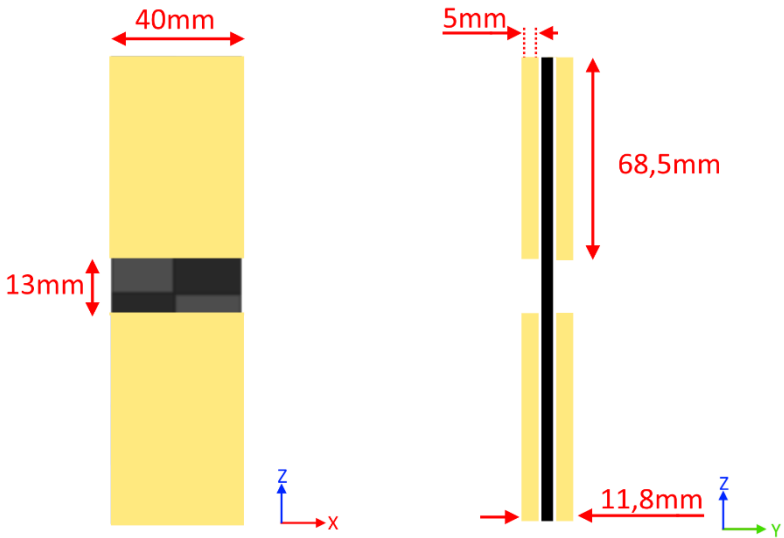


Figure 28: Tab dimensions for the compression specimens

### 3.6. TESTING

The main purpose of the material testing is to obtain a conservative estimate of the laminate constants for a combination of Textreme (76 gsm) and Renlam M1 resin. Abaqus uses the following laminate constants to simulate composite materials in plane stress.

$$E_1, E_2, \nu_{12}, G_{12}, G_{13} \text{ and } G_{23}$$

To use Tsai Wu as a failure criterion, the following laminate constants are needed.

$$X_T, X_C, Y_T, Y_C \text{ and } S_{12}$$

To limit the scope of this thesis, some assumptions had to be made. The difference between warp and weft is assumed to be negligible. All the tests of fiber in the longitudinal direction will therefore be tested in the weakest direction (weft). This assumption leads to the following assumption for the laminate constants.

$$E_1 = E_2$$

$$X_T = Y_T$$

$$X_C = Y_C$$

Further assumptions

$$\nu_{12} = 0,04$$

$$G_{13} = G_{12} * 0,4$$

$$G_{23} = G_{12} * 0,3$$

In plane, Poisson ratio  $\nu_{12}$  could be measured by attaching a horizontal strain gauge to the tension samples. However, this was not done due to lack of strain gauges. Finding the out on plane shear constants  $G_{13}$  and  $G_{23}$  would require separate tests. These constants have very little effect of the results and was therefore estimated.

All the testing where performed in the fatigue lab at IPM, NTNU. Specimen number 1, 2, 4, 5,8, 10 and 11 was equipped with a strain gauge. All the strain gauges used in this experiment had a gauge factor of 2.13

All the specimen where properly measured by a calliper before testing was started. The dimensions of the specimen samples are listed in Table 1, Table 2 and Table 3. For the compression specimen, there have been listed four lengths between the tabs, these are measured in each corner. This is due to nonalignment between the tabs.

Table 1: Dimensions for tension specimen

Tension					
Specimen number	Width top [mm]	Width bottom [mm]	Length between tabs [mm]	Thickness [mm]	Cross sectional area [mm <sup>2</sup> ]
1	57.24	57.35	182.91	0.3	17.1885
2	59.01	58.85	186.37	0.3	17.679
3	58.98	58.87	186.36	0.3	17.6775
4	58.93	59.05	183.13	0.3	17.697

Table 2: Dimensions for shear specimen

Shear					
Specimen number	Width top [mm]	Width bottom [mm]	Length between tabs [mm]	Thickness [mm]	Cross sectional area [mm <sup>2</sup> ]
1	57.96	58.42	181.51	0.3	17.457
2	58.78	59.3	181.32	0.3	17.712
3	59.65	58.85	176.5	0.3	17.775
4	59.2	58.44	180.67	0.3	17.646

Table 3: Dimension for compression specimen.

Compression						
Specimen number	Width top [mm]	Length between tabs 1 [mm]	Length between tabs 2 [mm]	Length between tabs 3 [mm]	Thickness [mm]	Cross sectional area [mm <sup>2</sup> ]
1	39.12	13.7	12.3	13.56	13.42	70.416
2	38.85	13.36	13.78	13.28	12.86	69.93
3	40.39	12.95	13.11	12.89	13.26	72.72
4	38.95	13.1	13.5	12.77	13.52	70.11

### 3.6.1. TEST SETUP FOR TENSION TESTING

A total of four specimens were tension tested with a speed of 2 mm/min. The Experimental setup is shown in Figure 29. To ensure the sample is orthogonal to the loading direction an alignment tool was used. Specimen 1,2 and 4 had a strain gauge mounted in the geometrical center on the smooth mould side of the specimen.



Figure 29: Experimental setup for tension testing

### 3.6.2. TEST SETUP FOR SHEAR TESTING

Four shear specimens were tested with a speed of 2mm/min. The experimental setup is shown in Figure 30. As for the tension test, an alignment tool was used to align the test sample with the loading direction.



Figure 30: Experimental setup for shear testing

### 3.6.3. TEST SETUP FOR COMPRESSION TESTING

A total of four compression tests were performed at a speed of 2 mm/min. Figure 31 shows how the test sample is clamped in at the bottom. Before the test is started, the upper part comes down and clamps around the specimen tabs. Because the compression samples are too short, the alignment tool couldn't be used and the specimen was therefore adjusted by eye. Specimen number 10 and 11 were fitted with a strain gauge at the geometrical center of the smooth side of the samples.

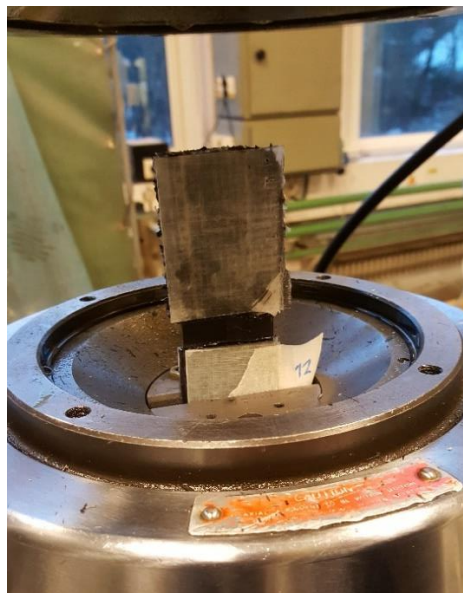


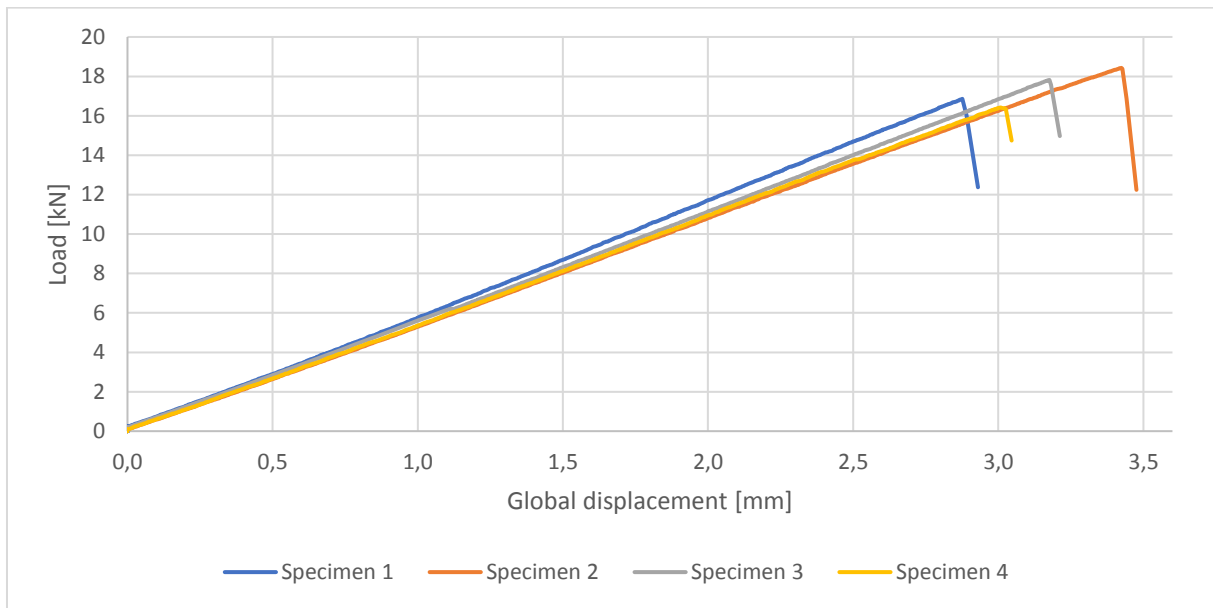
Figure 31: Experimental setup for compression test

### 3.7. TEST RESULTS

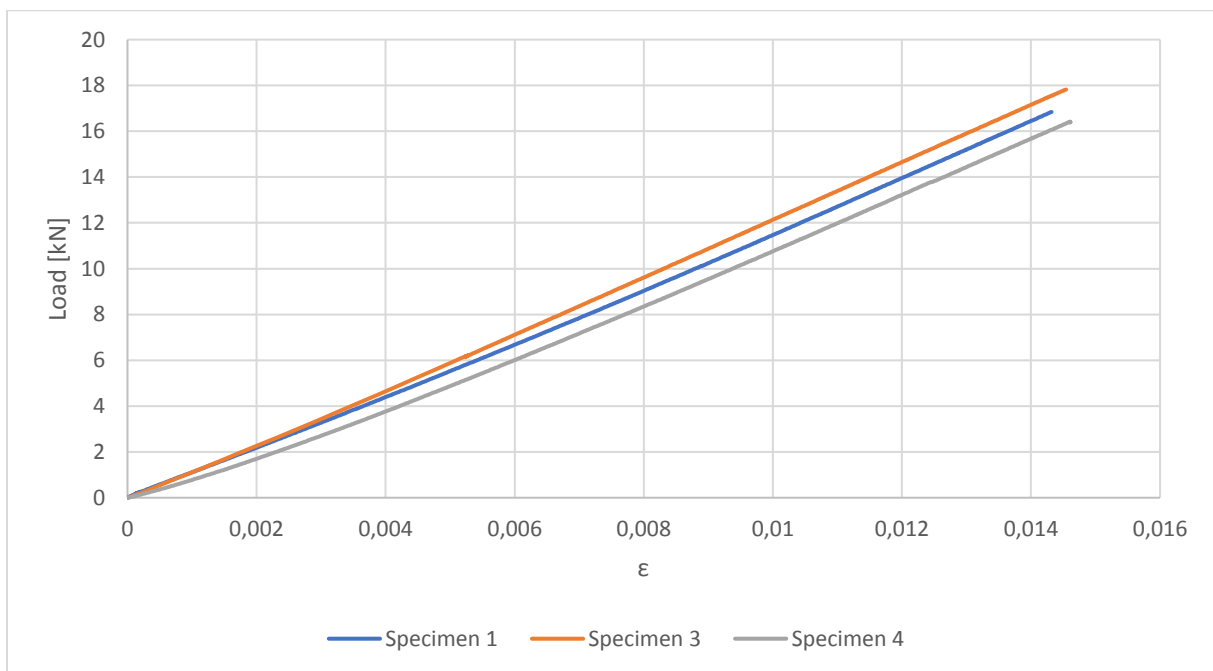
Because there were so few tests (less than 5 which is suggested by the ASTM standard) the average between the different tests was used to find the laminate constants. In many cases it is useful to use the worst results as laminate constants to be on the safe side.

#### 3.7.1. TENSION RESULTS

The load displacement curve for the tension samples are given in Graph 1. This graph illustrates that there is a spread between the maximum load and maximum strain. Graph 2 plots the load vs strain from strain gauge.



Graph 1: Load vs global displacement for Tension testing



Graph 2: Load vs strain for tension

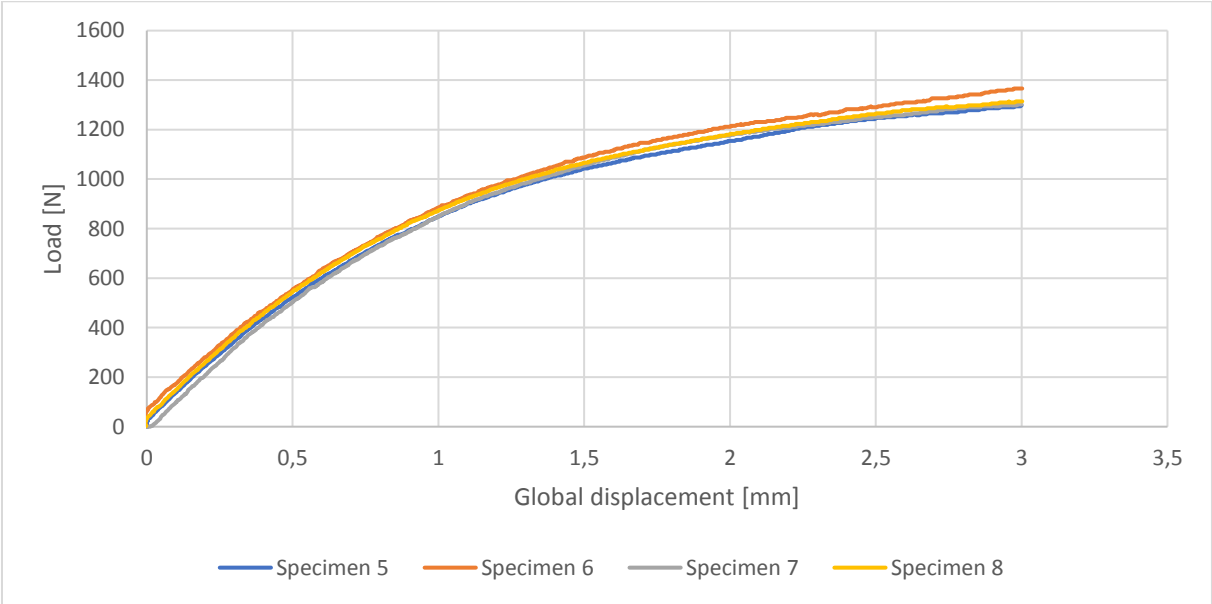
By using the values obtained from the test in equation (8) and equation (9), the laminate values in Table 4 was calculated.

**Table 4: Calculated laminate values for tension testing**

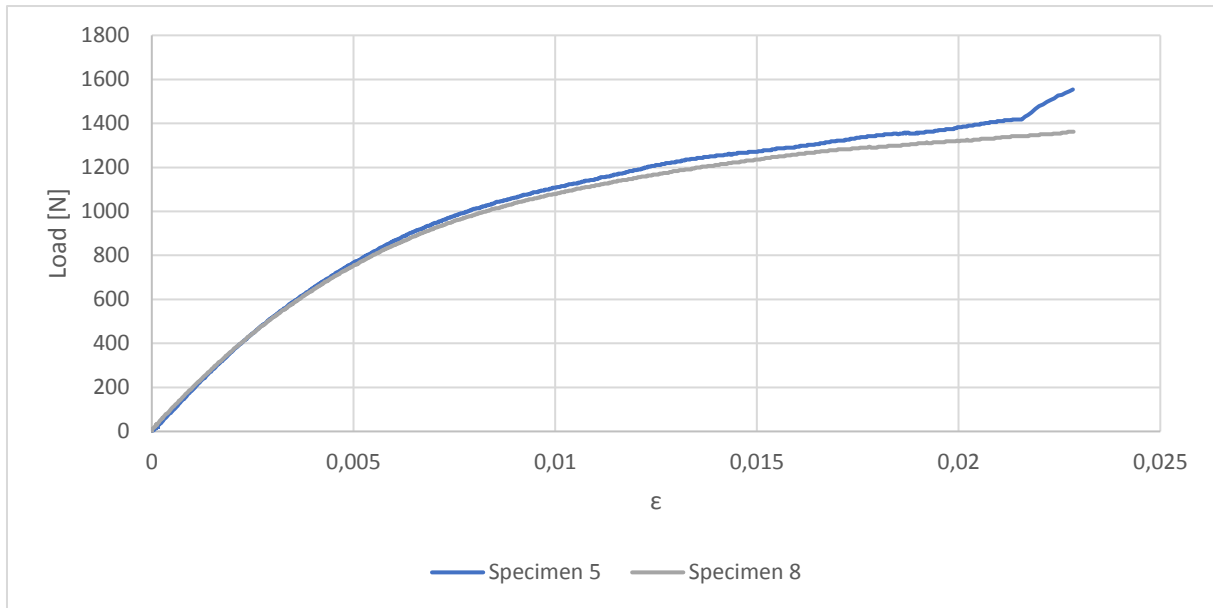
Tension results			
Specimen number	Maximum load [N]	Ultimate strength [Mpa]	Youngs modulus [Gpa]
1	16860	980.89	68.50
2	18430	1042.48	
3	17820	1008.06	69.31
4	16420	927.84	63.49
Average	17382.5	989.82	67.1

**3.7.2. SHEAR RESULTS**

The load displacement curve for the shear samples are shown in Graph 3. This graph is only from 0 to 3mm displacement. Graph 3 plots the load vs strain.



**Graph 3: Load vs global displacement for shear samples**



Graph 4: Load vs strain for specimen 5 and 6

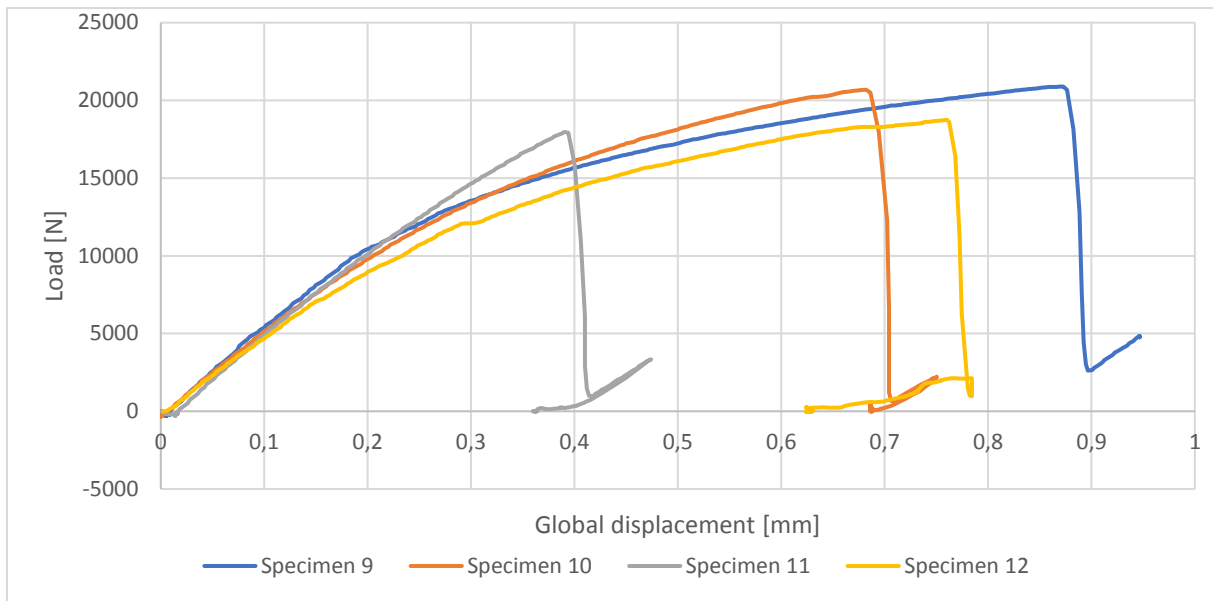
Using the values obtained from the experiment and combining them with equation (12) and Equation (13), an estimated value for maximum share and shear modulus  $G_{12}$  was found. The laminate constants calculated from the test can be seen in Table 5.

Table 5: Calculation of material properties in shear

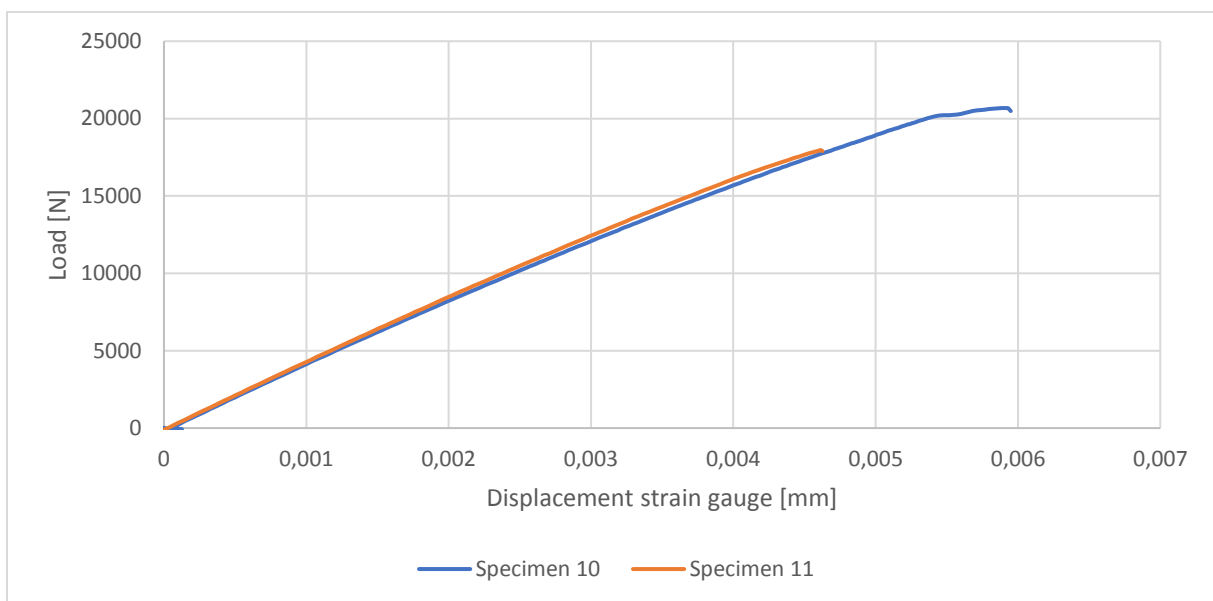
Shear results			
Specimen number	Maximum load [N]	Ultimate strength [Mpa]	Youngs modulus [Gpa]
6	1298	53.9	3563.68
6	1366		
7	1302		
8	1314	50.61	3375.78
Average	1320	52.26	3469.73

### 3.7.3. COMPRESSION RESULTS

The global load displacement curve is plotted in Graph 5. This graph illustrates the load vs displacement for the four compression tests. Graph 6 plots the relation between load and strain from the strain gauge.



**Graph 5: Load vs global displacement for compression samples**



**Graph 6: Load vs strain gauge displacement for specimen 10 and 11**

Using the data from the compressive tests and combining them with equation (11), the constants in Table 6 was calculated.

**Table 6: Calculation of material properties for compression samples**

Shear results		
Specimen number	Maximum load [N]	UTS comp [Mpa]
9	20890	296.67
10	20680	295.72
11	17970	247.17
12	18750	267.43
Average	19573	276.75

3.7.4. SUMMARY TESTING RESULTS

---

By conducting these experiments, material constants for a combination between Textreme (76 gsm) and Renlam M1 resin was found. Table 7 summarizes the laminate constants and summarizes the failure stress.

Table 7: Summary calculated material constants

	E1 [Mpa]	E2 [Mpa]	v12	G12 [Mpa]	G13 [Mpa]	G23 [Mpa]	X <sub>T</sub> [Mpa]	X <sub>C</sub> [Mpa]	Y <sub>T</sub> [Mpa]	Y <sub>C</sub> [Mpa]	S <sub>12</sub> [Mpa]
Textreme	67100	67100	0.04	3470	1388	1041	990	277	990	277	52

## 4. BLADDER MOULDING (CONCEPT 1)

This beam was produced at Kitemill's production facilities. The procedure described in this chapter is the exact same procedure as they use when producing the horizontal stabilizer beam for the 30kW prototype glider. It is also the same materials which is a combination between Textreme (76 gsm) and Renlam M1 epoxy. A total of two samples was made with this method.

The mould used was a two-piece closed mould milled out of solid aluminum. The bottom part of the mould was threaded, so bolts can pass through the top part and clamp the two pieces together. This concept of a closed mould is illustrated in Figure 32. The tricky part with a closed mould is to generate pressure to the composite to press it against the mould.

In this case a bladder moulding technique was used to generate pressure on the composite. This technique involves laying the composite around a bladder then close the mould. In this case a bicycle tire was used as the bladder. When the mould is fully closed and all the bolts are tightened the bicycle tire gets filled up with pressurized air. This pressure will generate pressure against the composite laminate, which helps distributing the epoxy.

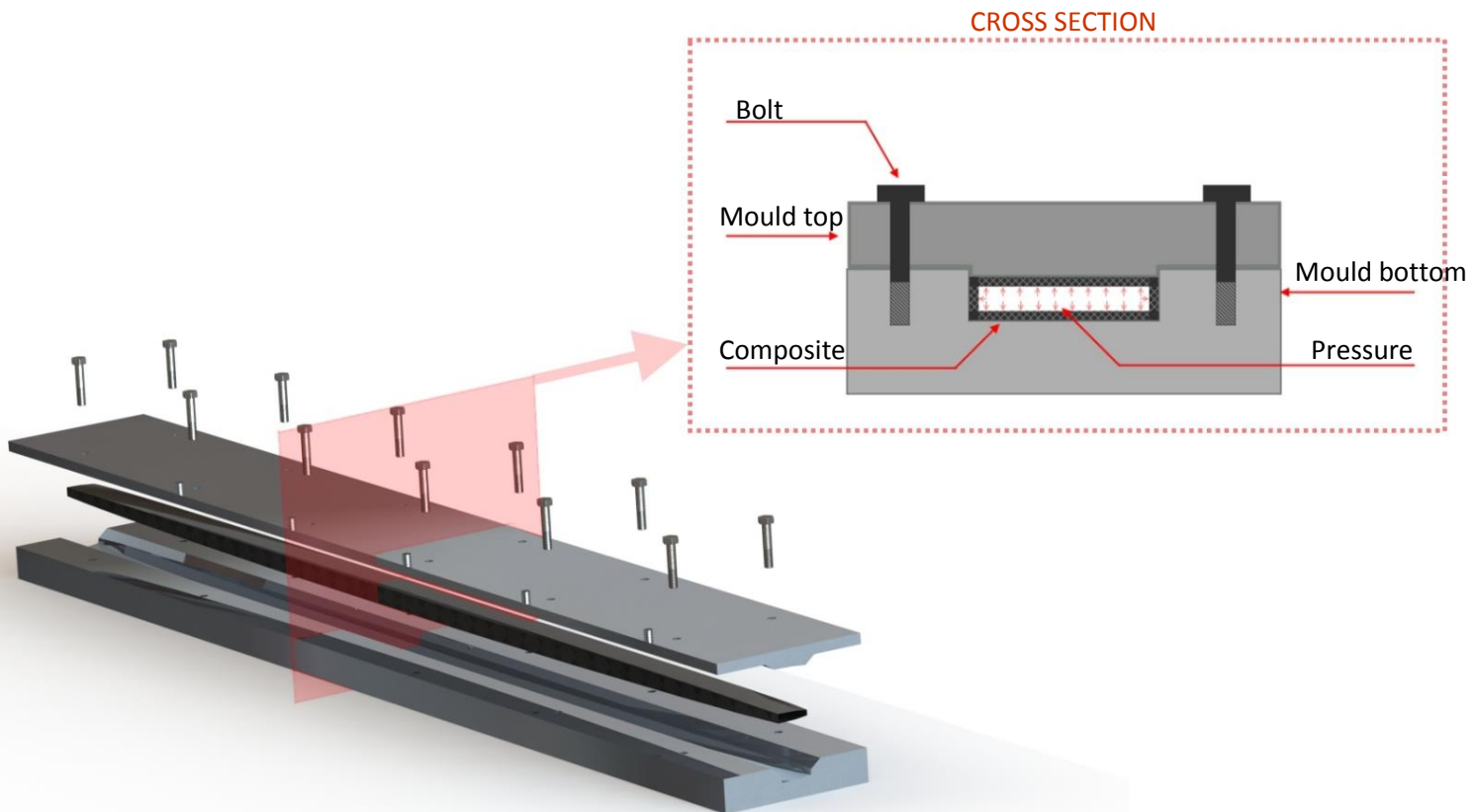


Figure 32: The concept of a closed mould

## 4.1. MOULD PREPARATION

Good preparation of the mould is important to be able to demould the composite part without any complications. This was done by first cleaning the excess epoxy and dust with methylated spirit. After cleaning, four separate layers of release coating was added to the mould. The mixture between beeswax and ethanol was applied with a clean cloth covering all the surfaces that was going to be in direct contact with the composite. A wipe on / wipe off technique was used with 20 minutes drying time between the four layers. The process of applying release coating is illustrated in Figure 33.



Figure 33: Process of applying release coating

## 4.2. CUTTING THE TEXTREME WEAVE

When dealing with wet lay-up of composites, time is crucial, because of the short curing time of the epoxy. Therefore, all the Textreme carbon fiber was cut and organized into lay-up sections before mixing the two component epoxy. The carbon fiber was cut using a wheel cutter and a ruler. Textreme has a special way of adding binder to the weave that prevents the material from flaring after cutting. This makes this material ideal for parts like this with a quite complex geometry. Figure 34 illustrates the anti-flaring properties of Textreme. Each spar consists of eight strips of carbon fiber measuring 30mm x 1300mm with an 0/90 orientation and 4 strips measuring 120mm x 1300mm with an +45/-45 orientation. This adds up to a total of 0.936m<sup>2</sup> of weave in the part, which is equal to 80g.

The Textreme fabric used had a quite rough weave where both the warp and the weft tow have a width of 20mm. It was noticeable while cutting that the strips with 30mm width had less resistance to flare than the wider strips.



Figure 34: The anti-flaring properties of textreme



Figure 35: Cutting the width

Because the strips were thinner than the width of the unit cell of the material, the weave wasn't braided properly together anymore. This problem can be seen in Figure 35.

### 4.3. WET LAY-UP OF CARBON FIBER

The epoxy used in this build is a combination of the Renlam M1 resin and Ren HY 956 hardener. The mixing ratio was 20g hardener for every 100g of resin. These two components were mixed together by hand for two minutes. After mixing, a single drop of black color was added to the mixture. The color made it easier to see by eye if the resin is distributed evenly in the laminate

First a thin film of epoxy was applied as a thin film to the mould. The idea is that this film makes a good surface finish on the product. The precut strips of carbon fiber were placed on a flat clean surface. A paintbrush was used to apply resin to the weave and a spatula was used to evenly distribute the resin within the weave. Figure 36 shows the epoxy being distributed into the weave on the 120mm x 1300mm +45/-45 strips. When distributing the resin with the spatula onto the thin strips, the tows showed a tendency to split.

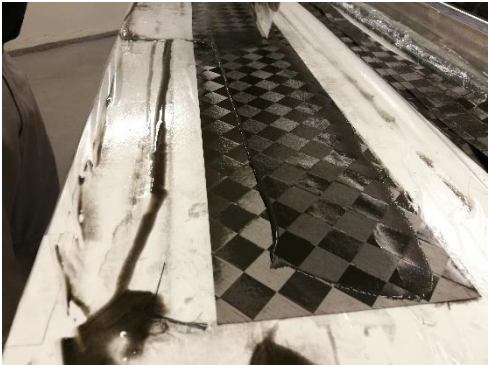


Figure 36: Coloured epoxy distributed on the weave with a spatula

### 4.4. STRUCTURE OF THE LAY-UP

When a bladder moulding technique is used the lay-up, time is critical. The epoxy has a short gel time, and all the strips of carbon fiber needs to be impregnated by hand before going into the mould. Because of this the lay-up is the same for every cross section along the length of the mould. The lay-up used in this spar is illustrated in Figure 37. The sequence of this lay-up is in chronological order from A – N where A is the first layer to be placed into the mould. Since it is a two piece mould, both the M and N layer was placed on the top part of the mould.

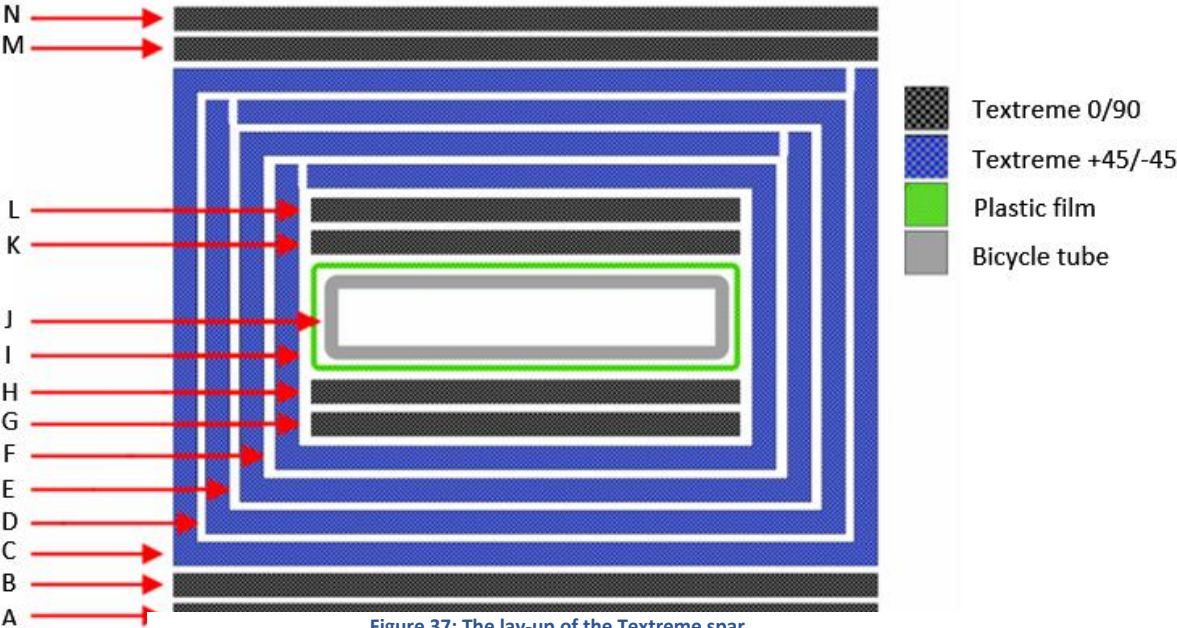


Figure 37: The lay-up of the Textreme spar

The carbon fiber strips were carefully peeled off the table and placed into the mould. Because the spar is a three-dimensional shape were the cross-sectional perimeter varies along the length, some of the square pieces didn't fit well into the mould. Figure 38 shows that layer square geometry of layer C, D, E and F doesn't fit properly near the ends of the mould. This problem was solved by folding double layer on the top of the spar near the ends. Figure 39 shows the bladder in the mould.



Figure 38: Lay-up process of the carbon fiber



Figure 39: The bladder in the mould

## 4.5. CURING

After lay-up, the first step was to make sure that the mould is properly closed and the bolts are pre-tensioned. The Bicycle tube was equipped with a valve in one end and sealed in the other end. The concept of the bicycle tube can be seen in Figure 40.



Figure 40: Mould after lay-up with bicycle tube and valve

Originally, the idea was to fill the bicycle tube with a pressure of 7 bar, but since the ends of the mould had an open-end design, the bicycle tube grew out of the mould and exploded when the pressure exceeded 2 bar. Therefore the Textreme spars were cured under a maximum pressure of 2 bar. Figure 41 illustrates the problem and a potential design change. When pressure was applied, the mould was heated to 40 °C for 14 hours.

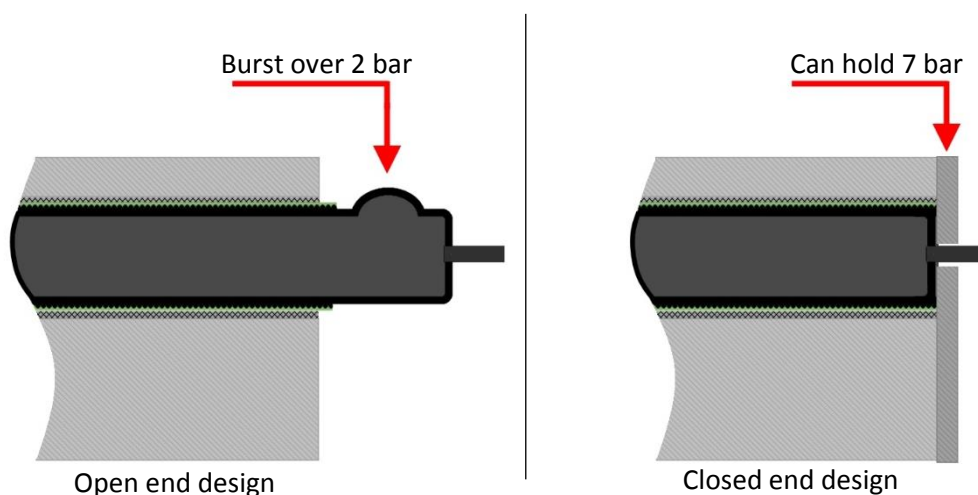


Figure 41: Open vs closed design. The illustration shows how the bicycle tube burst in an open-end mould

#### 4.6. DEMOULDING

---

The demoulding was done after the aluminum had cooled down to room temperature. This was done by first depressurizing the inflatable bicycle tube and cutting of the vent with a scissor. By removing the vent, the tube is small enough to pass through the inside of the hollow spar. The plastic film was still stuck in the laminate, but this thin film didn't add more than 2g of extra weight. The top part of the mould was removed, and pressurized air was used to separate the composite from the mould and demould the spar.

#### 4.7. RESULTS

---

Two spars were made with this method. Both samples seem to show a trend of dry spots on the outside, this could be due to lack of resin or poor pressure. Because the carbon fiber content was weighed before adding epoxy, it was possible to calculate the weight fraction of carbon in the final product for both samples.

The weight of the Textreme samples was:

Sample 1: 173,6g

Sample 2: 182,2g

The total weight of carbon fiber for each spar was 80.5g which gives a total of 93.1g resin in sample 1 and 101,7g of resin in sample 2.

The surface finish of these samples contained big craters. These craters can be seen in Figure 42. Both sample 1 and sample 2 had this kind of surface finish.



Figure 42: The craters on the surface

#### 4.8. 3-POINT BENDING TEST

---

It is difficult to find an accurate test method for the spar, because the lift distribution of the wing is an elliptical shape. However, A three-point bending test will have a rectangular distribution which is very similar. Figure 43 illustrates the wing with a load profile of three-point bending. The 3-point bending test is also easy to set up and cheap to perform. It was therefore chosen as the test method to verify the results in this thesis.

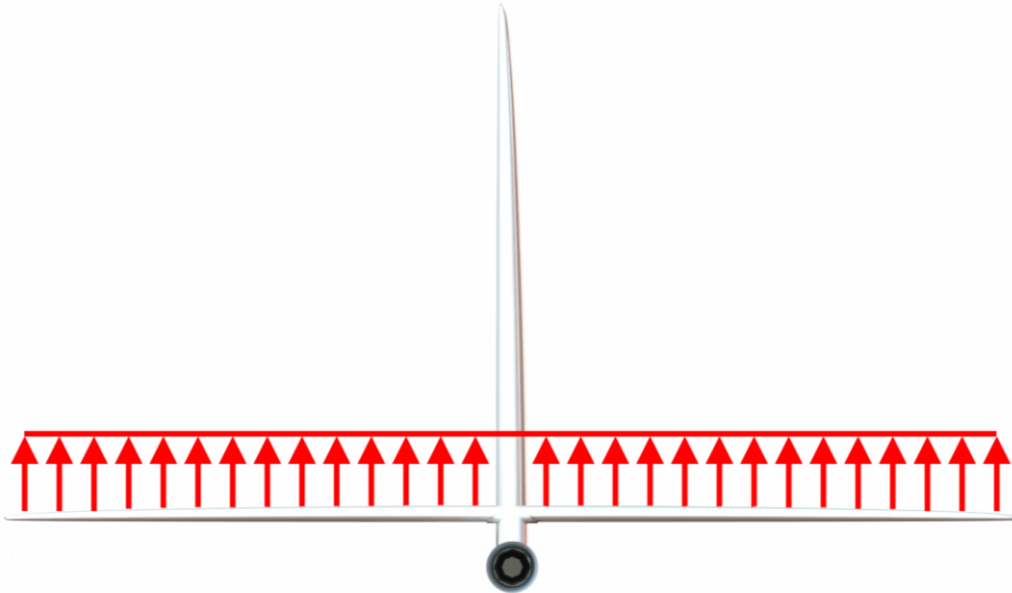


Figure 43: Load distribution with three-point bending.

The maximum load before failure was going to be found by physical testing before the benchmark load was set in the optimization program. Time constraints made this difficult and the benchmark loading therefore had to be estimated by simulation.

A parametric optimization was set up for this purpose. The target of this optimization was to find the load that was equal to a "Maximum stress" value of 1. This was a rather quick simulation to set up and run, and after a short time the failure load was found to be 360N.

## 5. OPTIMIZATION OF COMPOSITES

This chapter describes the process of making an optimization program for composites in Isight. The goal for this lay-up was to build a compression moulded sample that can take the same load as the original, but with less weight.

As described in chapter 2.7, Isight doesn't support iterative optimization of composites. This means that you must use programming and creativity to make an optimization loop that can iterate composites.

Two different methods were tested. The foundation for both methods was the macro function in Abaqus. The lay-up iteration was done by manipulating the macro input file and importing it into Abaqus using Isight. One of the methods used the data exchanger to manipulate the macro and the other method used a combination of Excel, Python and OS command.

### 5.1. BUILDING A FEA MODEL IN ABAQUS

In Isight, the user first builds an Abaqus model for a single simulation. The parameters that are going to be optimized are set as input to the simulation, and a field output is set as a result. Isight evaluates the result from each simulation and uses the optimization algorithm to decide the input for the next simulation. This is a process that requires a lot of computational power. Therefore, it was a high priority to reduce the computational power requirement for this simulation.

As described in chapter 2.2.2, the load distribution on an airfoil has an elliptical shape. This load distribution is difficult to duplicate when it comes to practical testing. Because of this, it was decided to test and simulate the samples in a three-point bending test.

#### 5.1.1. SYMMETRY CONDITIONS

The spar is symmetric about the cross-sectional plane in the length direction. The idea was to use this symmetry to only do simulations of half of the spar and save a lot of computational power. The symmetry plane is illustrated in Figure 9.

A normal three-point bending case is illustrated by Figure 45. Here the load is applied to the centre of the test sample. Figure 44 illustrates a way to do simulation on half of the beam. A simulation to verify both cases was performed and the results were different so all the simulations in this thesis were carried out without symmetry.

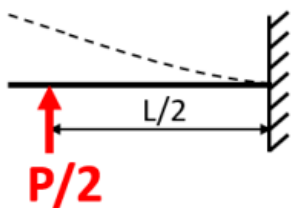


Figure 44: Three point bending with symmetry

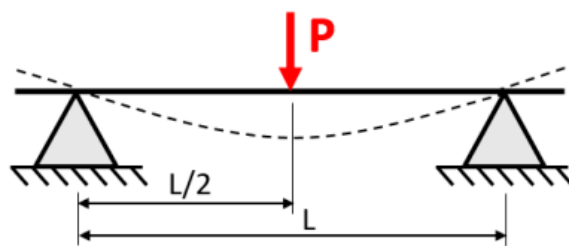


Figure 45: Conventional three-point bending setup

### 5.1.2. MATERIAL PROPERTIES AND DEFINITIONS

Two different materials were used for simulations. The laminate constants for the Textreme 76 gsm fiber was found by material testing (chaptre r4.7). The laminate constants for Hexply 6376 was provided by Kongsberg Defense and Aerospace. The material laminate constants and the failure stress for both materials can be found in Table 8.

Table 8: Material data for the two different materials

	E1 [Mpa]	E2 [Mpa]	$\nu_{12}$	G12 [Mpa]	G13 [Mpa]	G23 [Mpa]	X <sub>T</sub> [Mpa]	X <sub>C</sub> [Mpa]	Y <sub>T</sub> [Mpa]	Y <sub>C</sub> [Mpa]	S <sub>12</sub> [Mpa]
Textreme	67100	67100	0.04	3470	1388	1041	990	277	990	277	52
Hexply 6376	67000	67000	0.05	2840	1000	1000	1006	900	1006	900	100

The definition of the material orientation is given by Figure 46. The 0° direction is axial and the 90° direction is circumferential to the body. The material offset direction is towards the center of the spar.

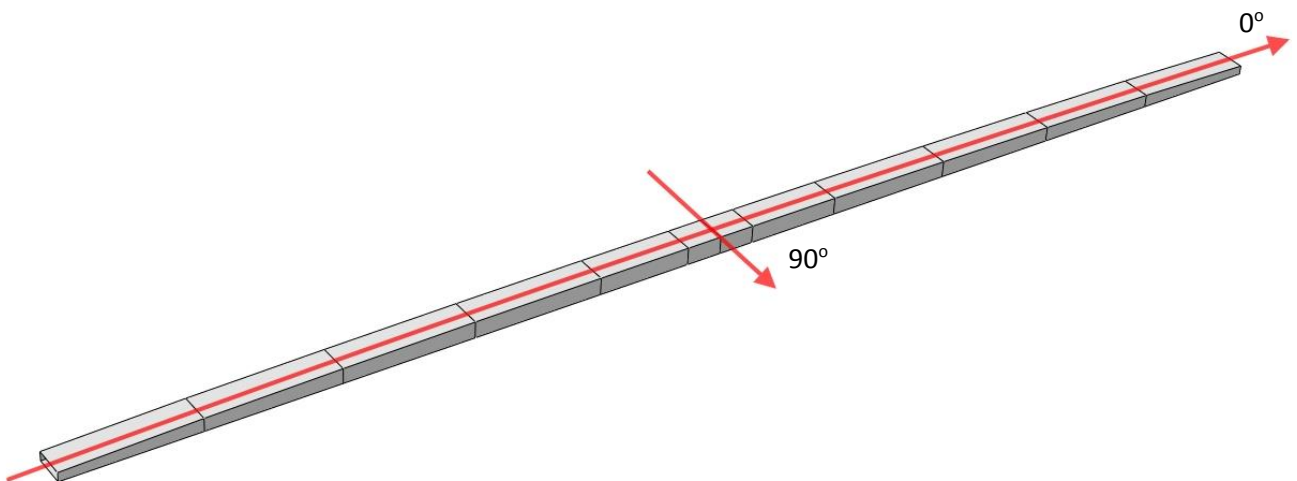


Figure 46: The definition of the material orientation of the Spar

### 5.1.3. INTERACTION

When contact is introduced in Abaqus, the problem becomes highly nonlinear. Which means that the simulation requires more computational power. Because of this, the roller supports were exchanged with boundary conditions and the applicator was exchanged with a point and a kinematic coupling. The loading point (RP-1) and the kinematic coupling are illustrated in Figure 47: The Kinematic coupling from RP-1 to the center of the spar. The kinematic coupling was chosen because the applicator distributes the forces evenly over the spar when testing. The distance from RP-1 to the spar is 10mm which is the same as the diameter of the load applicator.

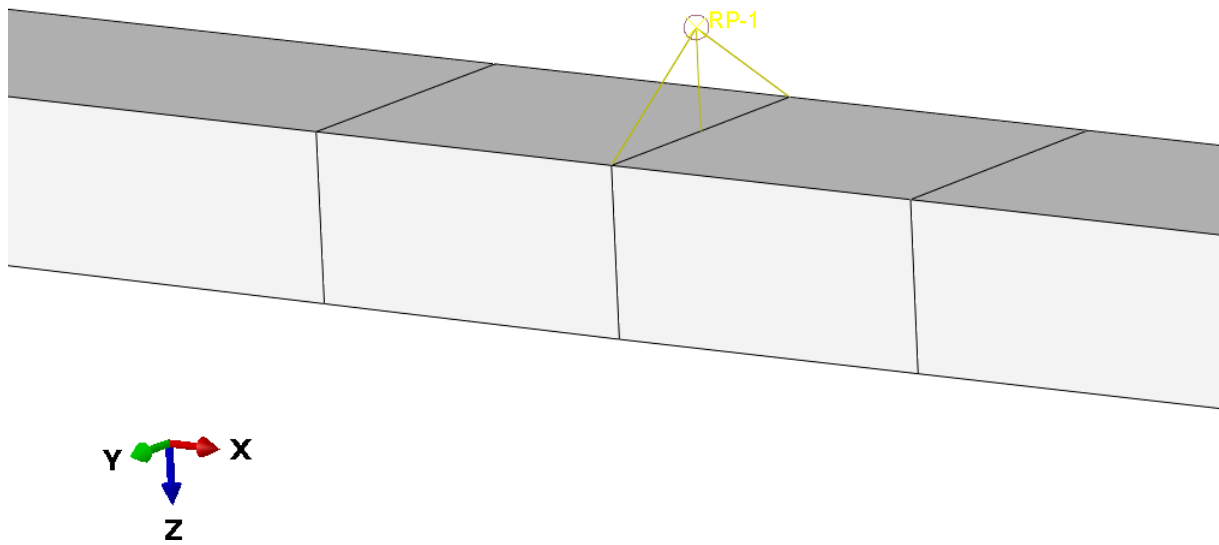


Figure 47: The Kinematic coupling from RP-1 to the center of the spar.

#### 5.1.4. BOUNDARY CONDITIONS

To avoid contact, boundary conditions was used at the contact point between the spar and the roller supports. The contact point can be seen in Figure 48. Referring to the coordinate system in the same figure, the boundary conditions for the roller supports was set to.

$$Y = 0$$

$$Z = 0$$

$$R_x = 0$$

$$R_z = 0$$

The boundary condition for the roller supports was applied to both sides of the spar.

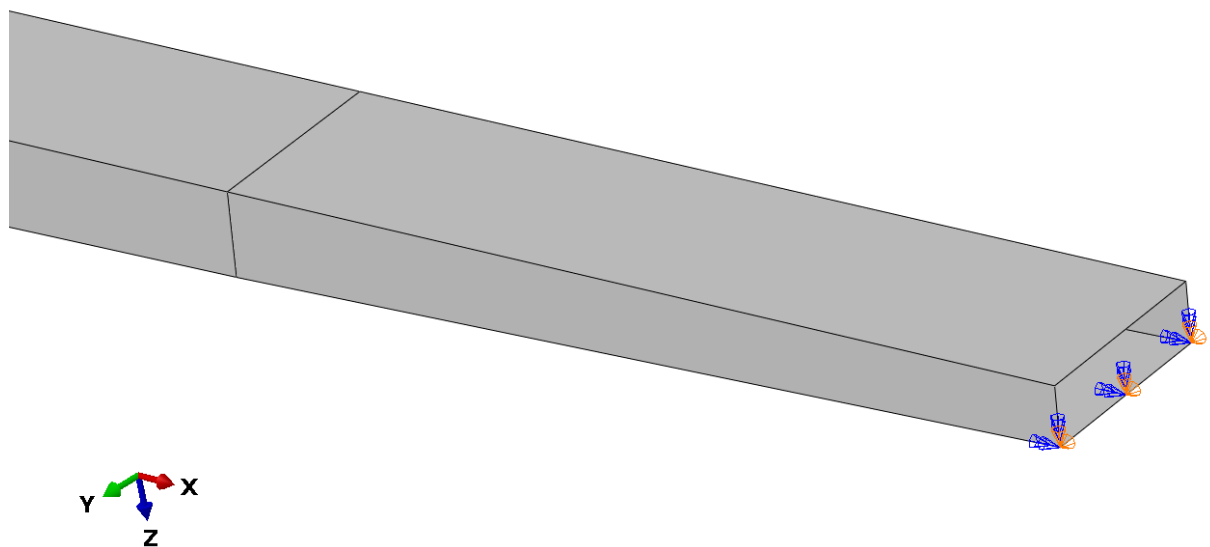


Figure 48: The boundary conditions on the roller support

#### 5.1.5. STEP AND LOADING

---

The simulations were set as a static general simulation. In this type of simulation all the inertia effects are ignored. The loading was a ramped load acting of the RP-1 point in the positive Z direction.

#### 5.1.6. SIMULATION ON A COMPRESSION MOULDED SAMPLE

---

The Texteme sample is a thin walled hollow structure. This means that this sample is suited for a conventional shell simulation. The Hexply sample was going to be compression moulded which means that there is a core material inside the composite. The core material was imported into Abaqus as a solid and the conventional shell was added to the surface of the solid using the “create skin” tool in Abaqus.

The core material used was Rohacell IG-F 71. It was given isotropic behavior with a young’s modulus of 1.5 and a Poisson’s ratio of 0.3.

#### 5.1.7. MESH

---

##### **Textreme sample:**

Total number of nodes: 1410

Total number of elements: 1400

- 1400 linear quadrilateral elements of type S8R (Texteme 76 gsm)

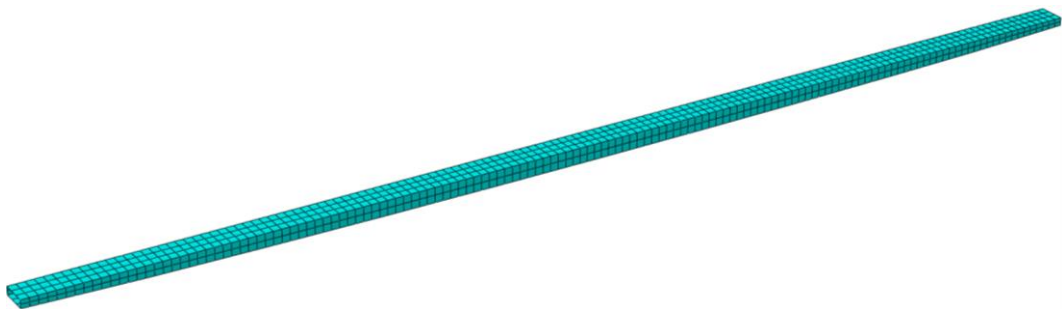


Figure 49: Documentation of mesh quality for Texteme simulation

##### **Hexply sample:**

Total number of nodes: 1692

Total number of elements: 2252

- 1412 linear quadrilateral elements of type S8R (Hexply 6376)

- 840 linear hexahedral elements of type C3D8R (Rohacell IG-F 71)

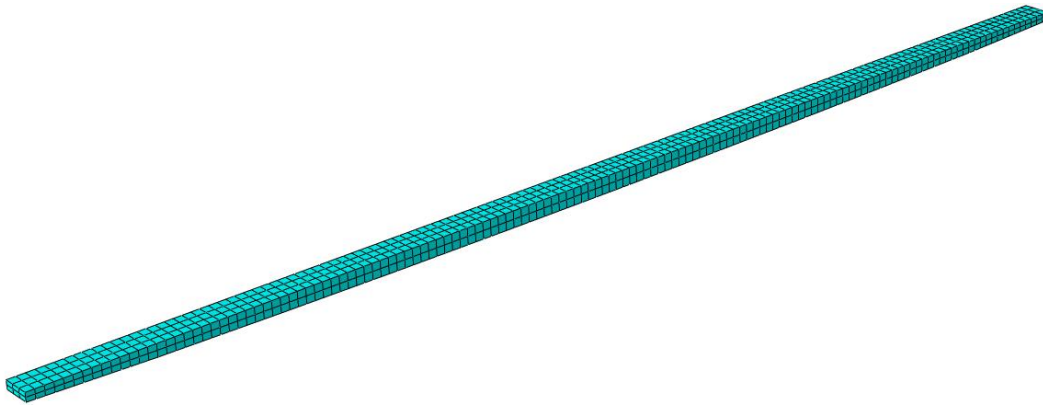


Figure 50: Documentation of mesh quality for Hexply simulation

A mesh convergence test was performed to decide number of elements. The results of the mesh convergence test can be seen in Figure 51. From this figure, the mesh is converging close to 1400 elements

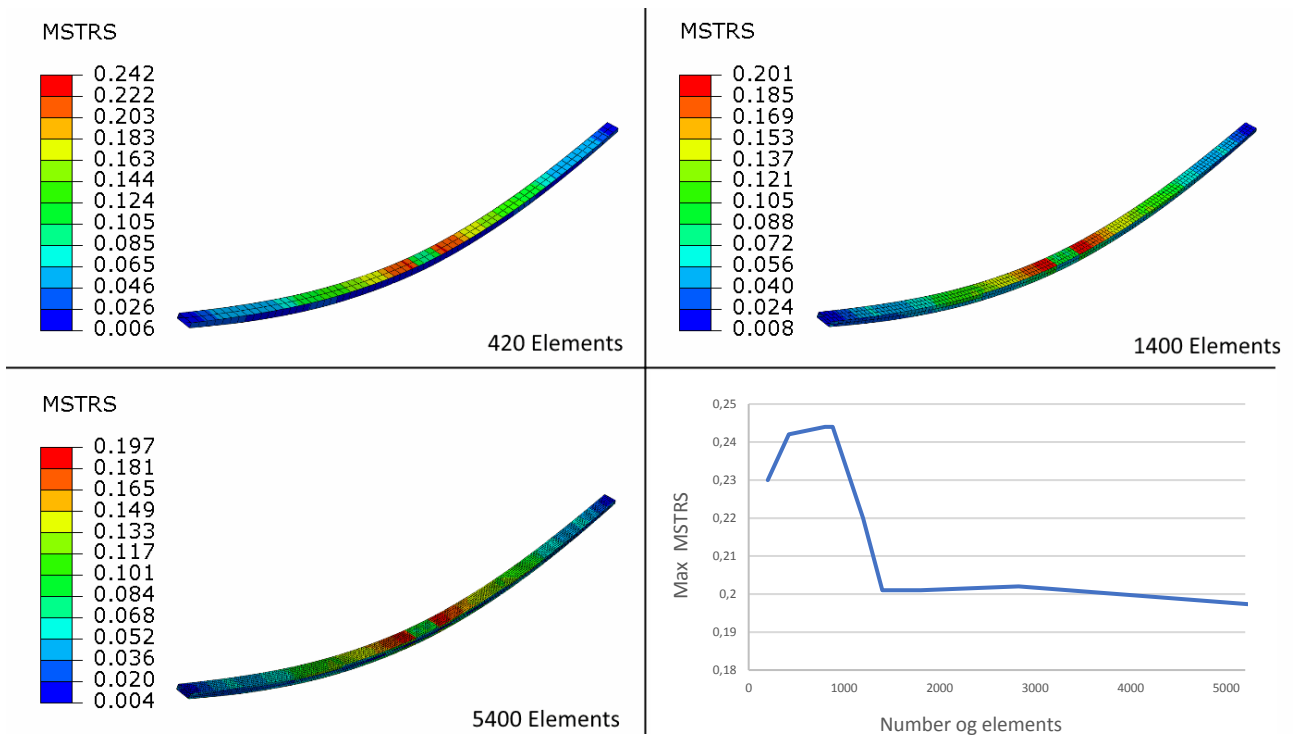


Figure 51: Mesh convergence test

## 5.2. LAY-UP ZONES

The spar was divided into 24 different sections. These sections were assigned to a “set” in Abaqus. Each of these sets could have a unique number of plies and each ply could have a unique orientation angle. The idea behind this was that the number of plies will be higher in the areas with high stress when looping the simulation. To make it easier to interpret the results it was necessary to make a notation system of all the different lay-up zones. This was done by naming the four different sides of the beam respectively TOP, BOT, SIDEF and SIDEB. Further, the beam was divided into 12 zones in the length (6 because of symmetry). The length of the zones is marked with green in Figure 52. These zones were given a number ranging from 1-6 where 1 is the zone closest to the symmetry plane. Figure 52 illustrates the notation system of the different zones on the beam. All the combinations within the symmetry plane are listed in Table 9. The “TOP” side of the spar will be under compression when the spar is loaded in what is believed to be the worst-case scenario.

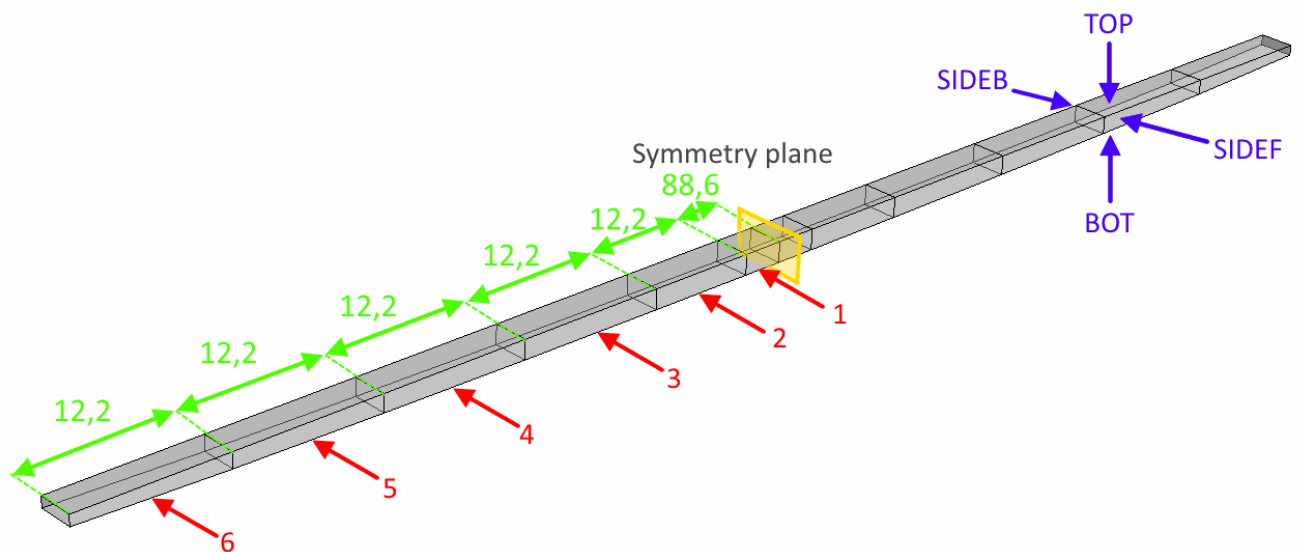


Figure 52: Name notations of the “sets” in Abaqus.

Table 9: Name notations within the symmetry plane

Distance from symmetry plane	Side of the spar			
		TOP1	BOT1	SIDEF1
	TOP2	BOT2	SIDEF2	SIDEB2
	TOP3	BOT3	SIDEF3	SIDEB3
	TOP4	BOT4	SIDEF4	SIDEB4
	TOP5	BOT5	SIDEF5	SIDEB5
	TOP6	BOT6	SIDEF6	SIDEB6

Later in the process, SIDEF and SIDEB was merged to reduce the number of iterations further. The notation was then renamed to SIDE.

### 5.3. ABAQUS MACRO

Two different methods were tested. The foundation for both methods was the macro function in Abaqus. The lay-up iteration was done by manipulating the macro input file and importing it into Abaqus using Isight. One of the methods used the data exchanger to manipulate the macro and the other method used a combination of Excel, Python and OS command.

The lay-up iterations were done manipulating a Abaqus macro. This was done by recording the macro of a lay-up process in Abaqus. The macro for generating a composite ply for a given set in Abaqus is illustrated and explained in Figure 53.

```
1 p = mdb.models['Model-1'].parts['Part-1']
2 region1=p.sets['TOP1']
3
4 compositeLayup = mdb.models['Model-1'].parts['Part-1'].CompositeLayup(
5 name='TOP1', description='', elementType=SHELL,
6 offsetType=BOTTOM_SURFACE, symmetric=False,
7 thicknessAssignment=FROM_SECTION)
8 compositeLayup.Section(preIntegrate=OFF, integrationRule=SIMPSON,
9 thicknessType=UNIFORM, poissonDefinition=DEFAULT, temperature=GRADIENT,
10 useDensity=OFF)
11 compositeLayup.ReferenceOrientation(orientationType=GLOBAL, localCsys=None,
12 fieldName='', additionalRotationType=ROTATION_NONE, angle=0.0,
13 axis=AXIS_3)
14
15 compositeLayup.CompositePly(suppressed=False, plyName='Ply-1',
16 region=region1, material='Hexply 6376',
17 thicknessType=SPECIFY_THICKNESS, thickness=0.20,
18 orientationType=SPECIFY_ORIENT, orientationValue=0,
19 additionalRotationType=ROTATION_NONE, additionalRotationField='',
20 axis=AXIS_3, angle=0.0, numIntPoints=3)
```

Annotations in the code block:

- A red arrow points from the text "Set" to the 'TOP1' set name in line 2.
- A blue arrow points from the text "Ply number" to the 'Ply-1' ply name in line 15.
- A blue arrow points from the text "Suppression [True /" to the 'False' suppression value in line 15.
- A blue arrow points from the text "Orientation angle" to the '0' orientation value in line 18.

Figure 53: Illustrates the Abaqus macro for importing the properties for a single ply in each set.

### 5.4. OPTIMALIZATION USING DATA EXCHANGER

The principle for this method is to use the data exchanger to directly manipulate the Abaqus macro for importing a composite lay-up. The flow loop for this process is illustrated in Figure 54.

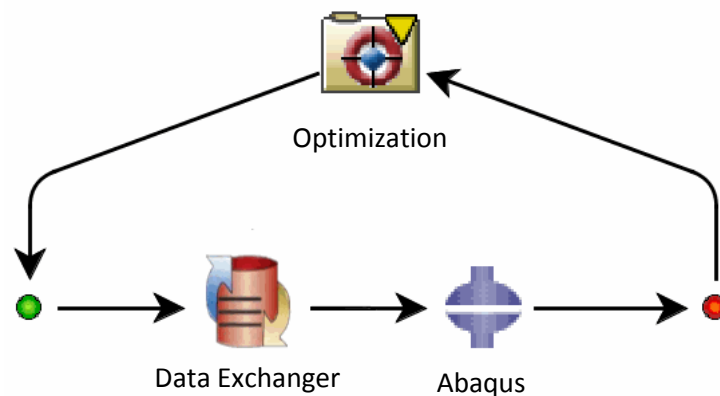


Figure 54: Flow loop of Data Exchanger

For this flow loop, the limitation of plies was restricted by how many times line 15 – 20 was repeated in the macro file (see Figure 53). In this case the maximum number of plies were set to 20. The data exchanger could suppress the layers by iterating between “True” or “False” in the code, and change the angle of the ply between 0 and 45.

This program was complicated to make because there are 24 different sets within the symmetry plane and each of these could have a maximum of 20 plies. This makes a total of 480 repetitions of the macro code. In each of these repetitions, the macro the characters going to be manipulated had to be manually selected. Figure 55 shows a screenshot from the Data Exchanger, the characters marked with red can be manipulated by the optimization loop.

```
467 compositeLayup.CompositePly(suppressed=True, plyName='Ply-2', region=region2,
468 material='Kitemill testet', thicknessType=SPECIFY_THICKNESS,
469 thickness=0.15, orientationType=SPECIFY_ORIENT, orientationValue=0,
470 additionalRotationType=ROTATION_NONE, additionalRotationField='',
471 axis=AXIS_3, angle=0.0, numIntPoints=3)
472
473 compositeLayup.CompositePly(suppressed=False, plyName='Ply-3', region=region3,
474 material='Kitemill testet', thicknessType=SPECIFY_THICKNESS,
475 thickness=0.15, orientationType=SPECIFY_ORIENT, orientationValue=0,
476 additionalRotationType=ROTATION_NONE, additionalRotationField='',
477 axis=AXIS_3, angle=0.0, numIntPoints=3)
```

Figure 55: Screenshot from the Data Exchanger

Since all the values going to be manipulated had to be manually selected, it wasn't possible to make a general program that could easily be implemented to optimize other composite parts.

As explained in chapter 2.7.1 it is important to keep numbers of iterations down when designing an optimization loop. When using the Data Exchanger to suppress the different layers you will end up with a lot of combinations that will end up with the same number of layers. Isight also iterated the angles on the suppressed plies, which doesn't affect the simulation in any way. This is unfortunate for the optimization loop, because it will take a long time to find convergence.

## 5.5. OPTIMIZATION USING OS EXCEL, OS COMMAND AND PYTHON

The lesson learned from the Data exchanger program was to find a way to reduce the number of iterations that doesn't affect the simulation. The optimization program should also be as general as possible so it easily could be used to optimize other composite parts. This could clearly not be done with the Data Exchanger application.

These problems were solved by using Python to communicate between the optimization algorithm and Abaqus. Isight is only compatible with a simple version of python and doesn't support any external libraries. It was therefore necessary to use OS Command to open a “.bat” file that automatically opens Python and submits the Python script.

The Python script rewrites the macro for each round in the optimization loop. This way all the plies could be set in a non-suppressed state, and the script will write line 15 – 20 a given amount of time based on the input from an Excel script, that was automatically updated by the optimization algorithm in Isight. The macro file is then picked up by Abaqus which updates the lay-up and submits the simulation. Figure 56 illustrates the flow loop for this optimization loop, and Figure 57 illustrates the local flow within the applications.

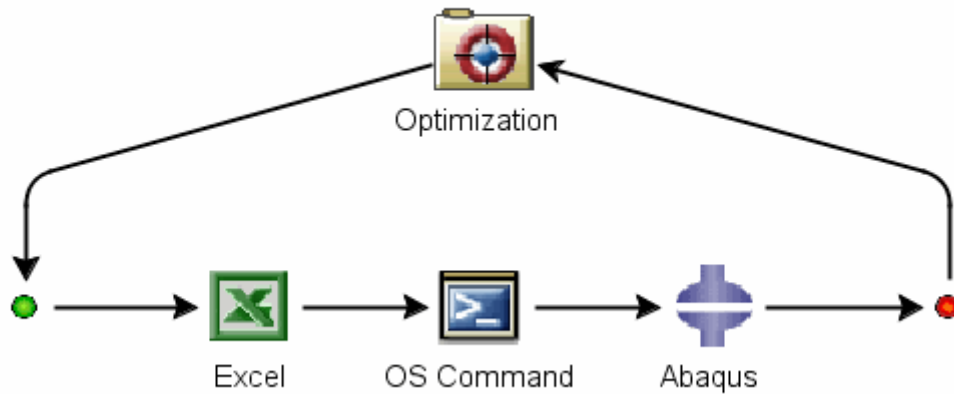


Figure 56: The flow loop in Isight

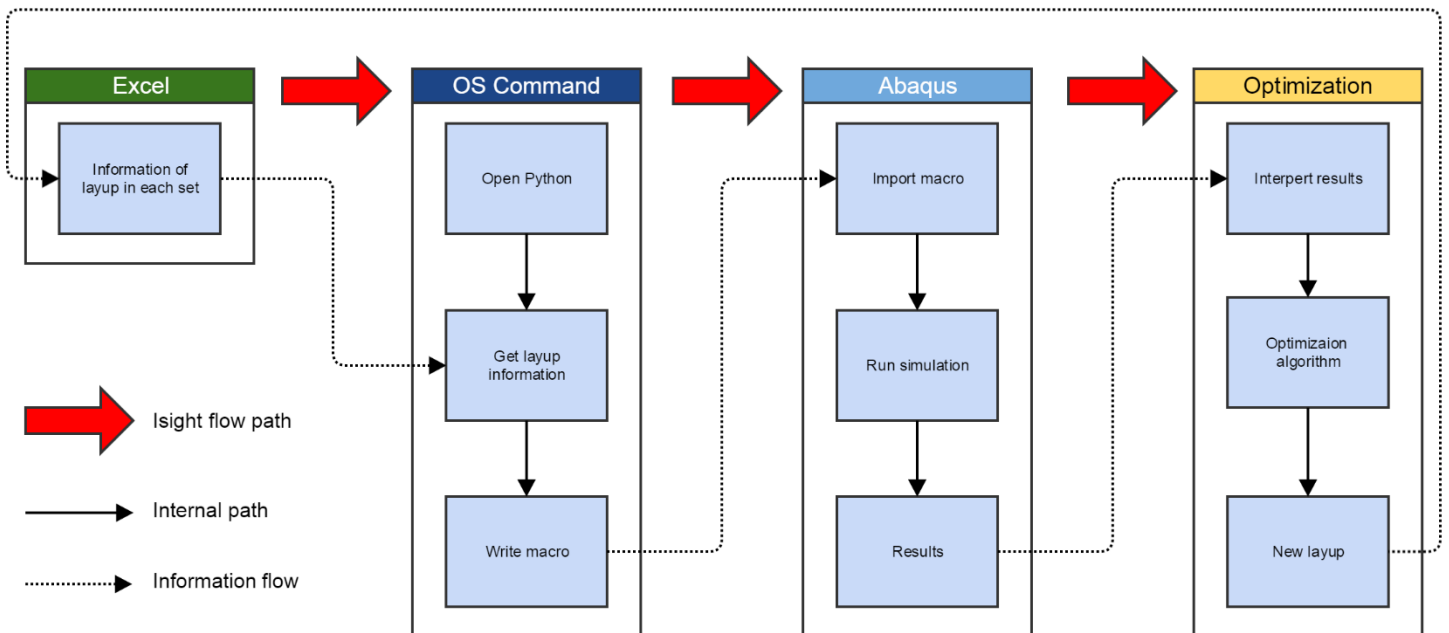


Figure 57: Local flow within applications

This method eliminates the possibility to have many lay-ups with the same number of plies within the same set, but the program will still make iterations for ply angle for all the layers whether they are in the lay-up or not. Because Python is the core of this optimization loop it is easy to make a general program where the user can modify the script to fit the needs.

## 5.6. PYTHON PROGRAM

The python program is designed to take values from an Excel spreadsheet and write an Abaqus macro based on this information. The script is not only useful for Isight, but can be used to quickly modify simulations with advanced lay-ups.

The excel sheet contains information about how many layer, and the orientation of each layer for a given set. Figure 58 is a screenshot of the excel sheet. Column A-C contains information about the lay-up for the TOP1 set in Abaqus.

	A	B	C	D	E	F	G	H	I	J	K	L	M	N	O	
1	TOP1	6			TOP2	8			TOP3	8			TOP4	8		
2	Ply	supressed	Angle		Ply	supressed	Angle		Ply	supressed	Angle		Ply	supressed	Angle	
3	1	False	45		1	True	0		1	True	0		1	True	45	
4	2	False	0		2	True	0		2	True	0		2	True	45	
5	3	False	0		3	True	45		3	True	0		3	True	0	
6	4	False	0		4	True	0		4	True	45		4	True	45	
7	5	False	45		5	True	45		5	True	45		5	True	45	
8	6	False	0		6	True	45		6	True	45		6	True	45	
9		True	0		7	True	0		7	True	0		7	True	45	
10		True	45		8	True	45		8	True	0		8	True	0	
11		True	0			False	0			False	0			False	45	
12		True	45			False	45			False	45			False	45	
13		True	45			False	45			False	0			False	45	

Figure 58: Screenshot of the excel sheet that is used for input to the python script

The information in excel is then imported to python which combines them with the macro text. This is done by splitting the text at the point where the imported value from excel is going to be pasted. Figure 59 is a screenshot from the Python script that illustrates how this is done.

```

80 #Information for first ply
81 t4 = """compositeLayup = mdb.models['Model-1'].parts['Part-1'].CompositeLayup(
82     name=""
83
84     t5 = """', description='', elementType=SHELL,
85     offsetType=BOTTOM_SURFACE, symmetric=False,
86     thicknessAssignment=FROM_SECTION)
87     compositeLayup.Section(preIntegrate=OFF, integrationRule=SIMPSON,
88     thicknessType=UNIFORM, poissonDefinition=DEFAULT, temperature=GRADIENT,
89     useDensity=OFF)
90     compositeLayup.ReferenceOrientation(orientationType=GLOBAL, localCsys=None,
91     fieldName='', additionalRotationType=ROTATION_NONE, angle=0.0,
92     axis=AXIS_3)
93
94     """
95
96
97     TOP1f = t4 + "TOP1" + t5
98     TOP2f = t4 + "TOP2" + t5
99     TOP3f = t4 + "TOP3" + t5
100    TOP4f = t4 + "TOP4" + t5
101    TOP5f = t4 + "TOP5" + t5
102    TOP6f = t4 + "TOP6" + t5
103
104    BOT1f = t4 + "BOT1" + t5
105    BOT2f = t4 + "BOT2" + t5
106    BOT3f = t4 + "BOT3" + t5
107    BOT4f = t4 + "BOT4" + t5
108    BOT5f = t4 + "BOT5" + t5
109    BOT6f = t4 + "BOT6" + t5
110

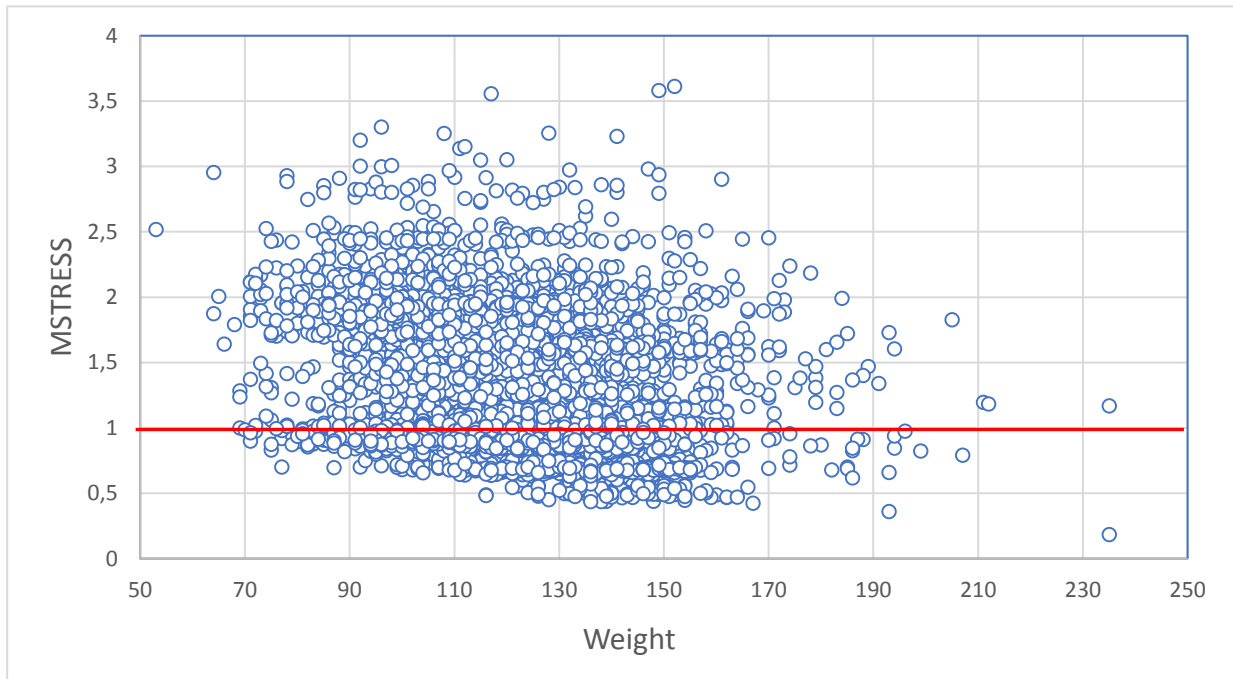
```

Figure 59: Sample from the python script

The same thing is done for the orientation of the plies. Eventually, python puts everything together to a long text and writes it to a document called userscript\_cae\_pre.py that is saved in the same folder. This script can be executed to the “run-script” command in Abaqus, which then automatically will generate the same lay-up as in the excel sheet and assign the lay-up to the steps with the corresponding name.

## 5.7. OPTIMIZED LAY-UP

This program went through a lot of iterations to fix different problems occurring. The result is a program that can iterate the lay-up in between specifically defined steps in Abaqus. Graph 7 shows a scatterplot of all the simulation results for the optimization for the compression moulded sample made with Hexply 6376. It took 76 hours to complete 5000 iterations.



Graph 7: Scatterplot of 5000 iterations

Each dot illustrates a simulation and all the dots above the red line will fail before the load reaches 360N. The x-axis illustrates the estimated weight. So, the dots closest to the bottom left corner should in theory represent the best lay-ups for this application.

There was a miscalculation in the weight estimation. This was due to a miscalculation of the gsm of the carbon fiber. This resulted in Isight estimating a lower weight than what it was. This doesn't affect the optimization, because weight is relative in this optimization.

The python program can be found in appendix.

## 6. COMPRESSION MOULDING (CONCEPT 2)

Compression moulding is a technique that takes advantage of the spring back force in a compressed foam core material inside a closed mould. This is because the core has been milled out to fit into the mould, but has been extruded 1-2% in height. When the mould is clamped together, this extra foam will generate pressure. The composite is squeezed between the foam and the mould, which distributes the resin throughout the laminate. This process will make a good surface finish all over the outer surface of the product.

This subchapter will explain the process of producing a mould for this process as well as production of the actual composite part. A variety of different materials was considered for the mould, but MDF was chosen because of price.

### 6.1.1. REDESIGN OF THE MOULD

For this process it was necessary with a small redesign of the part to ease the production of the spar. A slip angle was made to the sides of the part and the mould which would make it easier to squeeze the core material. The slip angle is marked with red in Figure 61. Figure 60 illustrates how the mould is closed. The core material is squeezed on the "TOP" side by the lid. To maintain high pressure throughout the whole curing process. The core material was extruded by 2% on the top, to generate high pressure on the composite. Figure 61 illustrates a cross section of the core material. The area marked with blue is the extruded part of the core. The slip angle will also generate higher pressure on SIDEB and SIDEF, as the core was slightly bigger than the mould on the sides. The cross section shown in Figure 60 and Figure 61 is representative for the whole length.

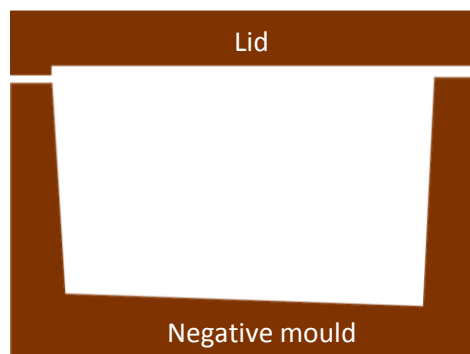


Figure 60: Cross section of the closed mould with slip angle.

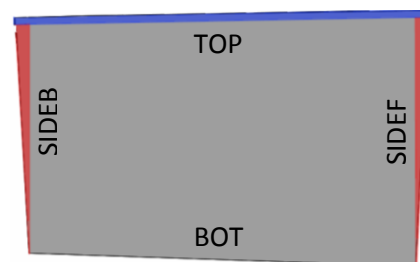


Figure 61: Cross section of the core material. Slip angle marked with red and expansion factor marked with blue

Squeezing the core material with the mould generates high pressure, and a lot of force is needed to close the mould with the core material inside. The mould was therefore designed with bolt holes, so the it could be closed by tightening bolts. To block the ends, there was milled a slot for bar clamps with could clamp a piece of wood to the ends. The design of the mould is shown in Figure 62.

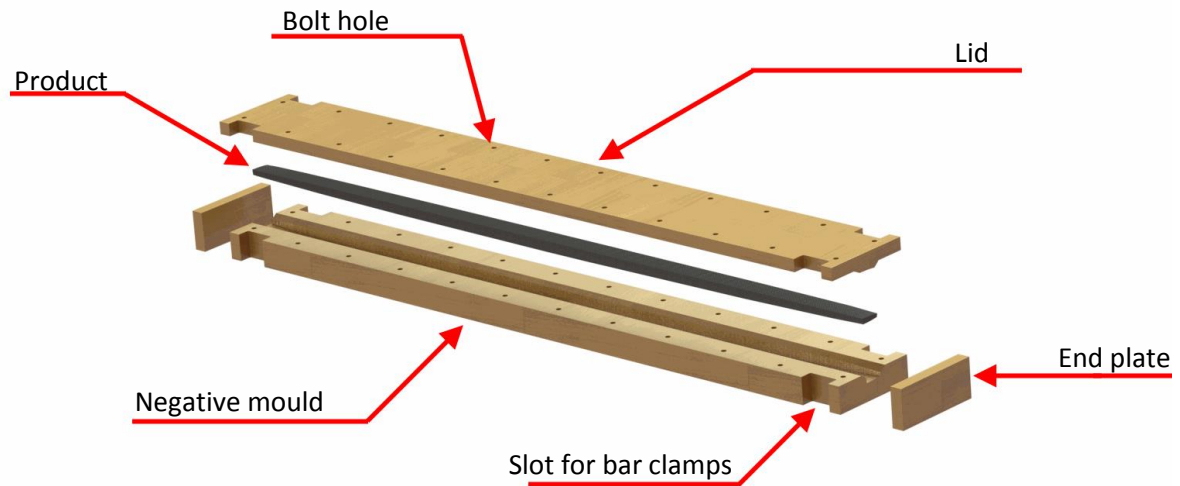


Figure 62: Render of the mould design

### 6.1.2. PREPARATION OF THE MOULD

Both the lid and the negative mould pieces were milled out from MDF with a 3-axis milling machine. Figure 64 illustrates the milling machine and the mould. After milling, the mould was sanded with rough sandpaper before adding a thin layer of epoxy. The resin used was Renlam CY 219 mixed with the hardener Ren HY5161. This was to seal all the air pores in the material, so they don't affect the composite product. The key here is to let the MDF absorb the epoxy. Figure 63 illustrates how the epoxy is absorbed.



Figure 63: Applying epoxy to the mould



Figure 64: Mould in the milling machine

The epoxy was cured at 50°C for 12 hours. After cooling down the mould was sanded carefully. Starting at 120 grits going up to 800 grit. It is important to not sand through the epoxy coating applied in the previous step. This was to prepare the surface for the two-component clear coat. A total of 4 layers of coating was applied with 20 minutes of drying between each layer. After the fourth layer, the mould was put into the oven to cure for 1 hour at 60°C and 2 hours at 90°C. Figure 65 illustrates the surface finish after the clear coating.



Figure 65: Surface finish after two component clear coat

The clear coat introduced some small dimples in the coating. The surface was therefore carefully wet sanded with fine grit sandpaper to remove these dimples. Sandpaper with a grit up to 2000 was used. After this the surface was polished with 3M fast cut plus compound, Extra fine compound and ultra-fine compound to obtain a shining surface.

The moulds were cleaned properly with a linen cloth and water before the surface was coated with Chemlease 712 EZ sealer. Six layers were applied using a wipe on / leave on technique where each layer was set to dry for 30 minutes. After the last layer, the mould was heated to 60°C for 20 minutes. This made a good base for the release agent Chemlease 2185. Four layers of release agent was applied using a wipe on / wipe off technique. Figure 66 illustrates the final surface finish.



Figure 66: The final surface finish

## 6.2. SIMPLYFING THE LAY-UP

Good design practice for composites is to have large plies with long fibers, especially in the direction of loading. Since the whole lay-up share the same mesh and there is no adhesive connection in the simulations. This means that Abaqus assumes that a connection between a 0/90 ply and a -45/+45 is as strong as a continuous ply. The lay-up was then changed so the first layer would go all over the part without being cut.

Because of this, the optimization came up with some suggestions that was unfavorable in terms of the design criteria. The lay-up was therefore modified to have as many continuous layers as possible. The modification was then control checked in Abaqus to make sure that it didn't fail. The simulation lay-up and the production lay-up are listed in Table 10 and Table 11.

Table 10: The simulation lay-up from the optimization loop

Simulation layup								
layer	1	2	3	4	5	6	7	8
TOP1	0							
TOP2	0							
TOP3	0							
TOP4	0							
TOP5	0	45	0	45	45	45	0	45
TOP6	45							
SIDE1	0	45	0	0				
SIDE2	45	45	45	0				
SIDE3	0							
SIDE4	45	45	0	0				
SIDE5	45							
SIDE6	0	45						
BOT1	0							
BOT2	0	0	45	0	45	45	0	0
BOT3	0							
BOT4	0	0						
BOT5	0	0						
BOT6	45	0						

Table 11: The modified lay-up. Changes marked with yellow

Production layup								
Layer	1	2	3	4	5	6	7	8
TOP1	0							
TOP2	0							
TOP3	0							
TOP4	0							
TOP5	0	45	0	45	45	45	0	45
TOP6	0	45						
SIDE1	0	45	0	0				
SIDE2	0	45	45	45				
SIDE3	0							
SIDE4	0	45	45	0				
SIDE5	0	45						
SIDE6	0	45						
BOT1	0							
BOT2	0	45	0	0	45	45	0	0
BOT3	0							
BOT4	0	0						
BOT5	0	0						
BOT6	0	45						

## 6.3. FIBERSIM

Fibersim is a computer program that can divide the 3D shape of the composite part into 2D plies. The Fibersim was made on the outside of the CAD model of the spar. This made the plies slightly bigger than the inside of the mould. The Idea behind this is that it will ease the lay-up process, because it is easier to shrink a ply than to stretch it. Figure 67 illustrated this process.

The file generated can be sent to a CNC cutting machine which can cut out all the plies accurate with the right orientation. This reduced a lot of variations compared to using scissors when it comes to cutting. To save as much material as possible, the Fibersim file was imported to Majestic. This is a

nesting software that uses advanced algorithms to nest the plies in an efficient way. The final cut material can be seen in Figure 68.

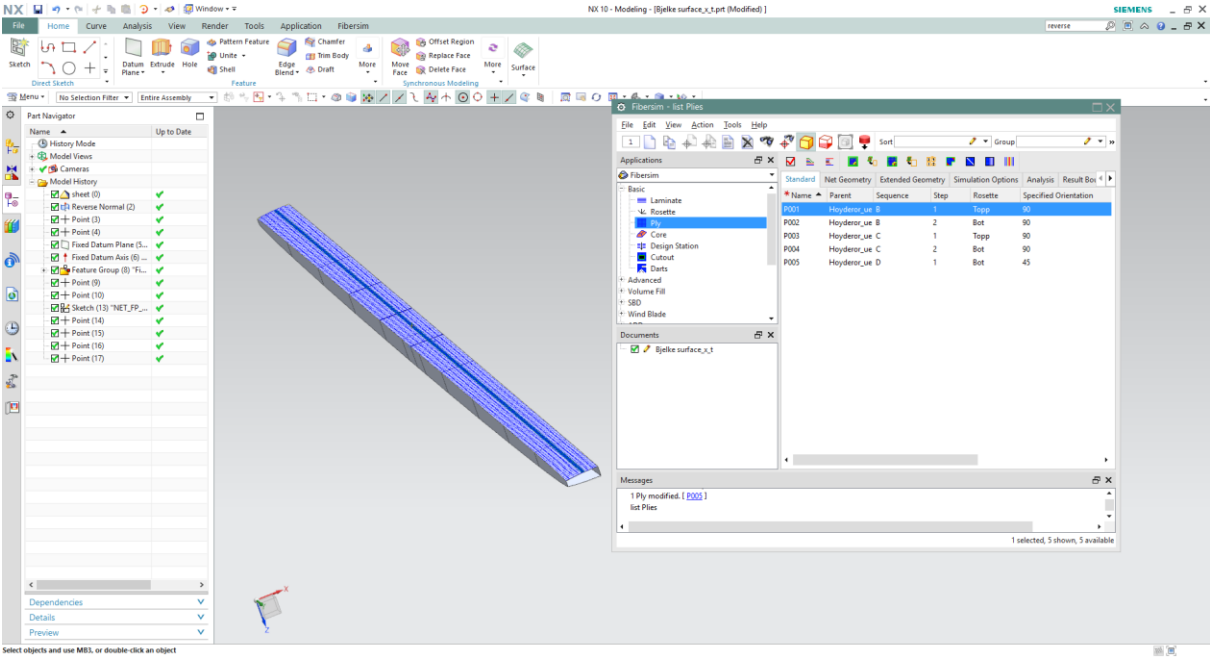


Figure 67: Fibersim of the spar

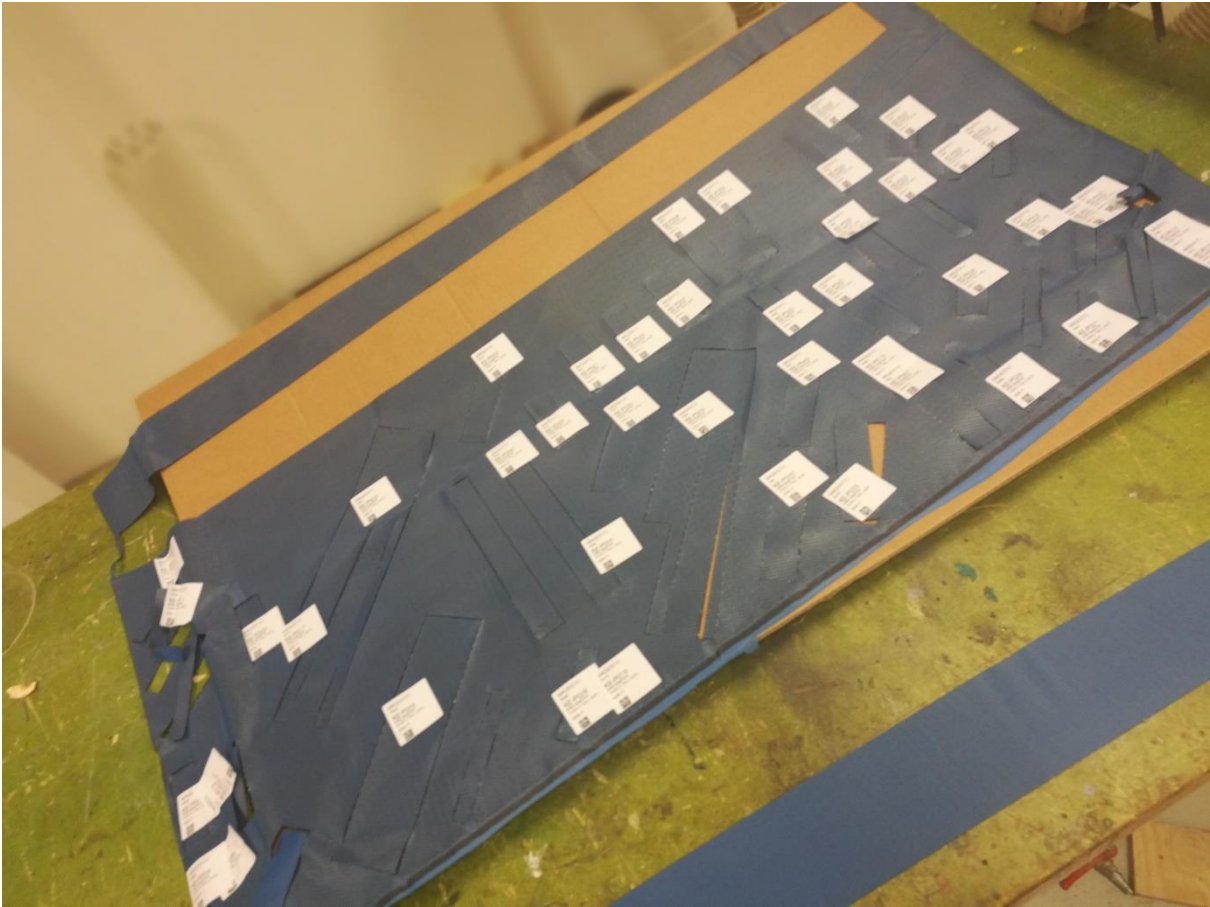


Figure 68: CNC cut plies

## 6.4. LAY-UP

---

All the material used in the compression moulded sample was expired prepreg material. Normally, the pre-preg composites stick to the walls of the composite. The surface finish of the mould was so smooth that the pre-preg materials slips off the wall. This problem was however solved by heating the mould to 40°C for 1 hour. The slightly warmer mould made it easier to place the pre-preg to the side walls.

To maintain a high-quality product with good surface finish it is important to press the material into all the fillets. This was done with a carbon fiber tool made for this purpose. As described in chapter 6.2, the first layer was made to go all around the spar without being cut. This ply can be seen in Figure 69.

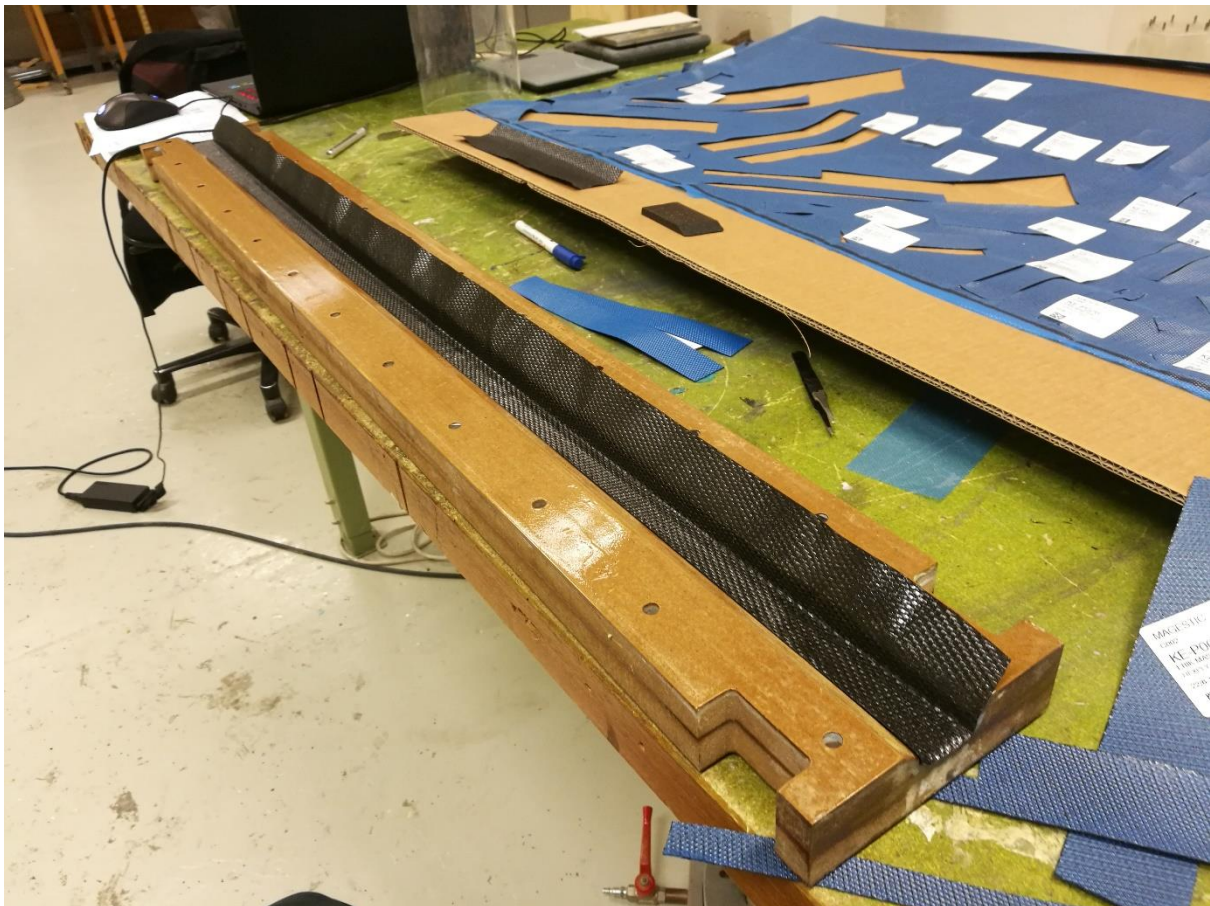


Figure 69: The first ply is placed into the mould

When all the carbon fiber was placed into the mould, it was debulked for 10 minutes in a vacuum bag. This process packed the carbon fiber harder together, which made it easier to squeeze in the core material with using the lid. The core material had been heated for 12 hours at 60°C to evaporate any liquids that could have been absorbed in the core material(17).

The core was first squeezed into the mould by the lid. When the core was in place, the mould was opened and the carbon fiber was placed on top of the core material. This is illustrated in Figure 70. The mould was closed and the bolts were tightened.

A strip of Teflon tape was put on a piece of wood which was clamped to the ends of the mould. The end piece with Teflon tape can be seen in Figure 71. In this way, all of the surface of the beam could be packed in carbon fiber, which eventually waterproofs the structure to some extent.

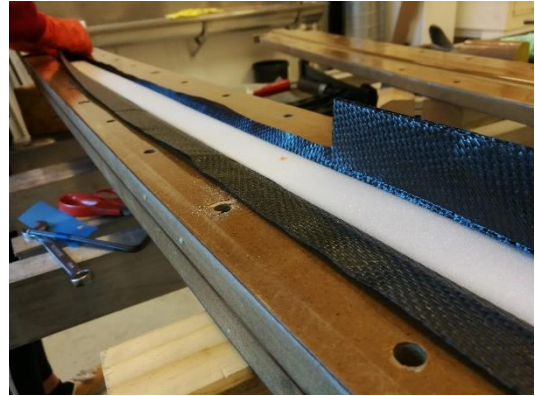


Figure 70: Packing carbon fiber around the core material

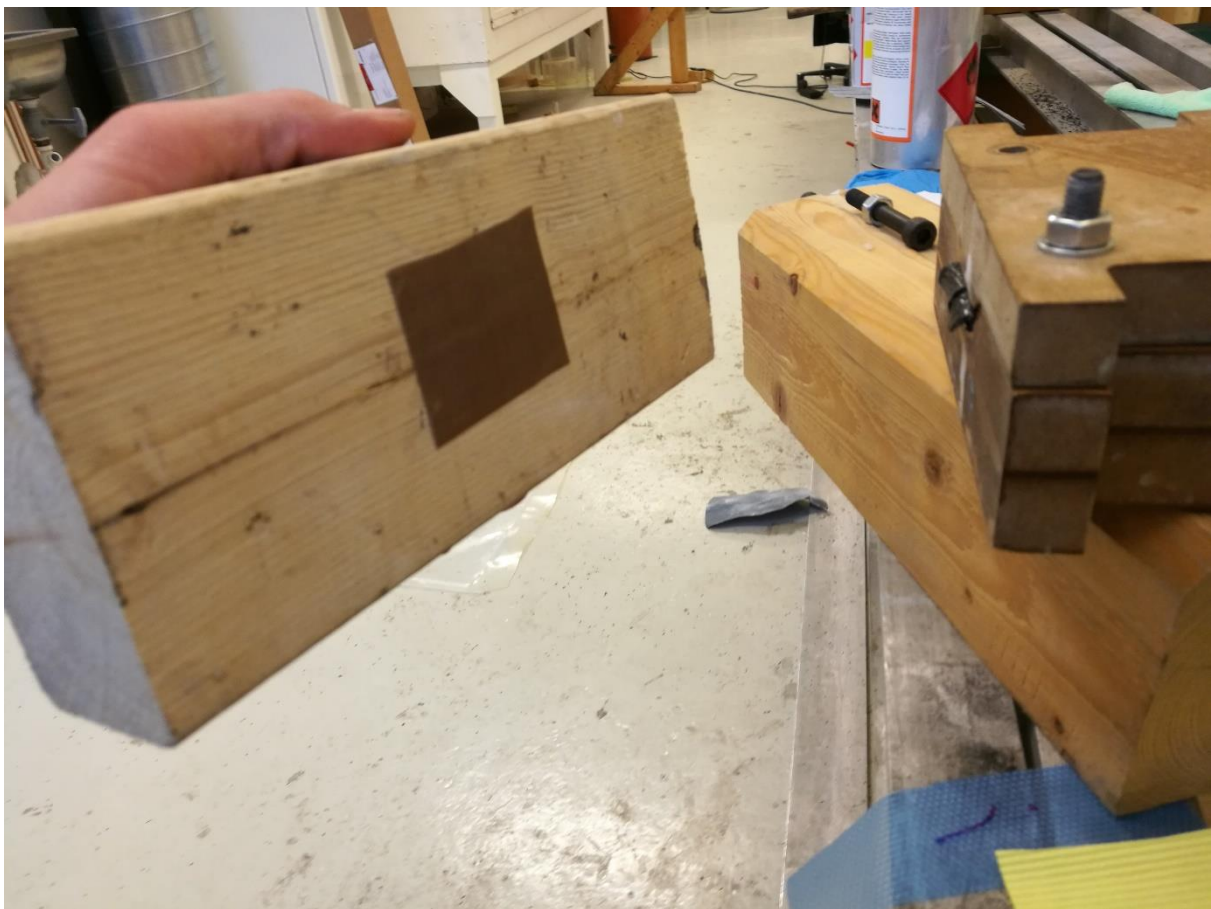


Figure 71: End piece with Teflon tape

## 6.5. CURING

Hexply 6376 should be cured at 175°C for two hours, but MDF can't take any more than 120°C without warping. Because of this, the part was cured at 120°C for 12 hours, then demoulded and heated again to 135°C for 4 hours. This is because the maximum temperature for the Rohacell IG-F core material is 130°C.

6.6. RESULT

In general, the surface finish on both samples was good. There was no sign of delamination between the core material on carbon fiber. On the first sample, the core material dragged down the carbon on the side wall and created a small crack between the SIDE and the TOP of the spar. There were no continuous fibers from the side to the top in the symmetry plane of the spar. This production flaw is illustrated in Figure 72.



Figure 72: Production flaw

This problem was solved on the sample 2 by placing an extra strip of carbon fiber from the sidewall and up to add extra friction to the slippery mould surface. This can be seen in Figure 73.

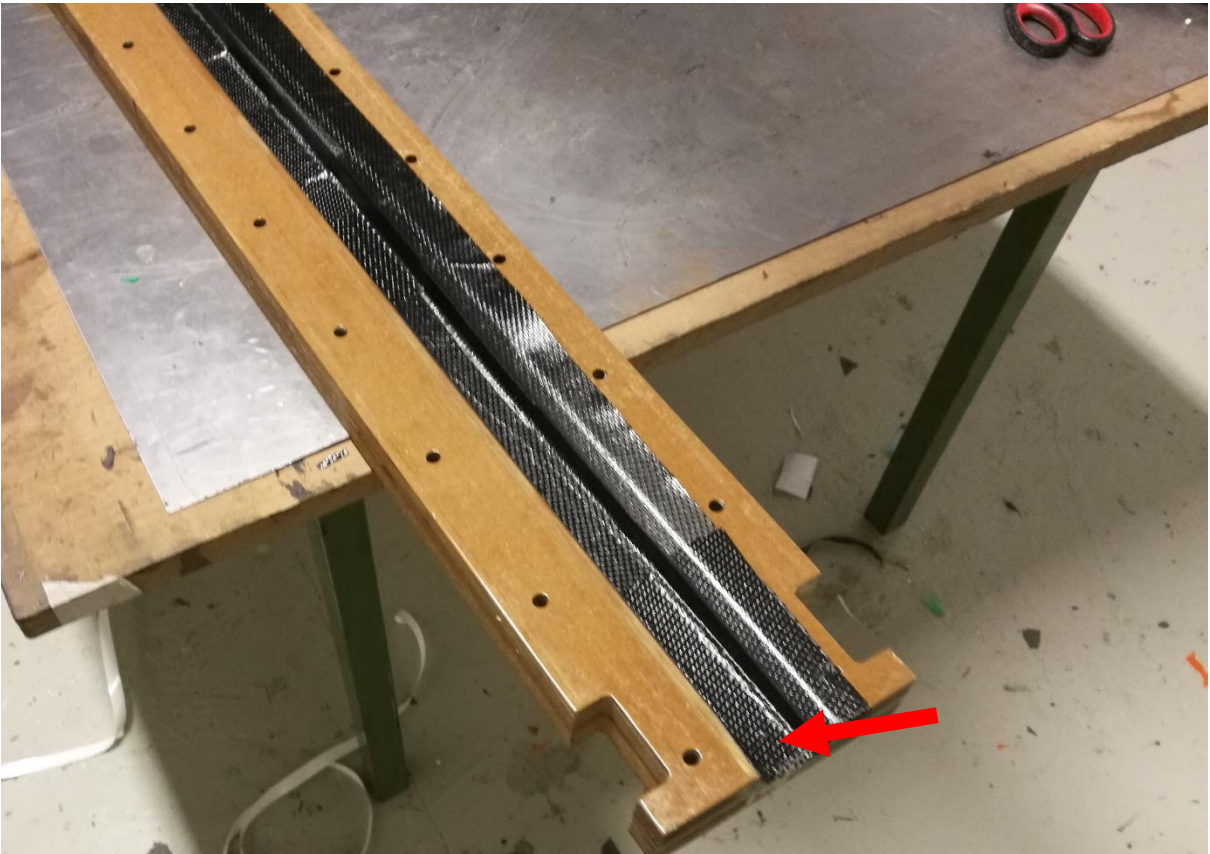


Figure 73: Extra strip of carbon to prevent the carbon from sliding down.

This method prevented the fiber from sliding down on sample 4. When examining the samples, it was however found sections with dry spots. The dry spots can be seen in Figure 74.



Figure 74: Finish Hexply 6376

The weight of the finished samples was:

Sample 3: 169.6g

Sample 4: 170g

## 7. TESTING

### 7.1. TESTRIG DESIGN

Since the spar is a 1,2m long composite part, a custom test rig had to be made to test the spar in three-point bending. The requirements for this design is that it had to behave like the boundary conditions in the simulations and there shouldn't be any rig compliance. The maximum deflection of the spar was believed to not be any greater than 90mm. The final design of the test rig can be seen in Figure 75. The load applicator used was a 25mm steel tube.

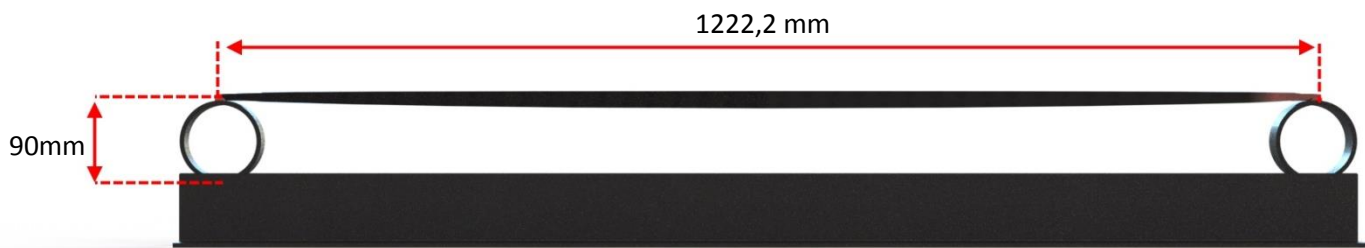


Figure 75: The design of the test rig

The BOT side of the spar follows the curvature of the airfoil, and is therefore not flat. This made it difficult to place the spar on the test rig parallel to the load applicator. Because of this, a spacer with the same geometry as the BOT side of the spar was designed to keep the spar steady while testing. This spacer was 3D printed in ABS plastic. The spacer can be seen in Figure 76.

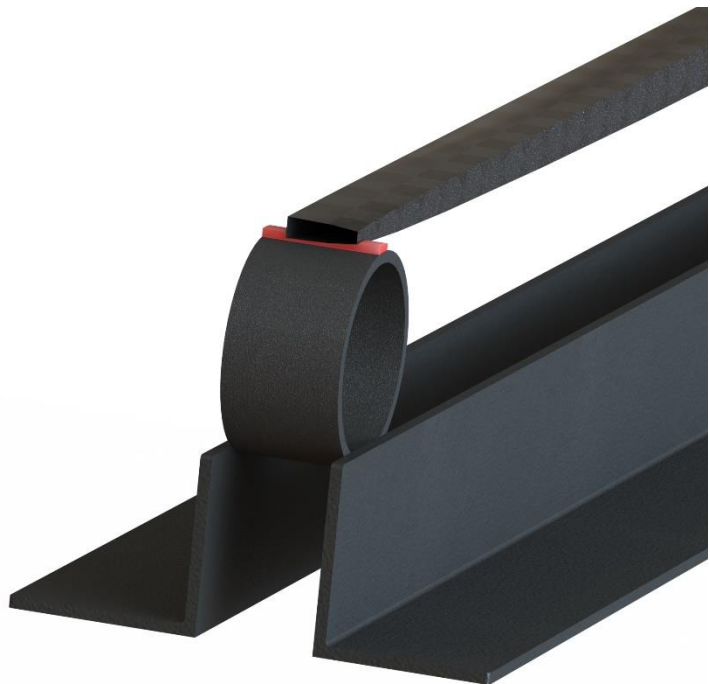


Figure 76: Spacer (Red) between test rig and the spar.

## 7.2. TEST SETUP

---

All the tests were done at NTNU's lab with assistance from the people working with these machines daily. The test setup can be seen in Figure 77. With this setup, the load applicator is pushed down to bend the spar.



Figure 77: Test setup for testing the spar

## 7.3. TEST RESULTS

---

Somehow the test machine didn't log any of the test results. Because of this there is no test results in this thesis. The focus is therefore changes to failure mode rather than the magnitude of the failure loads. The test results were however shown live on the computer monitor. This is what was observed:

### 7.3.1. BLADDER MOULDED SAMPLES

---

The bladder moulded samples didn't fail under testing. The maximum displacement of the test machine was less than the deflection to failure. The maximum load before the test was stopped was significantly higher than for the compression moulded samples.

### 7.3.2. COMPRESSION MOULDED SAMPLES

Both compression moulded samples failed before the maximum deflection was reached. The samples seemed to have a slightly different failure mode.

#### Sample 3:

As shown in Figure 72, there was a production flaw in sample 3. The failure mode of this production flaw seems to have been induced by this flaw. Figure 78 shows how the fiber separated from the core material. The core material is still bonded to the carbon fiber on the inside. The fibers are still intact, and if the spar is unloaded, the “air pocket” closes and the spar looks as good as new.



Figure 78: Failure of sample 3

#### Sample 4:

The failure mode of sample 4 was rather different. In this sample, all the fibers on the TOP and both SIDES failed at 140mm from the center of the spar. The edges are sharp and straight. The failure mode can be seen in Figure 79. The sample broke between two layup zones.



Figure 79: Failure mode of sample 4

## 8. DISCUSSION

### 8.1. TESTING TEXTREME

The overall results for the material testing are what could be expected from hand lay-up specimen. This production method isn't recommended by the ASTM standards, because the surface roughness in front and in the back, is different.

The strain gauges used on some of the samples had a length of 5mm. The ASTM standard says that the strain gauge should be at least the size of a unit cell, which is 40mm x 40mm. It also describes the minimum width of the tension and shear specimen to be 2 times the unit cell width. This means that the strain gauge used is too small and that the specimen is too narrow. It is difficult to say if this makes the results conservative or non-conservative without further testing.

To improve these results, I would recommend using pre-impregnated fabrics. This will enhance the production quality and hence, the material constants and failure stress would be higher. The downside is that the cost will go up. A gluing Jig to help aligning the clamping taps would probably improve the results. The taps also had a slight variation in thickness, which will make the laminate constants lower.

It is important to mention that the laminate constants used in this thesis are subtracted from an average of the tests results. Often the worst result is chosen to be on the safe side. These tests are however believed to be on the low end of the scale because of the uncertainties mentioned in this chapter. The production method used for this process is also not the same as for the bladder moulded sample. Even though it is the same materials the results could be different, due to production method specific flaws.

#### 8.1.1. TENSION TESTING

All the tension tests were destructive testing. The failure of the specimen seems to occur at the transition between the clamping tabs and the specimen. A typical specimen failure is shown in Figure 80. As shown, the sample failed in two different places. The first failure happened in tension, while the second fail in compression due to the energy release of the initial tension failure.



Figure 80: Typical tension specimen failure

### 8.1.2. SHEAR TESTING

---

The failure mode for the shear test was not the same as for the tension tests. Because there are no fibers crossing the specimen. The stiffness and the maximum load was significantly lower. The fibers tended to rotate inside the laminate, and failure occurred when the fibers had rotated out of the matrix. The typical failure mode can be seen in Figure 81.



Figure 81: Failure mode for shear samples

### 8.1.3. COMPRESSION TESTING

---

Figure 82 illustrates the air bubble trapped inside the laminate. This specimen was not tested, and there was no sign of air bubbles in the other tests. This air bubble is quite large and it is a clear indication that there could be a potential problem with bonding between the layers. This imperfection is most likely due to bad production quality. This can be caused by low vacuum or not enough epoxy, even though this can be difficult to avoid when producing an 18-layer laminate with hand lay-up. It is also important to emphasize that this laminate was produced on a flat surface.



Figure 82: Defect found in one of the compression samples.

## 8.2. BLADDER MOULDING

### 8.2.1. PRODUCT QUALITY

The way that this part was made might have introduced dry spots in the final sample. This is because layer C, D, E and F from Figure 37 is packed around the bicycle tube. When the tube inflates, it tensions the fibers. This prevents the fibers to go into the fillets of the mould. This problem might have been solved by making smaller plies that doesn't encircle the bicycle hose. Figure 85 illustrates the bike tube before it is blown up. In this case, the carbon fiber is not pressed completely into the corner. When the tube is inflated it generates pressure on the overlap which prevents increase of the perimeter. The concept is illustrated in Figure 84. This causes poor surface finish, because some of the carbon is not in contact with the mould. This can be seen in figure 83.

A solution to this problem would require better planning when it comes to cutting of the carbon fiber. Fibersim and a CNC cutting machine could easily solve this problem but then the cost would be a lot higher. Cutting templates could be a good and cheaper alternative, especially when making parts for prototype testing.



Figure 83: Surface of bladder moulded samples

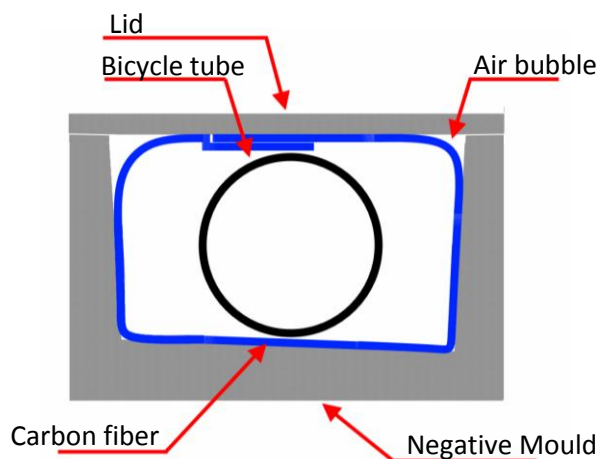


Figure 84: Before inflating the bicycle tube

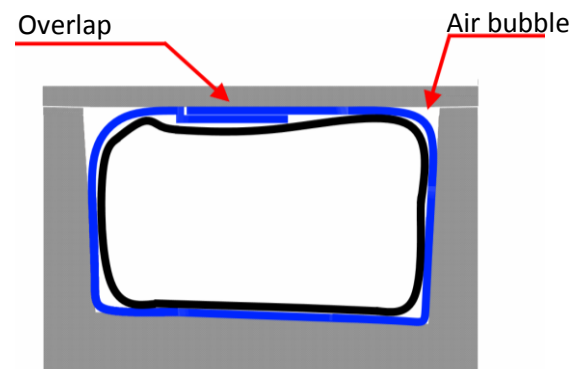


Figure 85: After inflating the bicycle tube

The surface of sample 1 and sample 2 was also studied in a light microscope to see if the fibers are covered in resin. The surface was full of small dry spots where you could see the fibers beneath the protective layer of resin. Figure 86 is a 5x magnitude photography from a light microscope studying the surface of sample 2.



Figure 86: 5x magnitude photography from light microscope

Since the part already is very light weight it is very difficult to save weight without influencing the quality of the product. The focus should therefore be on improving the quality instead of saving weight.

### 8.2.2. FINDING THE FAILURE LOAD

---

The failure load was originally going to be found by testing. The sample before starting the optimization program. Time constraints made this difficult and the benchmark failure load was found by simulation. Then the failure load of the simulation could be compared to the failure load of the spar in a later stage.

The compression moulded spar was going to be tested on a later stage, but as it is explained in Chapter 7.3, the test machine didn't log the load-deflection data from the tests. It is therefore unknown how accurate the simulation results are.

### 8.3. THE OPTIMIZATION PROGRAM

---

The structure of the program is pretty good. The Abaqus simulation is computational efficient and only small changes will make this a general optimization program for composites. The excel part of the program can probably be implemented into the python script to make it more computational efficient, but the interaction between Isight and excel is very smooth and easy to make changes fast.

There is still a long way to go before this program can generate an optimal lay-up in a reasonable amount of time. The program now uses 4 days on a laptop, and comes up with a lay-up that could be stronger.

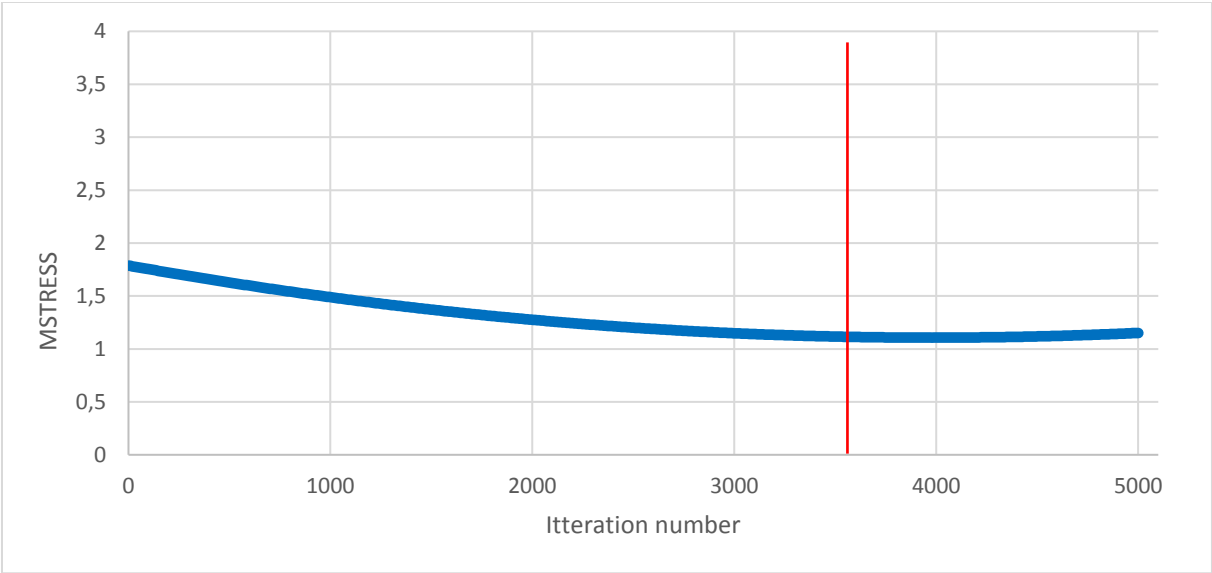
The main problem with the optimization is that it had to many lay-up zones. A lot of lay-up zones means a lot of iterations, which means that it requires more time to find the optimal result. In this case 5000 iterations were done and this is probably far from the optimum result. Considering the program has approximately  $10E+91$  possible iteration if it can iterate between 20 layers in each lay-up zone.

### 8.3.1. OPTIMALIZATION ALGORITHM

---

The process could also have been speed up by finding a better optimization algorithm. The evolution algorithm is well suited for nonlinear design spaces and long running simulations. The algorithm had three different stopping criteria, when it converges, hits the maximum amount of iteration's or when a given number of iteration's fail. In this case it stopped because it hit the maximum number of iterations.

Graph 8 represents the trendline of iteration number vs the "Maximum stress" failure criterion for composites. The trend is clearly going downward in the first 3500 iteration, before it seems to flatten out, or even go up when it goes towards 5000 iterations. The red line represents the iteration that was chosen, which was number 3699. If the optimization had seen a convergence pattern this should be below a MSTRESS value of 1, because this was the target set for this optimization. Fewer variables would make the program find convergence faster.



Graph 8: The trendline of iteration number vs MSTRESS

### 8.3.2. THE RESULT

---

The lay-up generated from this optimization is far from the optimized lay-up. This is mainly because of two reasons:

- 1) The bonding between plies in Abaqus is not right. This is explained in Chapter 8.3.3.
- 2) There are too many variables in this optimization program.

Both problems could probably be solved by having fewer sets. This would make the program have a lot less iterations and there would be bigger plies so less of this bonding between plies effect.

### 8.3.3. THE FEA SETUP

---

#### **Boundary conditions:**

It was chosen to use boundary conditions instead of contact in these simulations, because the stiffness of the spar is so low over this distance, a very small amount of reaction force is created. It is therefore expected that the difference between contact and boundary conditions are minimal. Having parts that are in physical contact will make the simulation highly nonlinear, which means that it would require more computational power.

#### **Material data:**

Two different materials have been used for simulations in this thesis. The laminate constants for the Textreme fiber were obtained by testing. The compression strength  $X_c$  and  $Y_c$  for this material is believed to be on the low-end due to buckling while testing.

The test data from the three-point bending test could give an indication on how accurate the laminate constants used in the simulations are.

#### **Static general:**

All the simulations were performed under the static general conditions. This means that there are no inertia effects in the simulation.

#### **Mesh:**

The mesh used in these simulations is a fine mesh with no irregularities. Two types of elements have been used for simulation, S8R (shell element) and C3D8R (Solid elements). Both elements should be well suitable for this kind of simulation.

A mesh convergence test was performed to check if the element size is adequate. The sweet spot for convergence seemed to be around 1400 elements. The simulation was only performed with reduced integration elements.

The main reason why this optimization program didn't work that well was due to a problem in Abaqus. Abaqus does not notice when a ply is not continuous. This is illustrated in Figure 87 where a 0/90 ply (to the left) -45/+45 to the right. This lay-up is obviously weaker than a continuous ply as shown in Figure 88. Abaqus will not see the splice between the two plies as a weak spot.

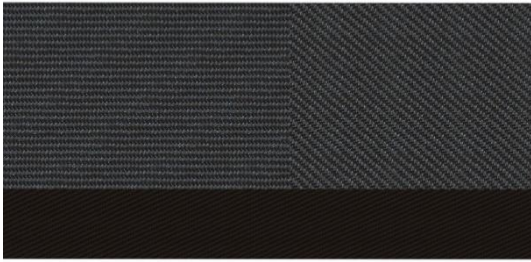


Figure 87: Two plies bonded together

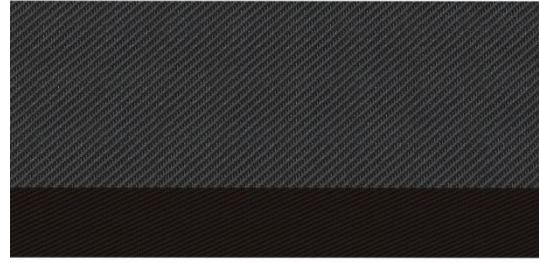


Figure 88: A single continuous ply.

There was not found a solution to this problem. This will therefore need further investigation.

### Failure criteria

In this program, the maximum MSTRESS value and the weight was used as criteria for the optimization. This because it is easier to find the failure mode from this criterion. Isight tries to find a solution that has a MSTRESS value below 1 and has as low weight as possible. Eventually what happens after a lot of iterations is that the whole spar will have a MSTRESS value close to 1. Which means that the whole beam is close to fail. Figure 89 illustrates the MSTRESS values in the lay-up that the optimization program suggested as the optimal lay-up.

The Rohacell material didn't have any failure criteria or failure load in these simulations. A core-material failure would therefore not be picked up by these simulations. The core material would however have a little effect on the failure of the spar. The core material is in this case mainly used for production purposes.

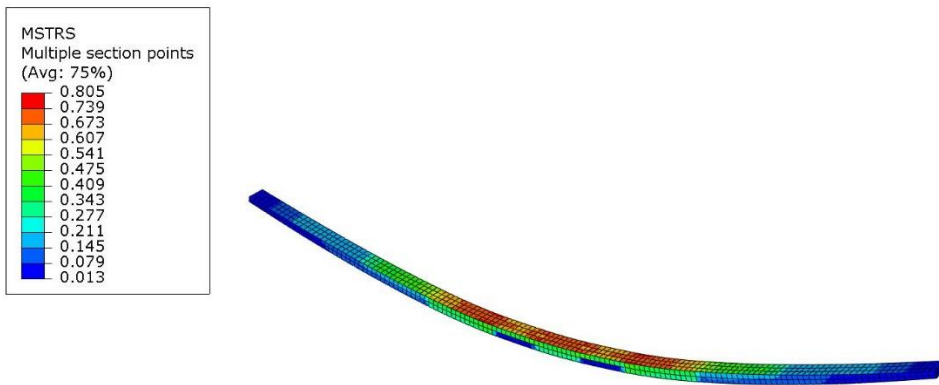


Figure 89: The simulation for the best lay-up according to the simulation program.

## 8.4. COMPRESSION MOULDING

### 8.4.1. QUALITY OF THE PRODUCT

The surface finish of the compression moulded parts looks good to the naked eye. However, when the samples were put under the microscope, a pattern of dry spots could be seen on the surface. The pattern is shown in Figure 90 with 5x magnification. From Figure 91 it is possible to see exposed

fibers. This pattern comes from the braiding pattern on the composite. Every time the weft goes over or under the web a small pocket is created. These pockets are usually filled with resin.



Figure 90: Dry spots in the braiding (5x magnification)

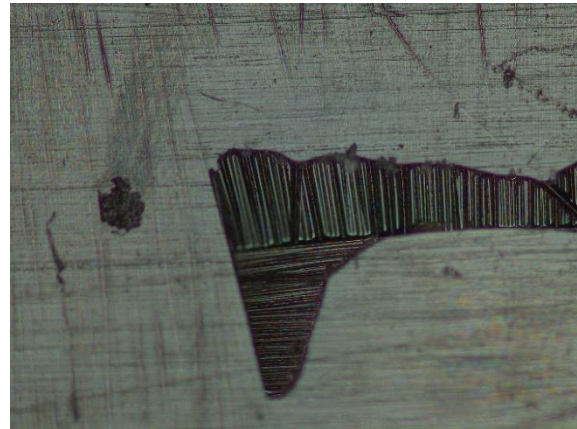


Figure 91: Dry spots in braiding (10x magnification)

Curing at a temperature which is 55°C below the recommended temperature has probably had an influence on the viscosity of the resin. The dry spots could also be caused by low pressure on the composite. Because of this uncertainty, the same process should have been tried with a pre-preg that has a lower curing temperature, or a mould that can take the temperature that is recommended by the datasheet.

It was rather complicated to put all these small plies into the mould. However, problem would be solved if the optimization program is tweaked to generate larger plies.

The compression moulded sample is without doubt an easier way to keep consistency to the process. These samples look a lot better compared to the bladder moulded samples and they feel like they have a higher quality. The bad result with the compression moulded parts is believed to be caused by the lay-up that was generated by the optimization program, but further testing is needed to provide more information.

## 8.5. TESTING

The testing was satisfactory and there were no issues with the test setup. Unfortunately, no data was logged during testing, but the live-graph in the screen showed that the strength of the bladder moulded samples was higher than for the compression moulded samples. This is believed to have been caused by lay-up generated from the optimization program.

The test results would be used to find the accuracy of the simulation results. If the simulation results were correlated with the results from the three-point bending, the confidence of the simulation setup and the laminate constants would be higher. This setup could then be used for other types of simulations.

If there was no correlation between the simulation results and the testing, the simulations must be tweaked to see if it is possible to find correlation. Parameters that could have been tweaked is mesh, boundary conditions, loading case, simulation type and laminate constants.

## 8.6. GENERAL DISCUSSION

---

The higher production quality of this process comes with a price. Pre-preg materials are more expensive than the dry fibers. The process also requires a Rohacell core material, and a 3-axis milling machine. In general, this is a much more expensive process and for this prototype stage it is probably not necessary, but if the production is going to be upscaled, this could be a good alternative.

The prototype glider contains a lot of expensive equipment and a crash could have catastrophic consequences for Kitemill and the concept. Because of this, it is recommended to change the production process of the bladder moulded technique. This could be done by having lids on the sides of the mould so higher pressure could be used while curing. Further testing is needed to say if this would have worked. The material could also be changed to a pre-preg material. Wet-lay-up introduces too much variation for aerospace applications.

As discussed in chapter 8.2.1, the material has problems with pressure in the fillets because of the way the carbon is folded around the bicycle tube. It is believed that it would be beneficial to cut the fiber in shapes that fits into the mould. This can be done by printing out templates from paper and cutting out the shapes needed to fit into the mould.

### 8.6.1. CROSS SECTION MICROSCOPY COMPARISON

---

After testing, the samples were cut and the cross-sectional plane was investigated to see how well the layers were bounded together. The results were clear, the cross section of the Bladder moulded samples had a lot more defects in the laminate. Figure 92 and Figure 93 shows the cross section of the different concepts. It is noticeable that the fibers are closer packed in the compression moulded samples. This trend was shown throughout all the samples.



Figure 92: Cross section of compression moulded sample



Figure 93: Cross section of bladder moulded sample

The samples were also put under a microscope to have a better picture of the production quality of the different concepts. Figure 94 and Figure 95 shows microscopy pictures taken with 5x magnification. The Bladder moulded sample clearly has more defects than the compression moulded sample.



Figure 94: Cross section microscopy of the bladder moulded sample

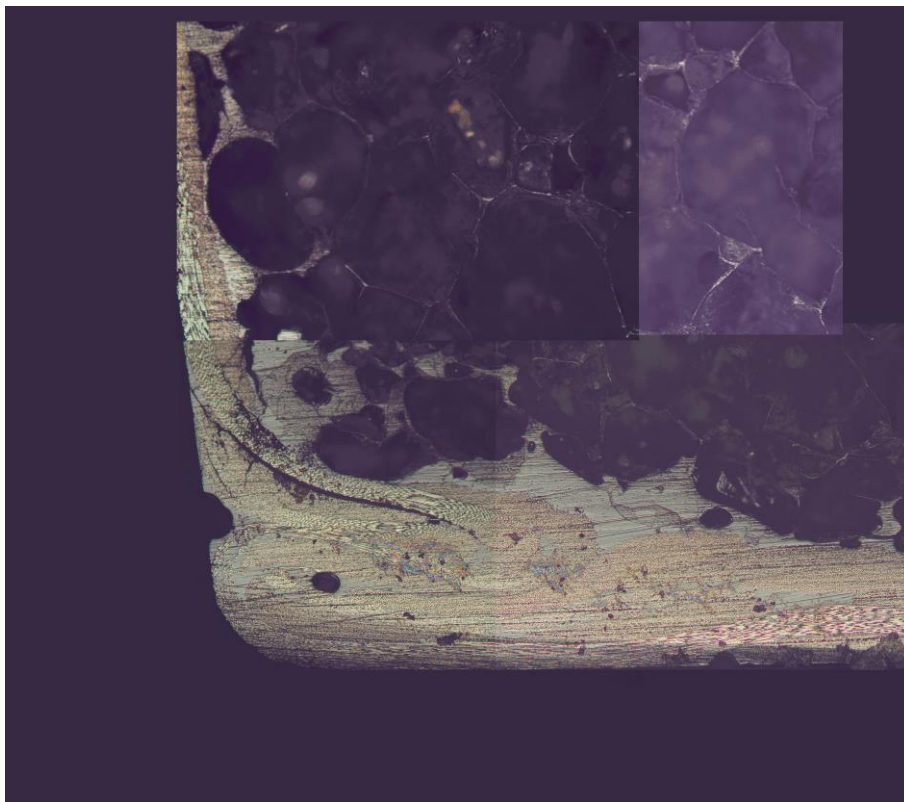


Figure 95 Cross section microscopy of the compression moulded sample

## 9. CONCLUSION

Two different concepts were tested, bladder moulding and compression moulding. There was used Textreme fiber with a wet-lay-up process for the bladder moulded samples and a pre-preg material was used for the compression moulded samples. The compression moulded process is believed to be the best process when it comes to reliability of the samples. They are however more expensive to make and is therefore not suitable for a prototype. A new method is suggested for prototype production. This process involves pre-preg material in a bladder moulding process with closed ends on the mould.

An optimization program was designed to create an optimized lay-up for the compression moulded samples. The structure of this program seems to work, but the lay-up generated is not the best possible lay-up. The conclusion is that this is caused by two factors. There are two main reasons for this. There are too many variables in the simulation and the ply size is too small. The simulation would benefit of having fewer and larger plies. There is also an issue with the simulation. Abaqus seemed to ignore the difference between a continuous ply and a non-continuous ply. The reason for this was not found, and will therefore need further investigation.

Unfortunately, no test results were logged when the samples were tested. These results would have been used for calibration of the simulation results. However, the failure modes were discussed to see if there was correspondence with the simulations.

Since the bladder moulded spar weights around 170g grams, there is very lite weight to be saved. The focus should therefore be changed to improving the quality of the product. The compression mould technique seemed more promising than the bladder moulding technique when the cross section of the samples were studied, but this is an expensive alternative for a prototype. It is therefore recommended to stay with the bladder moulding technique and try to improve the quality of the sample by using pre-preg materials and end plated on the mould.

## 10. FUTURE WORK

When it comes to the optimization of composites there is still a long way to go. This thesis is however a good start. The further work should focus on finding a new way to assign the lay-up iterations to the Abaqus sets with larger continuous plies. Find a way to vary the size of the sets so the ply can have different sizes. This would require some kind of “if” statement within the Isight loop.

This can be done by building the lay-up with the simulation. The optimization program will make a set in the region where the sample fail in the simulation, and add a ply to this area and run the simulation again. This would be continued until the sample could take the load without failing.

The focus should be changed from saving weight to increase the production quality of the product. The compression moulding technique seems to be processing for a production model. This concept needs further testing because the fiber used in this thesis did not reach the recommended curing temperature. It is recommended to make new samples that is cured at the right temperature.

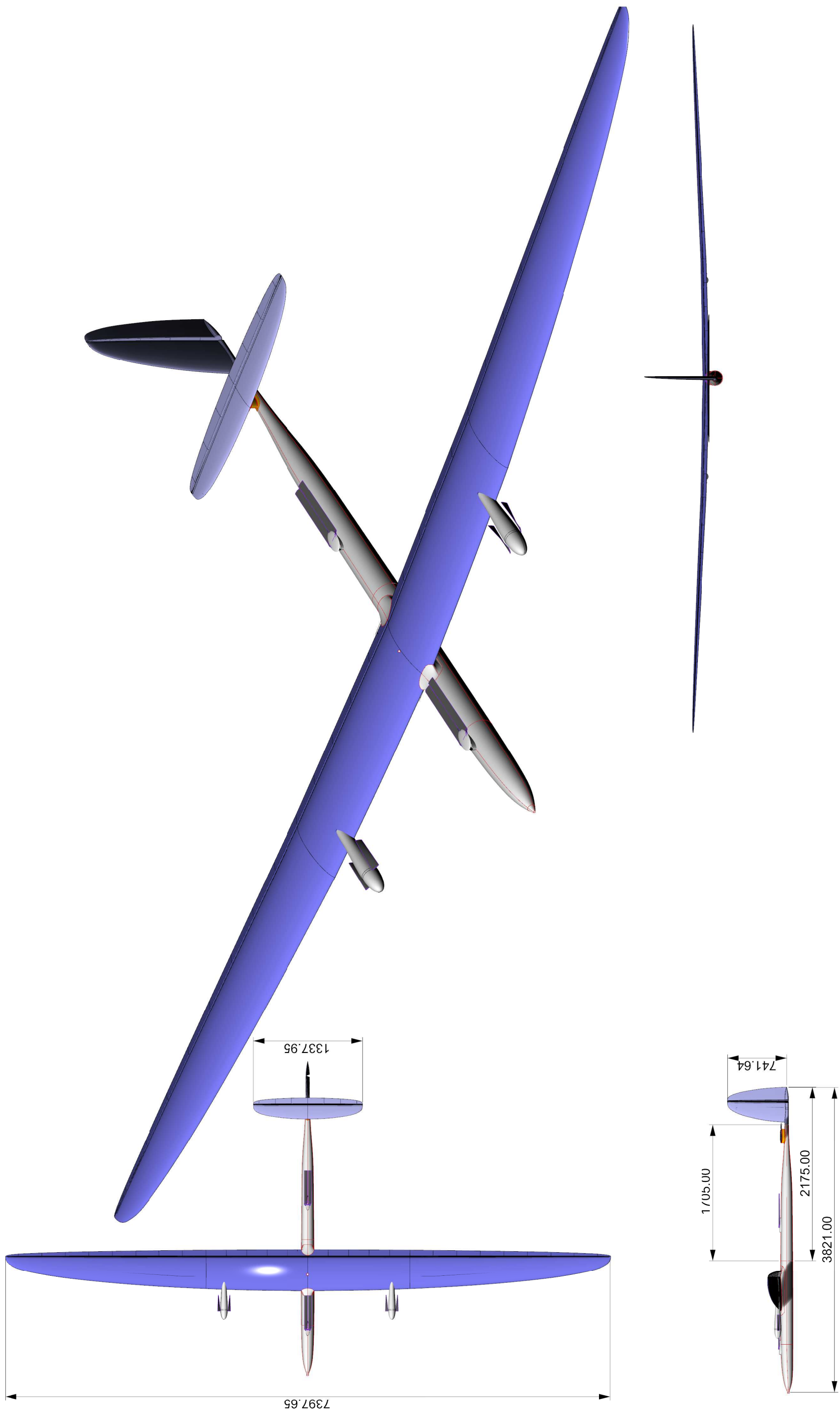
For the prototype, it is recommended to continue with the bladder moulded sample. The material should however be changed to a pre-peg, and there should be end plates on the mould.

## SOURCES

1. Abaqus Documentation 6.13. 28.1.1 Solid (continuum) elements: Abaqus 6.13; [cited 2017 26.07]. Available from: <http://129.97.46.200:2080/v6.13/books/usb/default.htm?startat=pt06ch28s01alm01.html>.
2. United Nations Framework Convention on Climate Change. The Paris Agreement. 2015.
3. Kitemill. 2008 [Available from: [www.kitemill.no](http://www.kitemill.no)].
4. John D. Anderson J. Fundamentals of Aerodynamics. 2nd Edition ed: MxGraw-Hill,Inc.; 1991.
5. Cook MV. Flight dynamics principles : a linear systems approach to aircraft stability and control. 3rd ed. ed. Amsterdam ;: Butterworth-Heinemann; 2013.
6. Abaqus Documentation 6.13. 3.6.8 Transverse shear stiffness in composite shells and offsets from the midsurface: Abaqus 6.13; [Available from: <http://129.97.46.200:2080/v6.13/books/stm/default.htm>].
7. Abaqus Documentation 6.13. 29.6.2 Choosing a shell element: Abaqus 6.13; [Available from: <http://129.97.46.200:2080/v6.13/books/usb/default.htm?startat=pt06ch29s06abo27.html>].
8. Abaqus Documentation 6.13. Shell element overview: Abaqus 6.13; [ 6.13:[Available from: <http://129.97.46.200:2080/v6.13/books/stm/default.htm>].
9. Abaqus Documentation 6.13. 6.2.2 Static stress analysis: Abaqus 6.13; [Available from: <http://129.97.46.200:2080/v6.13/books/usb/default.htm>].
10. Kollár LP, Springer GS. Mechanics of Composite Structures. New York, UNITED STATES: Cambridge University Press; 2003.
11. ASTM. Standard Guide for Testing Polymer Matrix Composite Materials 2016 [Available from: <https://www.astm.org/Standards/D4762.htm>].
12. ASTM. Testing Fabric-Reinforced "Textile" composite materials 2016 [Available from: <https://www.astm.org/Standards/D6856.htm>].
13. ASTM. Standard Test Method for Tensile Properties of Polymer Matrix Composite Materials 2014 [Available from: <https://www.astm.org/Standards/D3039.htm>].
14. ASTM. Standard Test Method for In-Plane Shear Response of Polymer Matrix Composite Materials by Tensile Test of a 645° Laminate 2013 [Available from: <https://www.astm.org/Standards/D3518.htm>].
15. ASTM. Standard Test Method for Compressive Properties of Polymer Matrix Composite Materials Using a Combined Loading Compression (CLC) Test Fixture 2014 [Available from: <https://www.astm.org/Standards/D6641.htm>].
16. Dassault Sys-temes. Isight documentation. 2006.
17. Evonik. Evonik; [Moisture Management: Moisture Uptake Is Reversible]. Available from: <http://www.rohacell.com/product/rohacell/en/processing/moisture-management/Pages/default.aspx>.

## APPENDIX

<u>KITEMILL SPARK 30KW .....</u>	<u>1</u>
<u>TECHNICAL DATASHEET TEXTREME 76 GSM .....</u>	<u>2</u>
<u>TECHNICAL DATASHEET RENLAM M1 EPOXY SYSTEM.....</u>	<u>3</u>
<u>TECHNICAL DATASHEET CHEMLEASE MPP 712 EZ .....</u>	<u>4</u>
<u>TECHNICAL DATASHEET CHEMLEASE 2185.....</u>	<u>5</u>
<u>TECHNICAL DATASHEET ARALDITE 4858 .....</u>	<u>6</u>
<u>PYTHON SCRIPT FOR OPTIMIZATION .....</u>	<u>7</u>
<u>TECHNICAL DATASHEET SPRAYMAX 2K CLEARCOAT .....</u>	<u>8</u>
<u>TECHNICAL DATASHEET HEXPLY 6376 .....</u>	<u>9</u>
<u>TECHNICAL DATASHEET ROHACELL IG / IG-F .....</u>	<u>10</u>
<u>RISK ASSESMENT.....</u>	<u>11</u>



# KITEMILL SPARK 30 kW

TeXtreme 76 PW M30SCWO/20:38/20:38-1000

## SPREAD TOW FABRIC SPECIFICATION

Warp tape: M30SC 18K 50C 38 gsm

Weft tape: M30SC 18K 50C 38 gsm

Stabilizing material: NM688 10 gsm

Total fiber weight: 76 gsm

Weave pattern: Plain Weave

Sizing: Epoxy compatible

Width of tape 0° /90° : 20 / 20 mm

Width of fabric: 1000 mm

Thickness of one ply laminate @ 60% Vf: 0.076 mm

## DISCLAIMER

The information in this technical data sheet is in accordance with Oxeon's information and from reliable sources, and, as far as Oxeon knows, correct at the stated date of revision based upon the state-of-the-art at that point in time. Whereas Oxeon believes that it has taken care to assemble this information, the information is provided "as is" and Oxeon does not warrant the accuracy, completeness, or usefulness of the information.

The information is intended for the purpose of guidance for safe handling, use, storage, transport etc. of this material and shall not be considered to constitute a warranty or representation of any kind, legal or other, or a quality specification. The information is specific to the named material(s) and does not apply for this material used in combination with any other material or processed together with another material unless explicitly stated in this text. The methods of your handling, storage and use of this product (and whether such use is suitable for this product, or if the product is used correctly in accordance with Oxeon's instructions or recommendations or not) are not within Oxeon's control and therefore, Oxeon disclaims all legal liability in relation to you, including, but not limited to, indirect damages.

Oxeon's legal responsibilities as regards product liability in relation to consumers shall, however, not be affected by this disclaimer to the extent that such legislation is compulsory in the applicable jurisdiction.

Notwithstanding the foregoing, Oxeon reserves the right of recourse in relation to you for any such undertakings.

All sales are made subject to our standard terms and conditions of sales (available at [www.oxeon.se](http://www.oxeon.se)) which include limitations on liability and other aspects. The fabric style listed here may not be available from inventory, and minimum order quantities may apply.



---

## Laminating Resin

### RenLam M-1 / Ren<sup>®</sup> HY 956

#### Low viscosity unfilled epoxy system

---

##### Key properties

- Low shrinkage and high dimensional stability
- High mechanical strength
- Highly compatible with glass fabrics and fillers

---

##### Applications

- Construction of jigs, foundry patterns and tooling aids

---

##### Product data

Property	Unit	RenLam M-1	Ren HY 956
Appearance Colour	visual	Liquid Pale yellow	Liquid Clear, pale yellow
Viscosity at 25°C	mPas	1250 – 1600	370 - 470
Density	g/cm <sup>3</sup>	1.1	1.0

---

##### Processing

Mix ratio	Parts by weight
RenLam M-1	100
Ren HY 956	20

Mix the two components thoroughly in the ratio indicated, then impregnate each layer of cloth as it is laid up to construct the laminate.  
Post-curing will improve final properties.

---

## Properties

Resin/Hardener mix:	Volume	Unit	M – 1 HY 956
Appearance			Liquid Pale yellow
Viscosity at 25°C		mPa s	1200
Pot life at 25°C	500 ml	min	30
Demoulding time		h	24

*After cure: 7 days at RT or 14 hours at 40 °C*

Density	ISO 1183	g/cm <sup>3</sup>	1.1
Deflection temperature	ISO 75	°C	50

---

## Storage

The resin and hardeners described in this instruction sheet have the shelf lives shown provided they are stored at 6 - 28°C in a dry place and sealed containers, preferably those in which they are supplied.

---

## Working conditions

The product should be used when in the temperature range 18-25°C.

---

## Packaging

System	M-1	HY 956
Quantity and Weight	4 x 5kg	6 x 1kg
Quantity and Weight	1 x 25kg	4 x 5kg
Quantity and Weight	1 x 225kg	-

---

## Handling precautions

### Caution

Vantico products are generally quite harmless to handle provided that certain precautions normally taken when handling chemicals are observed. The uncured materials must not, for instance, be allowed to come into contact with foodstuffs or food utensils, and measures should be taken to prevent the uncured materials from coming in contact with the skin, since people with particularly sensitive skin may be affected. The wearing of impervious rubber or plastic gloves will normally be necessary; likewise the use of eye protection. The skin should be thoroughly cleansed at the end of each working period by washing with soap and warm water. The use of solvents is to be avoided. Disposable paper - not cloth towels - should be used to dry the skin. Adequate ventilation of the working area is recommended. These precautions are described in greater detail in Vantico publication No. 24264/3/e Hygienic precautions for handling plastics products of Vantico and in the Vantico Material Safety Data sheets for the individual products. These publications are available on request and should be referred to for fuller information.

---

## Vantico Limited Adhesives and Tooling

All recommendations for the use of our products, whether given by us in writing, verbally, or to be implied from the results of tests carried out by us, are based on the current state of our knowledge. Notwithstanding any such recommendations the Buyer shall remain responsible for satisfying himself that the products as supplied by us are suitable for his intended process or purpose. Since we cannot control the application, use or processing of the products, we cannot accept responsibility therefor. The Buyer shall ensure that the intended use of the products will not infringe any third party intellectual property rights. We warrant that our products are free from defects in accordance with and subject to our general conditions of supply.

Duxford, Cambridge  
England CB2 4QA

Tel: +44 (0) 1223 493 000  
Fax: +44 (0) 1223 493 002

[www.renshape.com](http://www.renshape.com)

© Vantico Ltd, 2002

® Ren and RenShape are registered trademarks of Vantico AG, Basel, Switzerland

## Chemlease® MPP 712 EZ

### Mold Prep and Primer

Chemlease® MPP 712 EZ is formulated for sealing tooling in both the FRP and advanced composites sectors. Appropriate substrates include polyester gelcoat and non-gelcoat, epoxy and phenolic mold surfaces, and most metals. Chemlease® MPP 712 EZ is not recommended for sealing monolithic graphite or ceramic tooling.

#### General

Chemlease® MPP 712 EZ should be applied onto a clean mold surface. Chemlease® MPP 712 EZ is an excellent sealing material, but should not be used as a mold release agent. Use of this product without a release agent may result in severe damage to the mold. It has the ability to enhance the performance of semi-permanent release agents. In many cases, it has also been used as a means of re-surfacing a worn-out mold. The appropriate Chemlease® releasant should be applied on top of the product after it has been cured. For sealing purposes, a wipe on/wipe off application technique is used. To resurface a mold, use of a wipe on/leave on technique is typical.

#### Mold Preparation

1. After the mold has been buffed and polished with rubbing and polishing compounds, wash the mold surface thoroughly with clean water. The proper water wash will remove all fillers and water-soluble contaminants from the buffing and polishing compounds. Use liberal amounts of water. Wipe dry with clean cotton cloths (we recommend Chemlease® Cotton Cloth).
2. Following the water wash, apply Chemlease® Mold Cleaner EZ to remove all traces of solvent-soluble contaminants such as waxes, silicones, oils, etc. Use liberal quantities of Chemlease® Mold Cleaner EZ in a well-ventilated area, then wipe dry with clean cotton cloths until the mold is "squeaky clean" by thumb or hand rub test.

3. The wiping cloth should be changed regularly to ensure that a clean, absorbent surface of the wiping cloth is always presented to the mold surface. This procedure prevents recontamination of the mold by wiping cloths which carry contaminants lifted from the mold.

#### Application Instructions – Wipe On/Leave On

1. Apply Chemlease® MPP 712 EZ by wiping. Use clean, soft cotton cloths. A wipe on/leave on technique can be used, even for "Class A" finish molds, applying to an area of about four square feet at a time. Care should be taken on large structures to ensure that the overlap area is as small as possible and that the product on the area overlapped has not already cured. Generally, 1 or 2 coats are sufficient to seal. For sealing porous tooling blocks usually 6 – 12 coats are needed, which depends on the structure and material (PU or epoxy resin of different densities) and has to be individually tested before. Allow 30 minutes between each coat. After the final coat, allow a 1-2 hour cure at room temperature. The cure time can be reduced to 20 minutes by warming mold to 49-60°C. Note: a prismatic sheen may develop on the mold surface using this method. This sheen does *not* imprint onto the molded part in most situations.
2. When the product has cured, apply the appropriate Chemlease® mold release. Please refer to the proper Product Data Sheet for mold release application details and instructions.

#### Application Instructions – Wipe On/ Wipe Off

Follow instructions for Wipe On/Leave On. However, after material is wiped on, wipe off immediately using a clean, dry, soft cotton cloth being careful to wipe off evenly. Change cloths frequently for best results. Once material has begun to dry and cure, it will not be possible to wipe off without causing blemishes and streaks so it is important to wipe the sealer off immediately after it has been wiped on and is still wet. Generally, 1 or 2 wipe on/wipe off coats are sufficient to seal.

**PRODUCT DATA****Touch-Up Coats**

Touch-up coats are not possible once this product is applied and cured since a release agent must be applied over the top of it before the mold can be used in production.

**Cure Test**

Under the best conditions, Chemlease® MPP 712 EZ has been found to cure in as little as one hour. A simple test method for complete cure is: Apply one drop each of water and Chemlease® Mold Cleaner EZ onto a flange area that has been coated with the product. Wait a few seconds then wipe off with a clean cloth. If there is no evidence of the drops on the tool surface, the product is completely cured.

**Important**

The recommended number of coats and cure times are a general guideline found to be sufficient in a broad spectrum of molding conditions. When molding products with extreme geometries or experiencing low-humidity conditions in the shop, the customer may find it necessary to extend the cure time between coats and increase the number of coats applied to the mold. The efficiency of a release film is best determined through a combination of tape tests and experimentation.

**Storage**

The container should be kept closed at all times when not in use to prevent contamination, evaporation and/or premature curing. Do not store at temperatures above 38°C. Chemlease® MPP 712 EZ is flammable. Keep away from heat, sparks, flames and combustion sources during storage and use. If stored in cold temperatures, allow to warm to room temperature before using.

**Handling**

For more information, request a copy of Chem-Trend's Material Safety Data Sheet. Do not use if the use by date has been exceeded.

**Packaging**

Chemlease® MPP 712 EZ is available in container with 0,93 kg.

**Further Information**

Request information on our complete range of materials for this industry.

The information contained in this document is given in good faith based on our current knowledge. It is only an indication and in no way binding, particularly as regards infringement of or prejudice to third party rights through the use of our products. Chem-Trend warrants only that its products will meet its sales specifications. This information must on no account be used as a substitute for necessary prior tests which alone can ensure that a product is suitable for a given use. Users are requested to check that they are in possession of the latest version of this document and Chem-Trend is at their disposal to supply any additional information.

**Edition: 13.04.2012**

Amber Drive, Langley Mill  
Nottingham, NG16 4BE UK  
Tel: +44 (0) 1773 530899  
Fax: +44 (0) 1773 768687

E-mail: [tcacsales@tencate.com](mailto:tcacsales@tencate.com)

[www.tencateperformancecomposites.com](http://www.tencateperformancecomposites.com)

PRODUCT DATA

# Chemlease® 2185

## Semi-Permanent Release Agent for Composites

### Description

Chemlease® 2185 is a semi permanent, room-temperature curing release agent, effective for composites including polyester molding. It gives easy, multiple releases and does not require an extended cure. It is a ready-to-use liquid dispersion.

### Mold Preparation/Cleaning

Because Chemlease® semi-permanent release agents polymerize on the mold surface, all traces of prior release agents, sealers and buffers/polishes must be removed from the mold.

This method will remove not only wax release agents, but also waxes, silicones and water solubles that are contained in buffing and rubbing compounds. To clean the mold following buffing, take the following steps:

1. Using liberal quantities of clean water, wipe the mold with a clean, soft, lint-free 100% cotton cloth (in the following it is called just cloth) and wipe until dry (we recommend to use our Chemlease® Cotton Cloth).
2. Soak another clean, soft, lint-free cloth with a Mold Cleaner (we recommend to use our Chemlease® Mold Cleaner EZ).
3. Apply the cleaner to the mold surface.
4. Before the cleaner dries, use a second clean cloth to wipe off the dissolved wax and other contaminants.
5. Continue steps 3 and 4 until the surface is free of wax. When all traces of prior release agent have been removed, the hand/thumb will skid, and not slip, across the mold surface.

### Application

The ideal temperature of the mold for application is between 18-27°C.

If Chemlease® 2185 is applied below 18°C, allow a longer time than generally recommended for room-temperature curing. If applied when the mold surface is over 27°C, curing will be faster.

1. Shake or mix well before and during use. Soak a clean cloth until it is thoroughly wet.

2. Starting at one end of the mold, wipe a generous wet film over a section of about 0,5 m².
3. Repeat until the mold is completely covered. (see note after "5" which applies to very large molds)
4. Check the treated mold for any area that appears uncoated (where haze is not present). Coat as above.
5. After the product has dried to a haze on the mold surface, polish with a cotton cloth until a high gloss is obtained. To ensure that no release agent is re-deposited onto the mold, change cloth frequently.
 

**Note:** Do not allow any product to remain dry (hazed) for any longer than 30 minutes as it will become very difficult to buff out
6. Repeat steps 1-6 an additional four times for a total of five coats of Chemlease® 2185. This will allow the release agent to seal any mold pores and will give the necessary film thickness to permit multiple releases. A final polish with a clean cotton cloth will achieve a higher, Class A, gloss.
7. A cure time of 30 minutes is recommended prior to molding parts.

### Touch-Up Coats

As parts are removed from the mold, abrasion will gradually wear away the release film. When slight sticking is noticed, maintain the film by applying one or two touch-up coats (as required) as described above.

Molders should experience no buildup with Chemlease® 2185. Previously-applied Chemlease® does not have to be removed prior to touch-up. If the mold surface contains buildup of materials such as styrene, internal mold releases, UV absorbers, gel coats, "top coats" or other mold contaminants, clean the mold with a Chemlease® Mold Cleaner as specified under Mold Preparation/Cleaning.

# Chemlease® 2185

## Semi-Permanent Release Agent

**Important:**

The recommended number of coats and cure times are a general guideline found to be more sufficient in a broad spectrum of molding conditions. When molding products with extreme geometries or experiencing low-humidity conditions in the shop, the customer may find the need to extend the cure time between coats and increase the number of coats applied to the mold. The efficiency of a release film is best determined through a combination of tape tests and experimentation.

**Packaging**

Chemlease® 2185 is available in container with 0,69 kg and 3,4 kg.

**Safety Data**

For more information on storage, handling, hazards, etc., please request a copy of Chem-Trend's Material Safety Data Sheet, which must be consulted prior to use of this product.

**Further Information**

Request information on our complete range of materials for this industry from your Chem-Trend sales representative

The information contained in this document is given in good faith based on our current knowledge. It is only an indication and in no way binding, particularly as regards infringement of or prejudice to third party rights through the use of our products. Chem-Trend warrants only that its products will meet its sales specifications. This information must on no account be used as a substitute for necessary prior tests which alone can ensure that a product is suitable for a given use. Users are requested to check that they are in possession of the latest version of this document and Chem-Trend is at their disposal to supply any additional information.

**Edition 08.02.2013**

Amber Drive, Langley Mill  
Nottingham, NG16 4BE UK  
Tel: +44 (0) 1773 530899  
Fax: +44 (0) 1773 768687

E-mail: [tcacsales@tencate.com](mailto:tcacsales@tencate.com)

[www.tencateperformancecomposites.com](http://www.tencateperformancecomposites.com)

**Advanced Materials****Araldite® AW4858/ Hardener HW4858**

Structural Adhesives

**ARALDITE® AW4858/ Hardener HW4858  
Two component epoxy adhesive system****Key properties**

- Very high lap shear and peel strength
- Bonds a wide variety of materials (metal, composite and thermoplastics)
- Good moisture resistance
- Extremely tough and resilient adhesive
- Long pot life, ideal for large composite part assemblies

**Description**

ARALDITE® AW 4858/ Hardener HW 4858 is a two-component room temperature curing black coloured epoxy adhesive paste of high strength and toughness. Performances can be enhanced by post-curing at elevated temperature. It is suitable for bonding a wide variety of metals, and especially designed for bonding composites..

**Product data**

Property	Araldite® AW4858	Hardener HW4858	Mixed Adhesive
Colour (visual)	Black	Yellowish	Black
Specific gravity	1.2	1.0	approx. 1.1
Viscosity at 20°C (Pa.s)	20 - 30	2 - 5	thixotropic
Pot Life (100 gm at 25°C)			150 min

**Processing****Pretreatment**

The strength and durability of a bonded joint are dependent on proper treatment of the surfaces to be bonded.

At the very least, joint surfaces should be cleaned with a good degreasing agent such as acetone, iso-propanol (for plastics) or other proprietary degreasing agents in order to remove all traces of oil, grease and dirt.

Low grade alcohol, gasoline (petrol) or paint thinners should never be used.

The strongest and most durable joints are obtained by either mechanically abrading or chemically etching ("pickling") the degreased surfaces. Abrading should be followed by a second degreasing treatment

Mix ratio	Parts by weight	Parts by volume
Araldite® AW4858	100	100
Hardener HW4858	42	50

The resin and hardener should be blended until they form a homogeneous mix.

Araldite® AW4858/ Hardener HW 4858 is available in cartridges incorporating mixers and can be applied as ready to use adhesive with the aid of the tool recommended by Huntsman Advanced Materials

**Application of adhesive**

The resin/hardener mix is applied with a spatula, to the pretreated and dry joint surfaces.

A layer of adhesive 0.05 to 0.10 mm thick will normally impart the greatest lap shear strength to the joint.

The joint components should be assembled and clamped as soon as the adhesive has been applied. An even contact pressure throughout the joint area will ensure optimum cure.

**Mechanical processing**

Specialist firms have developed metering, mixing and spreading equipment that enables the bulk processing of adhesive.

We will be pleased to advise customers on the choice of equipment for their particular needs.

**Equipment maintenance**

All tools should be cleaned with hot water and soap before adhesives residues have had time to cure. The removal of cured residues is a difficult and time-consuming operation.

If solvents such as acetone are used for cleaning, operatives should take the appropriate precautions and, in addition, avoid skin and eye contact.

**Times to minimum shear strength**

Temperature	°C	23	40	60	100
Cure time to reach	hours	6			
LSS > 1N/mm <sup>2</sup>	minutes		90	25	< 5
Cure time to reach	hours	7	2		
LSS > 10N/mm <sup>2</sup>	minutes			35	15

LSS = Lap shear strength.

**Typical cured properties**

Unless otherwise stated, the figures given below were all determined by testing standard specimens made by lap-jointing 114 x 25 x 1.6 mm strips of aluminium alloy. The joint area was 12.5 x 25 mm in each case.

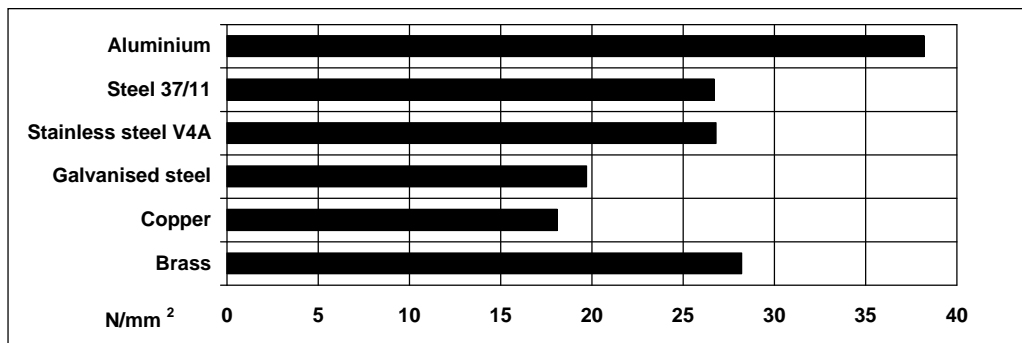
The figures were determined with typical production batches using standard testing methods. They are provided solely as technical information and do not constitute a product specification.

Note: The data in this edition is based on recent retesting of the product.

### Average lap shear strengths of typical metal-to-metal joints (ISO 4587)

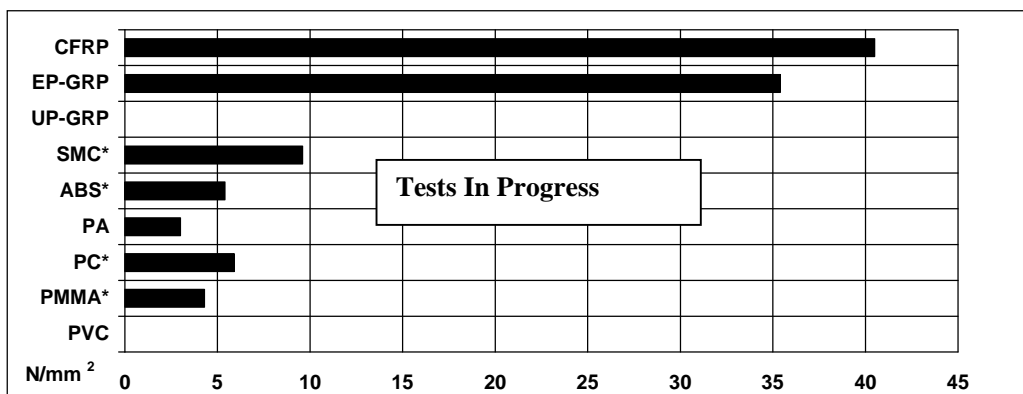
Cured for 16 hours at 40°C and tested at 23°C

Pretreatment - Sand blasting



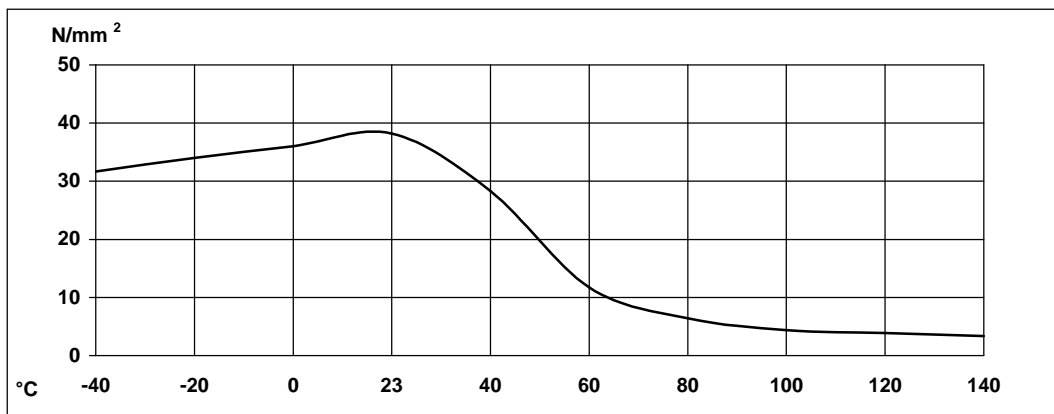
### Average lap shear strengths of typical plastic-to-plastic joints (ISO 4587)

Cured for 16 hour at 40°C and tested at 23°C. Pretreatment - Lightly abrade and alcohol degrease.



### Lap shear strength versus temperature (ISO 4587) (typical average values)

Cure: 16 hrs at 40°C, bonding on aluminium sandblasted and degreased



### Glass transition temperature

Cure: 16 hours at 40°C

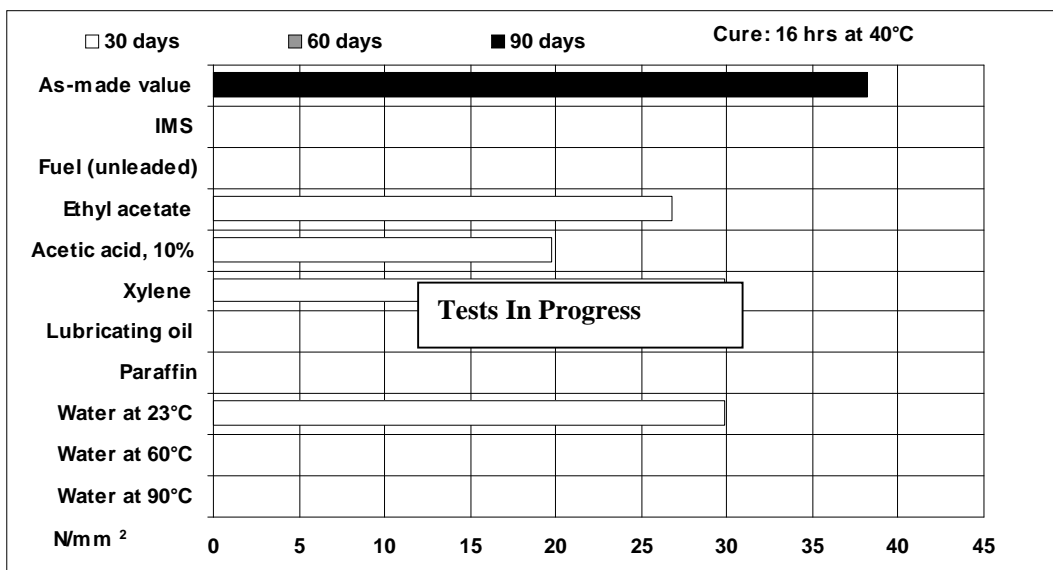
56°C by DSC

Cure: 16 hours at 40°C+ 1hour at 80°C

67°C by DSC

### Lap shear strength versus immersion in various media (typical average values)

Unless otherwise stated, L.S.S. was determined after immersion for 30,60 and 90 days at 23°C



### Tensile strength at 23°C (ISO 527)

31 MPa

E-modulus

1600 MPa

Elongation at break

7 %

### Flexural strength at 23°C (ISO178)

61 MPa

Flexural modulus

1650 MPa

### Shore Hardness (D scale) (ISO 868/03)

Cure 16 hours/ 40°C , tested at 23°C,

75 D

50%RH

### Shear modulus G'(ISO 6721)

Cure: 16 hours/ 40°

-40°C - 1.3 GPa

0°C - 980 MPa

23°C - 800 Mpa

60°C - 9.0 MPa

90°C - 7.2 MPa

---

**Storage**

ARALDITE® AW 4858 and Hardener HW 4858 may be stored for up to 3 years at room temperature provided the components are stored in sealed containers. The expiry date is indicated on the label.

---

**Handling precautions****Caution**

Our products are generally quite harmless to handle provided that certain precautions normally taken when handling chemicals are observed. The uncured materials must not, for instance, be allowed to come into contact with foodstuffs or food utensils, and measures should be taken to prevent the uncured materials from coming in contact with the skin, since people with particularly sensitive skin may be affected. The wearing of impervious rubber or plastic gloves will normally be necessary; likewise the use of eye protection. The skin should be thoroughly cleansed at the end of each working period by washing with soap and warm water. The use of solvents is to be avoided. Disposable paper - not cloth towels - should be used to dry the skin. Adequate ventilation of the working area is recommended. These precautions are described in greater detail in the Material Safety Data sheets for the individual products and should be referred to for fuller information.

---

**Huntsman Advanced Materials**

All recommendations for the use of our products, whether given by us in writing, verbally, or to be implied from the results of tests carried out by us, are based on the current state of our knowledge. Notwithstanding any such recommendations the Buyer shall remain responsible for satisfying himself that the products as supplied by us are suitable for his intended process or purpose. Since we cannot control the application, use or processing of the products, we cannot accept responsibility therefor. The Buyer shall ensure that the intended use of the products will not infringe any third party's intellectual property rights. We warrant that our products are free from defects in accordance with and subject to our general conditions of supply.

Huntsman Advanced Materials warrants only that its products meet the specifications agreed with the buyer. Typical properties, where stated, are to be considered as representative of current production and should not be treated as specifications.

The manufacture of materials is the subject of granted patents and patent applications; freedom to operate patented processes is not implied by this publication.

While all the information and recommendations in this publication are, to the best of our knowledge, information and belief, accurate at the date of publication, NOTHING HEREIN IS TO BE CONSTRUED AS A WARRANTY, EXPRESS OR OTHERWISE.

IN ALL CASES, IT IS THE RESPONSIBILITY OF THE USER TO DETERMINE THE APPLICABILITY OF SUCH INFORMATION AND RECOMMENDATIONS AND THE SUITABILITY OF ANY PRODUCT FOR ITS OWN PARTICULAR PURPOSE.

The behaviour of the products referred to in this publication in manufacturing processes and their suitability in any given end-use environment are dependent upon various conditions such as chemical compatibility, temperature, and other variables, which are not known to Huntsman Advanced Materials. It is the responsibility of the user to evaluate the manufacturing circumstances and the final product under actual end-use requirements and to adequately advise and warn purchasers and users thereof.

Products may be toxic and require special precautions in handling. The user should obtain Safety Data Sheets from Huntsman Advanced Materials containing detailed information on toxicity, together with proper shipping, handling and storage procedures, and should comply with all applicable safety and environmental standards.

Hazards, toxicity and behaviour of the products may differ when used with other materials and are dependent on manufacturing circumstances or other processes. Such hazards, toxicity and behaviour should be determined by the user and made known to handlers, processors and end users.

Except where explicitly agreed otherwise, the sale of products referred to in this publication is subject to the general terms and conditions of sale of Huntsman Advanced Materials LLC or of its affiliated companies including without limitation, Huntsman Advanced Materials (Europe) BVBA, Huntsman Advanced Materials Americas Inc., and Huntsman Advanced Materials (Hong Kong) Ltd.

Huntsman Advanced Materials is an international business unit of Huntsman Corporation. Huntsman Advanced Materials trades through Huntsman affiliated companies in different countries including but not limited to Huntsman Advanced Materials LLC in the USA and Huntsman Advanced Materials (Europe) BVBA in Europe.

Araldite is a registered trademark of Huntsman Corporation or an affiliate thereof.

Copyright © 2008 Huntsman Corporation or an affiliate thereof. All rights reserved.

**Huntsman Advanced Materials**

(Switzerland) GmbH  
Klybeckstrasse 200  
4057 Basel  
Switzerland

Tel: +41 (0)61 299 11 11  
Fax: +41 (0)61 299 11 12

[www.huntsman.com/advanced\\_materials](http://www.huntsman.com/advanced_materials)  
Email: [advanced\\_materials@huntsman.com](mailto:advanced_materials@huntsman.com)



## PYTHON SCRIPT

```
# -*- coding: utf-8 -*-
"""
Created on Mon May 01 12:22:47 2017

@author: ErikVassøy
"""

import openpyxl
wb = openpyxl.load_workbook('C:\Master\8 lag kitemill\sample.xlsx')
sheet = wb.get_sheet_by_name('Alt')

TOP1 = sheet['B1'].value
TOP2 = sheet['F1'].value
TOP3 = sheet['J1'].value
TOP4 = sheet['N1'].value
TOP5 = sheet['R1'].value
TOP6 = sheet['V1'].value

BOT1 = sheet['Z1'].value
BOT2 = sheet['AD1'].value
BOT3 = sheet['AH1'].value
BOT4 = sheet['AL1'].value
BOT5 = sheet['AP1'].value
BOT6 = sheet['AT1'].value

SIDE1 = sheet['BB1'].value
SIDE2 = sheet['BZ1'].value
SIDE3 = sheet['CD1'].value
SIDE4 = sheet['CH1'].value
SIDE5 = sheet['CL1'].value
SIDE6 = sheet['CP1'].value

# Abaqus start
start = """# -*- coding: mbc -*-
# Do not delete the following import lines
from abaqus import *
from abaqusConstants import *
import __main__

import section
import regionToolset
import displayGroupMdbToolset as dgm
import part
import material
import assembly
import step
import interaction
import load
import mesh
import optimization
import job
import sketch
import visualization
import xyPlot
import displayGroupOdbToolset as dgo
import connectorBehavior
layupOrientation = None

"""

#Abaqus macro for adding new layers
t1 = """p = mdb.models['Model-1'].parts['Part-1']
region"""
t2 = """=regionToolset.Region(skinFaces=(('""
t3 = """', faces), ))"""

#Information for first ply
t4 = """compositeLayup = mdb.models['Model-1'].parts['Part-1'].CompositeLayup(
name="""
```

```

t5 = "", description='', elementType=SHELL,
offsetType=BOTTOM_SURFACE, symmetric=False,
thicknessAssignment=FROM_SECTION)
compositeLayup.Section(preIntegrate=OFF, integrationRule=SIMPSON,
thicknessType=UNIFORM, poissonDefinition=DEFAULT, temperature=GRADIENT,
useDensity=OFF)
compositeLayup.ReferenceOrientation(orientationType=GLOBAL, localCsys=None,
fieldName='', additionalRotationType=ROTATION_NONE, angle=0.0,
axis=AXIS_3)

```

```

"""

```

```

TOP1f = t4 + "TOP1" + t5
TOP2f = t4 + "TOP2" + t5
TOP3f = t4 + "TOP3" + t5
TOP4f = t4 + "TOP4" + t5
TOP5f = t4 + "TOP5" + t5
TOP6f = t4 + "TOP6" + t5

```

```

BOT1f = t4 + "BOT1" + t5
BOT2f = t4 + "BOT2" + t5
BOT3f = t4 + "BOT3" + t5
BOT4f = t4 + "BOT4" + t5
BOT5f = t4 + "BOT5" + t5
BOT6f = t4 + "BOT6" + t5

```

```

SIDEF1f = t4 + "SIDEF1" + t5
SIDEF2f = t4 + "SIDEF2" + t5
SIDEF3f = t4 + "SIDEF3" + t5
SIDEF4f = t4 + "SIDEF4" + t5
SIDEF5f = t4 + "SIDEF5" + t5
SIDEF6f = t4 + "SIDEF6" + t5

```

```

SIDEB1f = t4 + "SIDEB1" + t5
SIDEB2f = t4 + "SIDEB2" + t5
SIDEB3f = t4 + "SIDEB3" + t5
SIDEB4f = t4 + "SIDEB4" + t5
SIDEB5f = t4 + "SIDEB5" + t5
SIDEB6f = t4 + "SIDEB6" + t5

```

```

t7 = ""compositeLayup.CompositePly(suppressed=False, plyName='Ply-""
t8 = "",
region=region""
t9 = "", material='Kitemill testet',
thicknessType=SPECIFY_THICKNESS, thickness=0.15,
orientationType=SPECIFY_ORIENT, orientationValue=""
t10 = "",
additionalRotationType=ROTATION_NONE, additionalRotationField='',
axis=AXIS_3, angle=0.0, numIntPoints=3)""

```

```

#Empty string for writing

```

```

TOP1a1 = ""
TOP1b1 = ""
TOP2a1 = ""
TOP2b1 = ""
TOP3a1 = ""
TOP3b1 = ""
TOP4a1 = ""
TOP4b1 = ""
TOP5a1 = ""
TOP5b1 = ""
TOP6a1 = ""
TOP6b1 = ""

```

```

BOT1a1 = ""
BOT1b1 = ""
BOT2a1 = ""
BOT2b1 = ""
BOT3a1 = ""
BOT3b1 = ""
BOT4a1 = ""
BOT4b1 = ""
BOT5a1 = ""

```

```
BOT5b1 = ""
BOT6a1 = ""
BOT6b1 = ""
```

```
SIDEF1a1 = ""
SIDEF1b1 = ""
SIDEF2a1 = ""
SIDEF2b1 = ""
SIDEF3a1 = ""
SIDEF3b1 = ""
SIDEF4a1 = ""
SIDEF4b1 = ""
SIDEF5a1 = ""
SIDEF5b1 = ""
SIDEF6a1 = ""
SIDEF6b1 = ""
```

```
SIDEB1a1 = ""
SIDEB1b1 = ""
SIDEB2a1 = ""
SIDEB2b1 = ""
SIDEB3a1 = ""
SIDEB3b1 = ""
SIDEB4a1 = ""
SIDEB4b1 = ""
SIDEB5a1 = ""
SIDEB5b1 = ""
SIDEB6a1 = ""
SIDEB6b1 = ""
```

```
# Write a1
for i1 in range(1, TOP1+1):
    TOP1a1+= t1 + '{}'.format(i1) + t2 + 'TOP1' + t3 + "\n\n"
for i2 in range(1, TOP2+1):
    TOP2a1+= t1 + '{}'.format(i2) + t2 + 'TOP2' + t3 + "\n\n"
for i3 in range(1, TOP3+1):
    TOP3a1+= t1 + '{}'.format(i3) + t2 + 'TOP3' + t3 + "\n\n"
for i4 in range(1, TOP4+1):
    TOP4a1+= t1 + '{}'.format(i4) + t2 + 'TOP4' + t3 + "\n\n"
for i5 in range(1, TOP5+1):
    TOP5a1+= t1 + '{}'.format(i5) + t2 + 'TOP5' + t3 + "\n\n"
for i6 in range(1, TOP6+1):
    TOP6a1+= t1 + '{}'.format(i6) + t2 + 'TOP6' + t3 + "\n\n"

for i7 in range(1, BOT1+1):
    BOT1a1+= t1 + '{}'.format(i7) + t2 + 'BOT1' + t3 + "\n\n"
for i8 in range(1, BOT2+1):
    BOT2a1+= t1 + '{}'.format(i8) + t2 + 'BOT2' + t3 + "\n\n"
for i9 in range(1, BOT3+1):
    BOT3a1+= t1 + '{}'.format(i9) + t2 + 'BOT3' + t3 + "\n\n"
for i10 in range(1, BOT4+1):
    BOT4a1+= t1 + '{}'.format(i10) + t2 + 'BOT4' + t3 + "\n\n"
for i11 in range(1, BOT5+1):
    BOT5a1+= t1 + '{}'.format(i11) + t2 + 'BOT5' + t3 + "\n\n"
for i12 in range(1, BOT6+1):
    BOT6a1+= t1 + '{}'.format(i12) + t2 + 'BOT6' + t3 + "\n\n"

for i13 in range(1, SIDEF1+1):
    SIDEF1a1+= t1 + '{}'.format(i13) + t2 + 'SIDEF1' + t3 + "\n\n"
for i14 in range(1, SIDEF2+1):
    SIDEF2a1+= t1 + '{}'.format(i14) + t2 + 'SIDEF2' + t3 + "\n\n"
for i15 in range(1, SIDEF3+1):
    SIDEF3a1+= t1 + '{}'.format(i15) + t2 + 'SIDEF3' + t3 + "\n\n"
for i16 in range(1, SIDEF4+1):
    SIDEF4a1+= t1 + '{}'.format(i16) + t2 + 'SIDEF4' + t3 + "\n\n"
for i17 in range(1, SIDEF5+1):
    SIDEF5a1+= t1 + '{}'.format(i17) + t2 + 'SIDEF5' + t3 + "\n\n"
for i18 in range(1, SIDEF6+1):
    SIDEF6a1+= t1 + '{}'.format(i18) + t2 + 'SIDEF6' + t3 + "\n\n"

for i19 in range(1, SIDEB1+1):
    SIDEB1a1+= t1 + '{}'.format(i19) + t2 + 'SIDEB1' + t3 + "\n\n"
for i20 in range(1, SIDEB2+1):
    SIDEB2a1+= t1 + '{}'.format(i20) + t2 + 'SIDEB2' + t3 + "\n\n"
```

```

for i21 in range(1, SIDEB3+1):
    SIDEB3a1+= t1 + '{}'.format(i21) + t2 + 'SIDEB3' + t3 + "\n\n"
for i22 in range(1, SIDEB4+1):
    SIDEB4a1+= t1 + '{}'.format(i22) + t2 + 'SIDEB4' + t3 + "\n\n"
for i23 in range(1, SIDEB5+1):
    SIDEB5a1+= t1 + '{}'.format(i23) + t2 + 'SIDEB5' + t3 + "\n\n"
for i24 in range(1, SIDEB6+1):
    SIDEB6a1+= t1 + '{}'.format(i24) + t2 + 'SIDEB6' + t3 + "\n\n"

# Write b1
for j1 in range(1, TOP1+1):
    TOP1b1+= t7 + '{}'.format(j1) + t8 + '{}'.format(j1) + t9 + str(sheet['C{}'.format(2 +
j1)].value) + t10 + "\n\n"
for j2 in range(1, TOP2+1):
    TOP2b1+= t7 + '{}'.format(j2) + t8 + '{}'.format(j2) + t9 + str(sheet['G{}'.format(2 +
j2)].value) + t10 + "\n\n"
for j3 in range(1, TOP3+1):
    TOP3b1+= t7 + '{}'.format(j3) + t8 + '{}'.format(j3) + t9 + str(sheet['K{}'.format(2 +
j3)].value) + t10 + "\n\n"
for j4 in range(1, TOP4+1):
    TOP4b1+= t7 + '{}'.format(j4) + t8 + '{}'.format(j4) + t9 + str(sheet['O{}'.format(2 +
j4)].value) + t10 + "\n\n"
for j5 in range(1, TOP5+1):
    TOP5b1+= t7 + '{}'.format(j5) + t8 + '{}'.format(j5) + t9 + str(sheet['S{}'.format(2 +
j5)].value) + t10 + "\n\n"
for j6 in range(1, TOP6+1):
    TOP6b1+= t7 + '{}'.format(j6) + t8 + '{}'.format(j6) + t9 + str(sheet['W{}'.format(2 +
j6)].value) + t10 + "\n\n"

for j7 in range(1, BOT1+1):
    BOT1b1+= t7 + '{}'.format(j7) + t8 + '{}'.format(j7) + t9 + str(sheet['AA{}'.format(2 +
j7)].value) + t10 + "\n\n"
for j8 in range(1, BOT2+1):
    BOT2b1+= t7 + '{}'.format(j8) + t8 + '{}'.format(j8) + t9 + str(sheet['AE{}'.format(2 +
j8)].value) + t10 + "\n\n"
for j9 in range(1, BOT3+1):
    BOT3b1+= t7 + '{}'.format(j9) + t8 + '{}'.format(j9) + t9 + str(sheet['AI{}'.format(2 +
j9)].value) + t10 + "\n\n"
for j10 in range(1, BOT4+1):
    BOT4b1+= t7 + '{}'.format(j10) + t8 + '{}'.format(j10) + t9 + str(sheet['AM{}'.format(2 +
j10)].value) + t10 + "\n\n"
for j11 in range(1, BOT5+1):
    BOT5b1+= t7 + '{}'.format(j11) + t8 + '{}'.format(j11) + t9 + str(sheet['AQ{}'.format(2 +
j11)].value) + t10 + "\n\n"
for j12 in range(1, BOT6+1):
    BOT6b1+= t7 + '{}'.format(j12) + t8 + '{}'.format(j12) + t9 + str(sheet['AU{}'.format(2 +
j12)].value) + t10 + "\n\n"

for j13 in range(1, SIDEF1+1):
    SIDEF1b1+= t7 + '{}'.format(j13) + t8 + '{}'.format(j13) + t9 + str(sheet['AY{}'.format(2 +
j13)].value) + t10 + "\n\n"
for j14 in range(1, SIDEF2+1):
    SIDEF2b1+= t7 + '{}'.format(j14) + t8 + '{}'.format(j14) + t9 + str(sheet['BC{}'.format(2 +
j14)].value) + t10 + "\n\n"
for j15 in range(1, SIDEF3+1):
    SIDEF3b1+= t7 + '{}'.format(j15) + t8 + '{}'.format(j15) + t9 + str(sheet['BG{}'.format(2 +
j15)].value) + t10 + "\n\n"
for j16 in range(1, SIDEF4+1):
    SIDEF4b1+= t7 + '{}'.format(j16) + t8 + '{}'.format(j16) + t9 + str(sheet['BK{}'.format(2 +
j16)].value) + t10 + "\n\n"
for j17 in range(1, SIDEF5+1):
    SIDEF5b1+= t7 + '{}'.format(j17) + t8 + '{}'.format(j17) + t9 + str(sheet['BO{}'.format(2 +
j17)].value) + t10 + "\n\n"
for j18 in range(1, SIDEF6+1):
    SIDEF6b1+= t7 + '{}'.format(j18) + t8 + '{}'.format(j18) + t9 + str(sheet['BS{}'.format(2 +
j18)].value) + t10 + "\n\n"

for j19 in range(1, SIDEB1+1):
    SIDEB1b1+= t7 + '{}'.format(j19) + t8 + '{}'.format(j19) + t9 + str(sheet['BW{}'.format(2 +
j19)].value) + t10 + "\n\n"
for j20 in range(1, SIDEB2+1):
    SIDEB2b1+= t7 + '{}'.format(j20) + t8 + '{}'.format(j20) + t9 + str(sheet['CA{}'.format(2 +
j20)].value) + t10 + "\n\n"
for j21 in range(1, SIDEB3+1):
    SIDEB3b1+= t7 + '{}'.format(j21) + t8 + '{}'.format(j21) + t9 + str(sheet['CE{}'.format(2 +
j21)].value) + t10 + "\n\n"
for j22 in range(1, SIDEB4+1):

```

```

        SIDEB4b1+= t7 + '{}'.format(j22) + t8 + '{}'.format(j22) + t9 + str(sheet['CI{}'.format(2 +
j22)].value) + t10 + "\n\n"
for j23 in range(1, SIDEB5+1):
    SIDEB5b1+= t7 + '{}'.format(j23) + t8 + '{}'.format(j23) + t9 + str(sheet['CM{}'.format(2 +
j23)].value) + t10 + "\n\n"
for j24 in range(1, SIDEB6+1):
    SIDEB6b1+= t7 + '{}'.format(j24) + t8 + '{}'.format(j24) + t9 + str(sheet['CQ{}'.format(2 +
j24)].value) + t10 + "\n\n"

```

```

# Print macro for Abaqus

```

```

with open('userscript_cae_pre.py', 'w') as f:

```

```

    f.write(start + TOP1a1 + TOP1f + TOP1b1 + TOP2a1 + TOP2f + TOP2b1 + TOP3a1 + TOP3f + TOP3b1
+ TOP4a1 + TOP4f + TOP4b1 + TOP5a1 + TOP5f + TOP5b1 + TOP6a1 + TOP6f + TOP6b1 + BOT1a1 + BOT1f +
BOT1b1 + BOT2a1 + BOT2f + BOT2b1 + BOT3a1 + BOT3f + BOT3b1+ BOT4a1 + BOT4f + BOT4b1+ BOT5a1 +
BOT5f + BOT5b1+ BOT6a1 + BOT6f + BOT6b1 + SDEF1a1 + SDEF1f + SDEF1b1 + SDEF2a1 + SDEF2f +
SDEF2b1 + SDEF3a1 + SDEF3f + SDEF3b1 + SDEF4a1 + SDEF4f + SDEF4b1 + SDEF5a1 + SDEF5f +
SDEF5b1 + SDEF6a1 + SDEF6f + SDEF6b1+ SDEB1a1 + SDEB1f + SDEB1b1 + SDEB2a1 + SDEB2f +
SDEB2b1 + SDEB3a1 + SDEB3f + SDEB3b1 + SDEB4a1 + SDEB4f + SDEB4b1 + SDEB5a1 + SDEB5f +
SDEB5b1 + SDEB6a1 + SDEB6f + SDEB6b1)

```

Peter Kwasny GmbH, Heilbronner Strasse 96,  
74831 Gundelsheim / Germany  
Telephone: +49 (0) 6269-95-0; Fax: +49 (0) 6269-95-80  
internet: [www.kwasny.de](http://www.kwasny.de) e-mail: [info@kwasny.de](mailto:info@kwasny.de)

Art. No.: 680 061  
**2K Clear Coat**  
**SprayMax®**

## TECHNOLOGY



- Wide jet spray (spray pattern is the same as a painting gun)
- High yield
- Constant spray pressure (until the can is completely empty)
- Professional results

## PRODUKT

SprayMax® 2K Clear Coat is a high-gloss 2-component clear coat for the permanent sealing of coated surfaces. Especially developed for parts and repair refinishing. This product has a long-lasting resistance to weathering and to chemicals, and excellent resistance to petrol; it is very easy to polish. SprayMax® 2K Clear Coat has excellent flow properties and is usually used for larger surfaces (1 or 2 car parts).

## SCOPE

Recommended for:

Spraying parts and spot repairs.

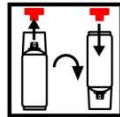
Suitable surfaces:

Solvent and water-thinnable base coat systems, dry old paintwork must be cleaned and sanded according to manufacturer's instructions.

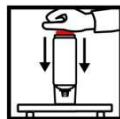
## TRIGGERING THE 2K CAN



Before triggering, shake can thoroughly for 2 minutes after hearing the shake balls.



Remove the red pushbutton from the cap. Turn the can by 180° and fit the pushbutton onto the pin in the base of the can.



Turn the can upside down and place on a firm surface. Press the red pushbutton all the way in with the palm of your hand.



After triggering, shake can thoroughly again for 2 minutes after hearing the shake balls.

## PROCESSING

Protection measures:



Wear person protection equipment.  
Respiratory mask type: A2/P2

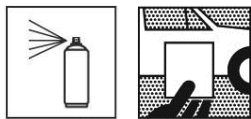


Protective gloves, e.g. made of nitrile or latex

Safety information:

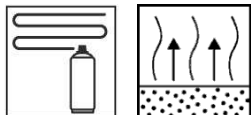
Ready-to-apply coating substances containing isocyanates may irritate mucous membranes – in particular the respiratory organs – and trigger hyper-sensitivity reactions. Hypersensitivity may be triggered if the vapours or spray mists are inhaled. Strictly observe all measures required for solvents coats when handling coating substances containing isocyanates. In particular, do not inhale vapours or spray mists. Allergy sufferers or persons with asthma or respiratory illnesses may not work with coating substances containing isocyanates.

Preparation:



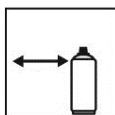
After shaking the can, test spray. The paint surface must be free of dust and grease.

Spray coats:

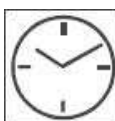


1 – 2 spray coats (approx. 20 µm dry film layer thickness per spray coat)  
Allow a 10 - 15 minute flash-off time between coats

Spray distance:



10 – 15 cm



The drying times refer to a dry film layer thickness of 35 µm.

Drying (20°C):

Dust dry: Drying level 1 acc. to DIN 53150	12 min.
Dry to touch: Drying level 3 acc. to DIN 53150	80 min.
Ready for polishing:	Over night

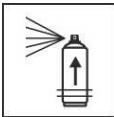
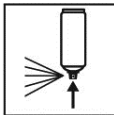
Drying (50°C):

Flash-off time:	10 min.
Dry to touch: Drying level 3 acc. to DIN 53150	60 min.
Ready for polishing:	110 min.
Completely dry:	3 h 35 min.

IR drying:  
shortwave



Flash-off time before IR:	10 min.
50% performance:	15 min.
100% performance:	20 min.
Cooling time:	10 min.
Ready for polishing:	55 min.
Completely dry:	110 min.

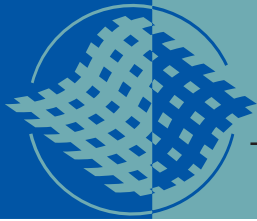
- Potlife:  Approx. 48 h at 20 °C room temperature. The potlife depends on the ambient temperature. Higher temperatures will shorten, lower temperatures will lengthen the drying time.
- End of work:  After painting, turn the can upside down and spray until the valve is empty.
- Disposal: The completely empty spray cans can be disposed of in the recycling waste container.

## KEY DATA

- Raw material base: Base paint: Two-component acrylate resins  
Hardener: Aliphatic polyisocyanates
- Solids content: Approx. 35 weight % in relation to thinned paint (without propellant)
- VOC value: see safety data sheet
- Identification: see safety data sheet
- Yield:  
theoretical: Approx. 0.5 – 0.75 m<sup>2</sup> / spray can at approx. 30 – 50 µm dry film thickness
- Shine: 84 - 92 GE at 20° measuring angle
- Storage stability:  36 months  
 The usage data refers to unused cans stored correctly at a temperature of 15-25°C and a relative humidity of below 60%. Store and transport the can upright in a dry place protected against chemical or mechanical influences. Observe the safety provisions on the can and all statutory regulations applicable to the storage place.  

- Comment: For use by professionals only.

SprayMax® is a registered trademark of the Peter Kwasny Group. This information describes our products and the respective application possibilities, and corresponds to our current information status. It does not aim to promise certain properties or suitability for a specific purpose. The warning information on the product labels must be observed. Please also observe any protection rights.



# HexPly® 6376

175°C curing epoxy matrix

## Product Data

### Description

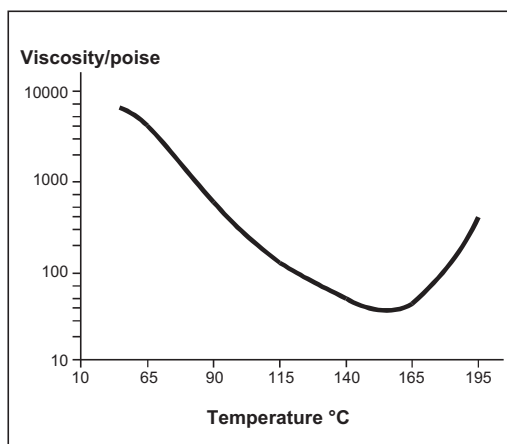
HexPly 6376 is a high performance tough matrix formulated for the fabrication of primary aircraft structures. It offers high impact resistance and damage tolerance for a wide range of high temperature applications.

### Benefits and Features

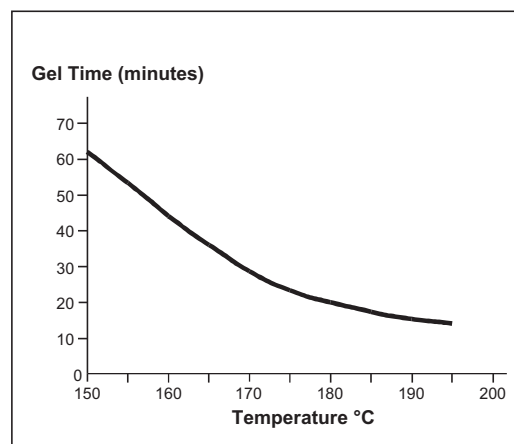
- Excellent toughness and damage tolerance
- Simple straight-up cure cycle
- Controlled matrix flow for ease of processing
- Effective translation of fibre properties
- Good hot/wet properties up to 150°C

### Resin Matrix Properties

Rheology



Gel Time





## Cured Matrix Properties (cured at 175°C)

		Method
Tensile strength	105 MPa	ISO R527 type 1
Tensile modulus	3.60 GPa	ISO R527 type 1
Tensile strain	3.1%	ISO R527 type 1
Flexural strength	144 MPa	ISO 178
Flexural modulus	4.4 GPa	ISO 178
Toughness $G_{IC}$	432 J/m <sup>2</sup>	Tested in accordance with EGF Task Group on Polymers and Composites protocol.
Cured density	1.31 g/cm <sup>3</sup>	

## Prepreg Curing Conditions

2 hours at 175°C and 700kN/m<sup>2</sup> (7 bar) pressure.

Heat up rate 2°C to 5°C.

Components up to 30 mm thick can be cured without a dwell in the schedule provided that the heat-up rate is not more than 3°C/minute. There is no deterioration in performance after 3 times the recommended cure schedule (verified by interlaminar shear strength tests).

## Prepreg Storage Life

- Tack Life @ 23°C 10 days (still processable for up to 21 days).
- Guaranteed Shelf Life @ -18°C 6 months (minimum)
- Storage conditions.

HexPly 6376 prepregs should be stored as received in a cool dry place or in a refrigerator. After removal from refrigerator storage, prepreg should be allowed to reach room temperature before opening the polythene bag, thus preventing condensation. (A full reel in its packaging can take up to 48 hours).

## Precautions for Use

The usual precautions when handling uncured synthetic resins and fine fibrous materials should be observed, and a Safety Data Sheet is available for this product. The use of clean disposable inert gloves provides protection for the operator and avoids contamination of material and components.

## Important

All information is believed to be accurate but is given without acceptance of liability. Users should make their own assessment of the suitability of any product for the purposes required. All sales are made subject to our standard terms of sale which include limitations on liability and other important terms.

©Copyright Hexcel Corporation  
Publication FTA051b (March 2007)

## For More Information

Hexcel is a leading worldwide supplier of composite materials to aerospace and other demanding industries. Our comprehensive product range includes:

- Carbon Fibre
- RTM Materials
- Honeycomb Cores
- Continuous Fibre Reinforced Thermoplastics
- Carbon, glass, aramid and hybrid prepregs
- Reinforcement Fabrics
- Structural Film Adhesives
- Honeycomb Sandwich Panels
- Special Process Honeycombs

For US quotes, orders and product information call toll-free 1-800-688-7734

For other worldwide sales office telephone numbers and a full address list please go to:

<http://www.hexcel.com/contact/salesoffices>

## ROHACELL® IG/IG-F



ROHACELL® IG and ROHACELL® IG-F products are closed-cell rigid foams based on polymethacrylimide (PMI) chemistry, which do not contain any CFC's.

The "IG" in ROHACELL® IG stands for "Industrial grade." It is the standard product in our range of rigid foams and is suitable for a variety of automotive, medical and industrial applications.

ROHACELL® IG-F is a foam grade with a finer cell structure, but the same mechanical and thermal properties as ROHACELL® IG. Because of the smaller size of its cells, ROHACELL® IG-F

takes up less resin at the surface, where the cells have been cut open.

ROHACELL® IG and ROHACELL® IG-F are particularly suitable for prepreg processing, but can also be used in, for example, resin infusion and RTM processes up to temperatures of 130°C (266°F) and pressures of 0.3 MPa (44 psi).

The thermoformability of ROHACELL® provides a tremendous manufacturing advantage.

ROHACELL® IG and ROHACELL® IG-F are also easy to shape by machining.

## ROHACELL® IG/IG-F properties

Property	Standard	Unit	ROHACELL® 31 IG/IG-F	ROHACELL® 51 IG/IG-F	ROHACELL® 71 IG/IG-F	ROHACELL® 110 IG/IG-F
Density	*	kg/m <sup>3</sup>	32 ± 7	52 ± 12	75 ± 15	110 ± 21
	*	lbs/ft <sup>3</sup>	2.00 ± 0.44	3.25 ± 0.75	4.68 ± 0.94	6.87 ± 1.31
Compressive Strength	ISO 844	MPa	0.4	0.9	1.5	3.0
	ASTM D 1621	psi	58	130	217	435
Tensile Strength	ISO 527-2	MPa	1.0	1.9	2.8	3.5
	ASTM D 638	psi	145	275	406	507
Shear Strength	DIN 53294	MPa	0.4	0.8	1.3	2.4
	ASTM C 273	psi	58	116	188	348
Elastic Modulus	ISO 527-2	MPa	36	70	92	160
	ASTM D 638	psi	5,220	10,150	13,340	23,200
Shear Modulus	DIN 53294	MPa	13	19	29	50
	ASTM C 273	psi	1,885	2,755	4,205	7,250

Technical data of our products are typical values for the nominal density.

\* Density values are valid for full-size sheets with a minimum thickness of 10 mm (0.39 inch) only. Other density ranges are available upon request.

ROHACELL® is a registered trademark of Evonik Industries and its subsidiaries

This information and all technical and other advice are based on Evonik's present knowledge and experience. However, Evonik assumes no liability for such information or advice, including the extent to which such information or advice may relate to third party intellectual property rights. Evonik reserves the right to make any changes to information or advice at any time, without prior or subsequent notice. EVONIK DISCLAIMS ALL REPRESENTATIONS AND WARRANTIES, WHETHER EXPRESS OR IMPLIED, AND SHALL HAVE NO LIABILITY FOR, MERCHANTABILITY OF THE PRODUCT OR ITS FITNESS FOR A PARTICULAR PURPOSE (EVEN IF EVONIK IS AWARE OF SUCH PURPOSE), OR OTHERWISE. EVONIK SHALL NOT BE RESPONSIBLE FOR CONSEQUENTIAL, INDIRECT OR INCIDENTAL DAMAGES (INCLUDING LOSS OF PROFITS) OF ANY KIND. It is the customer's sole responsibility to arrange for inspection and testing of all products by qualified experts. Reference to trade names used by other companies is neither a recommendation, nor an endorsement of the corresponding product, and does not imply that similar products could not be used.

**Evonik Resource Efficiency GmbH**  
High Performance Polymers  
64293 Darmstadt, Germany  
Phone +49 6151 18-1005  
E-mail rohacell@evonik.com  
www.rohacell.com

**Americas**  
**Evonik Foams Inc.**  
Theodore, Alabama, USA  
Phone +1 866 764-6235

**Evonik Specialty Chemicals**  
**(Shanghai) Co., Ltd.**  
Shanghai, China  
Phone +86 1391 6212034

NTNU		Utarbeidet av		Nummer		Dato	
		HMS-avd.		HMSRV2601		22.03.2011	
		Godkjent av		Erstatter			
HMS		Rektor				01.12.2006	
<b>Risikovurdering</b>							

**Enhet:** Institutt for produktutvikling og materialer, laboratorie for polymerer og kompositter

**Dato:** 03.08.2017

**Linjeleder:** Torgeir Welø

**Deftakere ved kartleggingen (m/ funksjon):** Nils Petter Vedvik, Erik Vassøy Olsen

**Risikovurderingen gjelder hovedaktivitet:** Masteroppgave student: Erik Vassøy Olsen.

**Tittel på oppgaven:** Lay-up, Production Process And Parametric Optimization Of A Composite Horizontal Stabilizer Spar

**Signaturer:** Ansvarlig veileder:  Nils Petter Vedvik

Student:  Erik Vassøy Olsen

ID nr	Aktivitet fra kartleggings-skjemaet	Mulig uønsket hendelse/ belastning	Vurdering av sannsynlighet (1-5)	Vurdering av konsekvens:			Risiko-Verdi (menneske)	Kommentarer/status Forslag til tiltak	
				Menneske (A-E)	Ytre miljø (A-E)	Øk/ materiell (A-E)			Om-dømme (A-E)
1	Blanding av epoxy	Epoxyssøl på hud eller klær	3	B	A	A	A	B3	Vernebriller hansker avtrekk
1	Blanding av epoxy	Varmeutvikling	3	B	B	B	B	B3	Sørge for at den står et sted hvor den ikke kan antenne annet brennbart materiale
2	Påføring av epoxy	Epoxyssøl på hund eller klær. Innhalering av skadelig avgass	3	B	A	A	A	B3	Hansker og pustemaske
3	Mekanisk testing	Skade på testutstyr	1	A	A	B	B	A1	Vernebriller
3	Mekanisk testing	Personskade	2	B	A	A	A	2B	Vernebriller

NTNU	Kartlegging av risikofylt aktivitet			Utarbeidet av	Nummer	Dato
				HMS-avd.	HMSRV2601	22.03.2011
HMS				Godkjent av	Ersatter	
				Rektor		01.12.2006
						

Dato: 03.08.2017

Deltakere ved kartleggingen (m/ funksjon): Nils Petter Vedvik, Erik Vassøy Olsen

Kort beskrivelse av hovedaktivitet/hovedprosess: Komposittproduksjon

Tittel på oppgaven: Tittel på oppgaven: Lay-up, Production Process And Parametric Optimization Of A Composite Horizontal Stabilizer Spar

Er oppgaven rent teoretisk? (JA/NEI): Nei

Signaturer: Ansvarlig veileder:  Nils Petter Vedvik Student:  Erik Vassøy Olsen

ID nr.	Aktivitet/prosess	Ansvarlig	Eksisterende dokumentasjon	Eksisterende sikringsiltak	Lov, forskrift o.l.	Kommentar
1	Blanding av epoxy	Erik Vassøy Olsen	Sikkerhetsdatablad	Vernebriller, hansker, avtrekk og pustemaske	Arbeidsmiljøloven, Kjemikalieforskrift en, lab- og Verkstedhåndbok en NTNU	
2	Påføring av epoxy	Erik Vassøy Olsen	Sikkerhetsdatablad	Vernebriller, hansker, avtrekk og pustemaske	Arbeidsmiljøloven, Kjemikalieforskrift en, lab- og Verkstedhåndbok en NTNU	
3	Mekanisk testing	Erik Vassøy Olsen	Romopplæring, HMS-kurs	Vernebriller og hørselvern	Arbeidsmiljøloven Verkstedhåndbok en NTNU	